



**Improving small power energy estimations for energy audits in
offices**

by

Ana Rodriguez-Arguelles

Thesis submitted for the degree of Doctor of Engineering (EngD)

**Technology for Sustainable Built Environments Centre
School of Construction Management and Engineering**

May 2019

University of Reading

Abstract

Approximately 40% of global energy use can be attributed to buildings; in commercial buildings around 20% of the total energy used comes from small power loads. In the UK, this percentage is expected to reach up to 50% in highly efficient offices in the next 20 years. This trend makes small power loads in commercial buildings one of the fastest growing load categories.

Quantitative energy audits for the analysis of the energy performance of buildings are conventionally divided into two approaches, *calculation*, based on algorithms and equations, and *measurement*, which performs some level of direct monitoring. These quantitative energy audit approaches are common tools for evaluating the potential for reducing energy demand in buildings. Small power load estimations in office buildings present challenges for both approaches due to the large number of such loads and their heterogeneous nature, and results in significant uncertainty in these estimations. This thesis investigates the sources of uncertainty of the small power energy estimations for the different audit approaches, and proposes and tests a number of methods and techniques to overcome these weaknesses in the auditing process.

For the calculation approach, insufficient input parameter specifications have been identified as the main source of uncertainty, which is associated with variability in the model output. A sensitivity analysis method has been developed to identify the inputs that most contribute to such output variability and that require additional effort to strengthen their accuracy in order

to minimize the likely error in calculated small power energy consumption. These influential parameters have been found to depend not only on the information sources available, but also on the calculation method used and the type of load estimated.

Regarding the measurement approach, its uncertainty is related to the number of meters used, which increases the quality of the information, but also the complexity of the hardware installation. An extrapolation method for providing the relationship between the number of appliances monitored and the accuracy obtained in the final energy estimations has been proposed. Results showed a logarithmic relationship between the number of desks monitored in a case study office and the relative standard uncertainty percentage obtained in the energy estimations for the aggregated load of the PCs. The method informs about the level of metering infrastructure required in accordance with the level of uncertainty that can be accepted for the small power energy estimations.

Non-Intrusive Appliance Load Monitoring (NIALM) methods, as a solution for small power individual load estimation in office buildings, have also been explored through a practical study. The disaggregation capabilities for the different electrical signatures, and their dependence on appliance type and number have been investigated. Although the overall accuracy in the disaggregation process was found to be significantly smaller for offices than for domestic scenarios, some signature combinations, such as the *Root Meter Square Increments* and the *Steady Harmonic Increment*, were found to achieve up to 90% of accuracy in the disaggregation process. The outcomes from this study contribute to the extension of the use of existing NIALM methods from domestic to office buildings in the field of small power disaggregation.

Declaration

I confirm that this is my own work and the use of all material from other sources has been properly and fully acknowledged.

Ana Rodriguez Arguelles

11th June, 2018

Acknowledgements

I would like to thank Dr Ben Potter and Dr Stefan Smith, they have been, in the wider meaning of the words, excellent supervisors, not only for their support and guidance throughout my doctoral training, but also for instilling in me their own enthusiasm and integrity for research.

Also many thanks to Alan Kiff for his availability and thoughtful feedback on my writing.

Special thanks goes to Dr Emmanuel Essah, who encouraged me to embark on the EngD journey and who has been always available to chat and provide kind advice.

Many thanks also to the energy team from the University of Reading who kindly facilitated my data collection for an important part of this research project, and to Ian Jones for helping me with the meter installation.

At the TSBE centre, I would like to give thanks Jenny, Emma, and David for the running of the centre with professional and supportive spirits, always with a smile and kind words, and to my research fellows, for sharing this sense of community and solidarity that makes the TSBE such a wonderful place in which to work. Especially to Timur and Max, always willing to help and share their knowledge with me over a cup of coffee.

My profound gratitude to my parents, Luque and Consuelo, for their unconditional support during my whole life and for showing me the value of work and perseverance.

A special mention to my son, Gael, he joined me on the final stage of this journey and has, in his

own way, inspired me to finish it.

And lastly, but most importantly, I would like to express my gratitude to Gabi, for motivating, helping, and believing in me to the end. I could not have done this without you.

Table of Contents

Abstract	ii
Declaration	iv
Acknowledgments	v
Table of Contents	xi
List of Tables	xiii
List of Figures	xvii
List of Abbreviations	xxi
1 Introduction	1
1.1 Background	2
1.2 Thesis motivation	3
1.2.1 Quantitative audit approaches	6
1.3 Problem statement, objectives and scope	11
1.3.1 Problem statement	11
1.3.2 Objectives	12

1.3.3	Scope	13
1.4	Thesis contribution	14
1.4.1	Publications	15
1.5	Thesis outline	16
2	Literature review	18
2.0.1	Energy audits for buildings	18
2.0.2	Energy performance assessment criteria for existing buildings	19
2.0.3	Quantitative energy audit approaches	20
2.0.3.1	Small power in quantitative energy audits, the challenge	22
2.1	Calculation models for energy audits	23
2.1.1	Sensitivity Analysis for energy audit	24
2.1.1.1	Sensitivity analysis classification	25
2.2	Measurement techniques for energy audits	27
2.2.1	Top-down	28
2.2.2	Bottom-up	29
2.3	NIALM: Alternative measurement method for energy audits in commercial buildings	30
2.3.1	Monitoring hardware	32
2.3.2	Event detection	34
2.3.3	Electrical signature	35
2.3.4	Machine learning techniques for load disaggregation	37
2.3.4.1	Algorithms for supervised machine learning	40
2.4	Conclusion and literature gaps	42
3	Improving the calculation approach	45

3.1	Introduction	45
3.1.1	Morris method	47
3.2	Methodology: The adapted SA method	48
3.2.1	Refinement adaptive measures	49
3.2.2	Implementation methodology	52
3.2.2.1	Starting points	53
3.2.2.2	SA implementation	55
3.2.2.3	Results interpretation	60
3.2.3	Explanatory example for the adapted SA method	65
3.3	Case-study	77
3.3.1	Calculation models	77
3.3.1.1	Calculation models input parameters	81
3.3.2	Information sources	82
3.3.3	Results	85
3.3.3.1	Visual result representation	90
3.4	Summary and discussion	99
4	Improving the measurement approach	102
4.1	Introduction	102
4.2	Methodology: metering techniques for small power loads	103
4.2.1	Monitoring hardware	104
4.3	Result analysis	107
4.3.1	Data meter comparison	107
4.3.2	Energy audit benefits obtained from aggregated appliances energy use data	111
4.3.2.1	Analysis of top-down existing techniques	112

4.3.2.2	Use of bottom-up techniques at the aggregated level	116
4.3.2.3	Bottom-up method validation	124
4.3.3	Energy audit benefits obtained from individual appliance energy use data .	125
4.3.3.1	Analysis of bottom-up existing techniques	125
4.3.3.2	Use of top-down techniques at the individual appliance level . . .	130
4.3.3.3	Top-down method validation	135
4.4	Summary and discussion	137
5	NIALM performance for small load appliance identification	141
5.1	Introduction	141
5.2	Methodology	143
5.2.1	First NIALM stage: Monitoring system installation	144
5.2.1.1	Monitoring equipment considerations	144
5.2.2	Second NIALM stage: Event detection	147
5.2.2.1	Signal preprocessing	147
5.2.2.2	Event detection algorithm	148
5.2.3	Third NIALM stage: Electrical signatures extraction	150
5.2.3.1	Steady- state in time domain signature	151
5.2.3.2	Steady-state in frequency domain signature	152
5.2.3.3	Transient signatures in time domain signature	153
5.2.3.4	Transient signatures in frequency domain signature	153
5.2.4	Fourth NIALM stage: The disaggregation algorithm implementation	154
5.2.4.1	Accuracy metric	156
5.2.5	Individual profile database	157
5.3	Results analysis and discussion	158

5.3.1	Individual appliance signal patters analysis	158
5.3.1.1	Signature characteristic parameters	166
5.3.2	Signature dataset	168
5.3.3	Individual appliance identification	170
5.3.4	Aggregated appliances identification	171
5.3.4.1	NIALM for domestic appliance disaggregation	172
5.3.4.2	NIALM for office appliances disaggregation	175
5.4	Summary and discussion	177
6	Discussion and thesis conclusions	180
6.1	Research summary	181
6.2	Research contributions	184
6.3	Further work	189
6.4	Concluding remarks	190
	References	191
A	CIBSE TM22 methodology	210
B	Informative monitored appliances table for Chapter 4 case study	214
C	Schematic layout of smart plugs for the bottom-up metering techniques	216
D	Individual power consumption profiles for appliances with high frequency content	219
E	Decision tree classifier algorithm	222
F	Validation methods for the decision three algorithm	225
G	Decision Tree code in KNIME	228

List of Tables

1.1	Total savings by switching off equipment during a 60 hour weekend*	5
1.2	Total site annual electrical energy break-down in the 1,500m ² commercial building targeted [1]	8
3.1	Maximum and minimum values for the inputs in the explanatory example.	66
3.2	Representative feature parameters for each input factor.	71
3.3	Description table for input data to energy models	81
3.4	Value ranges for the input parameters presented in Table 3.3 for a typical office. . .	84
3.5	Value ranges for the input parameters presented in Table 3.3 for a co-working office.	85
3.6	Input factor impact ranking for PCs from the <i>typical office</i> case study.	90
4.1	MTU monitoring layout explanation.	107
4.2	Case study data bases	108
4.3	Compensated errors band vales for ε'_k and ε''_k	111
4.4	Relative error for each of the extrapolation method estimations	124
4.5	Relative error for each of the NIALM method estimations.	137
5.1	ON period, power rate, and amperage for the different appliances under monitoring.	158
5.2	Steady Sate Signature Dataset	169

5.3 Transient State Signature Dataset 169

5.4 Individual loads precision recognition averaged over 10 iterations 171

5.5 Overall accuracy recognition averaged over 10 iterations 171

5.6 Overall accuracy for all the possible Signature combinations for the domestic scenarios 174

5.7 Overall accuracy for all the possible Signature combinations for the office scenario 176

A.1 TM22 methodology input data by assessment levels. 213

List of Figures

- 1.1 Annual energy usage of 300 case study of office buildings. 6
- 1.2 Percentage energy break down per equipment before and after the energy reconciliation in in the $1,500m^2$ commercial building targeted [1], resulting in a 4% percentage difference for the “small powers” estimates. 9
- 1.3 Deficiencies identified in the implementation of the two main quantitative energy audits approaches in terms of small power estimations in office buildings. 11
- 2.1 Proposed electrical signature classification 38
- 3.1 Input factors classification graph obtained from the Primary SA, based on the direct (horizontal axis) and indirect (vertical axis) effects of each input X over the model output. 63
- 3.2 Input factors classification graph obtained from the Secondary SA, based on the degrees of non-monotonicity (horizontal axis) and skewness (vertical axis). 64
- 3.3 Results interpretation for the X_1 input 72
- 3.4 Results interpretation for the X_2 input 73
- 3.5 Results interpretation for the X_3 input 73
- 3.6 Primary SA 75
- 3.7 Secondary SA 76

3.8	Primary SA graphs: Estimated mean (μ^*) of the absolute values and standard deviation (σ) of the different input factors of the four case-study models (applied on PCs' energy estimation)	86
3.9	Secondary SA graphs: Estimated degree of non-monotonicity (Φ) and degree of skewness (ξ) of the different input factors of the four case-study models (applied on PCs' energy estimation)	88
3.10	Primary SA chrome maps: impact of the different input factors (x-axis) for each of the small power considered in the typical office case study (y-axis)	92
3.11	Primary SA chrome maps: impact of the different input factors (x-axis) for each of the small power considered in the co-working office case study (y-axis)	94
3.12	Secondary SA chrome maps: complexity of the different input factors (x-axis) for each of the small power considered in the typical office case study (y-axis)	96
3.13	Secondary SA chrome maps: complexity of the different input factors (x-axis) for each of the small power considered in co-working office case study (y-axis)	98
4.1	4-noks metering system experimental set-up	105
4.2	MTU monitoring equipment and installation.	106
4.3	Comparisons of the MTU and Plugs power profile reads for the printer.	109
4.4	Power and energy consumption profiles from 21 st August to 3 rd September.	113
4.5	Power consumption profiles from the 21 st August to the 10 th September 2017	114
4.6	Power consumption profiles from the 21 st to the 27 th of August.	115
4.7	Hot desk leaved on from 23 rd to 24 th of August	116
4.8	RUP of the aggregated desk energy estimation depending on the number k of meter used	119

4.9 RUP logarithmic values of the aggregated desk energy estimation depending on the number k of meter used	120
4.10 Box plot graphical of the normalised energy distribution against the number of desks monitored.	122
4.11 Skewness percentage of the energy distribution set against the number of meter. .	123
4.12 Fridge power and energy consumption profiles from 18 th August to 4 th September, 2017.	126
4.13 Desks power and energy consumption profiles from 18 th August to 4 th	127
4.14 Printer power and energy consumption profiles from 18 th August to 4 th	128
4.15 Energy consumption percentage classification representations.	129
4.16 CT-A power reading event detection, for the morning of the 21 st of August 2017 . .	132
4.17 CT-B power reading event detection, for the morning of the 21 st of August 2017 . .	133
4.18 CT-C power reading event detection, for the morning of the 21 st of August 2017 . .	134
4.19 Detected switching on and off events in circuit 6L3 from 21 st to 28 th of August. . .	136
5.1 NIALM model work flow	143
5.2 Different components of the high-resolution monitoring system.	146
5.3 Zero crossing points in a wave cycle.	148
5.4 Steady state and transient segment wave definition.	149
5.5 Proposed electrical signature classification	151
5.6 Kettle electrical signal profiles.	159
5.7 Microwave electrical signal profiles.	160
5.8 Coffee machine electrical signal profiles.	161
5.9 Heater electrical signal profiles.	162
5.10 Fan electrical signal profiles.	163

5.11 Incandescent lamp electrical signal profiles.	164
5.12 Desk (PC and screen) electrical signal profiles.	165
5.13 RMS aggregated MATLAB profiles for the domestic scenario.	173
5.14 RMS aggregated MATLAB profiles for the office scenario.	175
6.1 Proposed methods for overcoming the deficiencies detected in the different small power load estimations.	183
A.1 TM22 tree diagram illustrating the breakdown of energy use.	211
C.1 Smart plugs schematic layout for room A	217
C.2 Smart plugs schematic layout for room B	218
D.1 Printer power profile at 100Hz sample rate.	220
D.2 PC power profile at 100Hz sample rate.	221
E.1 k-fold cross validation method.	226
E.2 Holdout validation method.	227
G.1 Decision Tree code in KNIME	228

Nomenclature

i	Sub-index relative to the sample point value
j	Sub-index relative to the input parameter value
X	Input parameter
n	Sample range size
r	Number of elementary effect evaluations
x	Sample point within the input parameter range
t	Sample point within the normalized trajectory range
x_{min}	Minimum sample point within the input parameter range
x_{max}	Maximum sample point within the input parameter range
y	Model output
Δ	Sample point perturbation
F	Distribution function
μ	Mean
μ^*	Mean of the absolute values
μ_m	Average of the elementary effect mean
σ	Standard deviation
ϕ	Degree of non-monotonicity
d	Euclidean distance

Ω	Experimental space
k	Number of input factors
Φ	Degree of non-monotonicity
ξ	Degree of skewness
se	Standardized elementary effect distribution
e	Elementary effect distribution
m	Median
E_T	The total annual energy consumption
U_n	The number of installed units
P_L	The nameplate load
F_L	The load factor
O_h	The operational hours
F_{ON}	The ON load factor
F_w	The wastage load factor
P_{ON}	The average ON power
P_W	The average waste power
O_d	The annual averaged occupancy density
P_r	The annual total number of persons
T_w	The waste time factor
α	Fix positive current threshold

T	Fix positive period threshold
I	Raw current value
P	Raw powers value
M	Moving window of samples
ε	Relative error
CF	Crest Factor
Sh	Steady Harmonic Increment
Th	Transient Harmonic Increment
ϕ	RMS current Increment

List of Abbreviations

CT Current Transformer

OAT One At a Time

SEA Sensitivity Analysis

SEE Standardized elementary effect

AC Alternating current

API Application Programming Interface

BSI British Standards Institution

BSRIA Building Services Research and Information Association

CF Crest Factor

CIBSE Chartered Institution of Building Services Engineers

CM Coffee machine

CT Clamp Transformer

DC Direct current

DECC British Department of Energy and Climate Change

DFFT Discrete Fast Fourier Transform

F Fan

FFT Fast Fourier Transform

FFT Fast Fourier Transform

Fl Fluctuations

H Heater

IFFT Inverse Fast Fourier Transform

IL Incandescent lamp

ISO International Standards Organization

K Kettle

M Microwave

MIT Massachusetts Institute of Technology

MTU Measuring Transmitting Unit

NIALM Non Intrusive Appliance Load Monitoring

OAT One at a Time

PC Personal computer

PD Profile Difference

RMS Root Meter Square

RUP Relative Uncertainty percentage

SA Sensitivity Analysis

Chapter 1

Introduction

”Great things are done by a series of small things brought together.”

Vincent Van Gogh (1853– 1890)

The aim of the research presented in this thesis is to contribute to the field of quantitative energy audits in office buildings by improving the ways in which small power energy consumption is estimated. For this, the different existing quantitative approaches are investigated, recognizing their weaknesses, and a number of methods and techniques are proposed, developed, and assessed to overcome those weaknesses. This chapter presents the background and motivation for the research on the basis of the identified challenges and opportunities associated with the energy assessment process in the small powers category. The problem statement is defined and split into a set of research objectives along with the scope of the thesis. Contributions of the research are stated and the thesis outline is presented at the end of the chapter.

1.1 Background

Tackling climate change is one of the greatest challenges facing the 21st Century. Energy saving constitutes a primary measure for the protection of the environment and for the reduction of the use of polluting fossil fuels. Energy audits are a crucial tool to ascertain the efficiency of energy use and a basis on which to make any decision for enhancing energy management [2].

Currently, the global energy use contributed by buildings is about 40%, of which a significant proportion might be wasted due to faults at the operation stages [3]. It is estimated that the potential energy savings to be achieved in the building sector could be between 20% and 40% [4]. Environmental awareness is one of the drivers for the implementation of energy efficiency measures, other underlying reasons being financial rewards and environmental policies.

International environmental policies, such as ISO 50002 [5] released by the International Organization for Standardization (ISO) in June 2011, defines the minimum set of requirements leading to the identification of opportunities for the improvement of energy performance. At national level, some of the main institutions delivering standards related to building practices are organizations such as the Building Services Research and Information Association (BSRIA), the Chartered Institution of Building Services Engineers (CIBSE), the British Standards Institution (BSI), and the ASHRAE.

Energy consumption of existing buildings can often be reduced by introducing cost-effective measures and cost savings that contribute to the profitability of organizations once the initial capital cost has been repaid [6]. This estimate is derived from changes that can be achieved with little or even negative cost, such as reducing behavioural barriers [7]. However, other initial investment costs required for energy management strategies are considerable and it is necessary to analyse the potential energy-saving effects of the energy strategies in advance, so that electricity use can be more accurately estimated and the return on investment can be more

accurately analysed.

The building sector accounts for approximately 40% of the global primary energy demand and, within the commercial sector, office and retail buildings are those with the biggest CO_2 emissions [8]. This energy consumption has been forecast to increase in the coming years, thereby having a direct impact on resource and environmental exhaustion [9]. Private initiatives, together with government intervention, which promote energy efficiency, limit energy consumption, and raise social awareness about the rational use of energy will be essential to make possible a sustainable energy future [10].

Energy audits can provide a basis on which decisions can be made for the achievement of energy savings [4]. It is required, then, to implement an energy audit approach that reflects the aforementioned awareness of environmental issues, as well as to account for energy policies and to implement new available technologies to facilitate the process. However, there is no unanimous agreement on how to assess the energy aspect of building performance and judge whether any unnecessary energy use is occurring in a building [11]. This research analyses the main approaches concerning building energy performance assessment, particularly for office buildings, focusing on small power load estimations.

1.2 Thesis motivation

Electricity is primarily used for cooling, lighting, and powering appliances across all sectors - residential, commercial, and industrial [12]. The importance of energy efficiency for office equipment however, is becoming more relevant as manufacturers continue to drive down the capital cost of such equipment while operation costs increase. According to Kamilaris et al. [13], small power in commercial buildings contribute significantly to the total overall energy consumption, accounting for more than 20% of primary energy used in commercial buildings in the U.S., with

this percentage expected to increase by 40% in the next 20 years. This has made small power loads in non-commercial buildings one of the fastest growing load categories in the U.S. [14]. This trend is followed by others countries, such as the UK, where small power appliances have also become a significant source of energy end-use, accounting for up to 50% in high-efficient buildings [15].

An experimental study highlighting the importance of small power loads in non-commercial buildings, is the “Blackout event” project launched by the sustainable service team at the University of Reading, UK ¹ ². The university sustainability team participated in the a “Blackout project” held on Friday November 2015, where the amount of energy that could be saved over one weekend was monitored by auditing buildings after switching off all small appliances, where possible. The project was carried out by volunteers students and staffs who explored 15 buildings on the University of Reading Whiteknights campus, switching off all the small appliances that were being left on across the university, with the aim of working out how much energy is being wasted over a typical weekend. The audit took place from Friday the 8th November at 4pm to Monday 11th November at 10am. Table 1.1 shows the savings achieved by switching off equipment over the 60 hour weekend.

¹sustainability.nus.org.uk/blackout/articles/students-lead-the-way-with-university-energy-audits

²storify.com/carboncountdown/blackout

Table 1.1: Total savings by switching off equipment during a 60 hour weekend*

Equipment	Number switched off	Power (kW)	Energy (kWh)	Economic (£)**
PC (on-sleep)	205	18450	1107	129
Monitor (on-off)	486	2430	146	17
Printer / photocopier	41	4100	246	29
Desk fan	390	7800	468	54
Electric heater	11	16500	990	115
Water boilers	3	60	4	0.48
Total	1136	49340	2960	344

*This information has been provided by the Sustainable Service Team of the University of Reading.

**Electricity cost 0.12 £/ kWh

Extrapolating results in Table 1.1 to a complete year (52 weekends), would result in an annual savings of 153,920 kWh and £17,888.

In office buildings the rapid market penetration of consumer electronics has expanded the small power category and consumption from plug loads has significantly increased. However, the energy use and reduction strategies for plug loads have so far received little attention. Small power equipment in offices are evolving into dominant loads and the identification of strategies for reducing their consumption has been recognised as an effective measure to improve energy use for office buildings by making them part of the basic building design and educating tenants and owners on their efficient energy use [16].

Rumsey Engineers measured the energy consumption of a representative selection of small power loads at 334 Packard Foundation offices [17]. The engineers assumed equipment and practices to be unchanged and estimated and compared the buildings' annual energy usage

baselines after implementing efficiency measures (in heating, ventilation, air conditioning (HVAC), and lighting) and again after implementing the efficiency measures alongside reducing plug load consumption. The study presents plug loads as a relevant proportion of the building and shows how, as the offices become more energy efficient, this relevance increases significantly (see Figure 1.1).

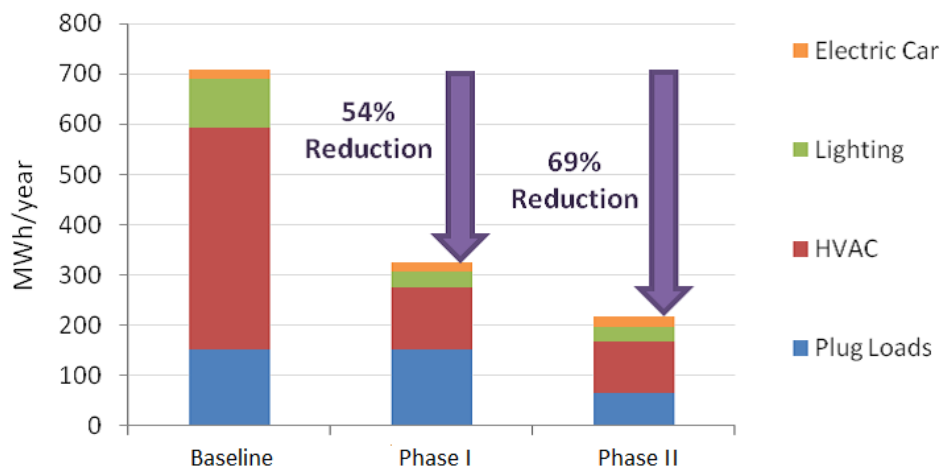


Figure 1.1: Annual energy usage of 300 case study of office buildings.

1.2.1 Quantitative audit approaches

Quantitative energy audits for the analysis of the energy performance of buildings, are popular tools for achieving energy savings in buildings [4]. Historically, quantitative audits can be divided into two types or approaches, *calculation* and *measurement*. Small power load estimations in office buildings, due to their large number and heterogeneous nature, present challenges for both approaches.

Calculation approach, based on algorithms and equations for delivery of the final energy estimations [18], carry out an intrinsic uncertainty associated with the model inputs. For small power loads in offices, the high dependence of energy consumption on end-use behaviour [19], makes

their specific input extremely variable and case dependent, leading to a degree of uncertainty around each input parameter and, therefore, the accuracy of the model outputs [20].

Measurement approach, perform some level of direct monitoring, that can range from the use of individual appliance/system hardware meters, in *bottom-up* metering techniques, to the use of a single meter for the monitoring of the whole building/area energy consumption, which is then broken down using calculation models, in *top-down* metering techniques. Both techniques present a compromise in terms of the number of meters, which increase the quality of the information, but also in terms of the complexity of the hardware installation. This relationship is more critical in the case of small power equipment in offices due to their large numbers.

A number of researchers, such as Pieter de Wile [21], Hong et al. [4] and Menezes et al. [15], the latter focus on small power equipment, have performed practical studies highlighting the gap between predicted, or calculated, and measured energy performance of buildings, presenting this gap as a new framework for investigation.

Engineers from AECOM, the industry sponsor for the present thesis research, followed the energy assessment methodology reported in CIBSE TM22 technical report [22] to conducted energy audits in commercial buildings [1, 23–25]. The TM22 quantitative energy assessment methodology, originally developed by the PROBE studies in 1999, is currently extensively used in the UK industry and overseas and provides a systematic way of undertaking an energy survey (see Appendix A). For practical reasons, a common practice for conducting these audits is the attribution of the *unknown energy percentage* (unmatched energy between measurement and calculated estimations) to small power, resulting in an overloading of small power to the detriment of other systems.

One of those reviewed audits [1], taken as an example to illustrate the above-mentioned audit practice, provides the following (Table 1.2) annual electrical energy break-down by end use

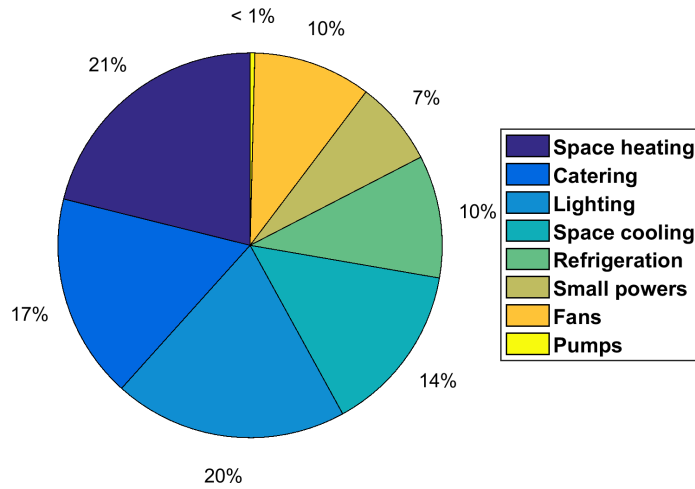
system over a total area of $1,500m^2$.

Table 1.2: Total site annual electrical energy break-down in the $1,500m^2$ commercial building targeted [1]

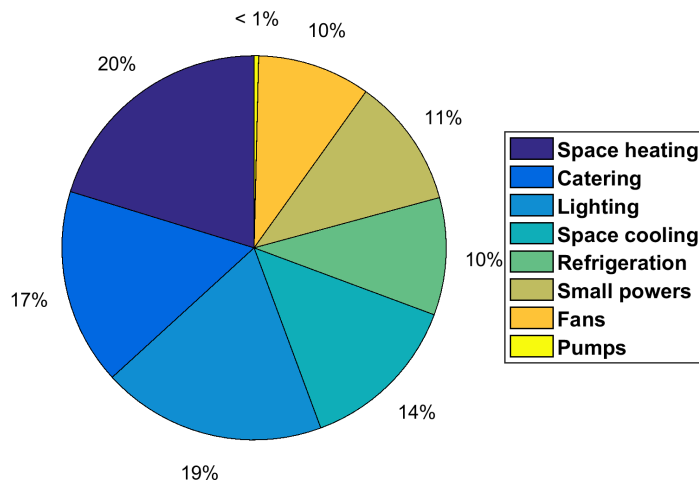
Equipment	Annual kWh
Space heating	353290
Catering	287860.9
Lighting	328870.8
Space cooling	238674
Refrigeration	172268.6
<i>Unmeasurable small power</i>	<i>71055.9</i>
Small power	118980.4
Fans	165686.6
Pumps	6622.6
Measured	1684513

According to the audit report, the initial calculated energy consumption was 1,613,462.1 kWh, but, in order to reconcile this value with that measured (2,243,791.5 kWh), the difference (71,055.9 kWh), called *Unmeasurable small power*, was attributed to the “Small powers” equipment category. This practice is very common and saves time for auditors, but can result in an overestimation of the contribution of small power and lower percentage estimation for the rest of the equipment. Figure 1.2 shows the initial and the reconciled energy break down³ obtained using the *calculated* and the *measured* total energy value.

³The reconciliation has been done by replacing the estimated with the measured values, following the standard TM22 procedure.



(a) Initial, using the calculated value



(b) Reconciled, using the measured value

Figure 1.2: Percentage energy break down per equipment before and after the energy reconciliation in the $1,500m^2$ commercial building targeted [1], resulting in a 4% percentage difference for the “small powers” estimates.

There is an increase of 4% in the energy consumption percentage of the “small powers” between

piechart 1.2a (where total energy consumption = 1613462.1 kWh) and piechart 1.2b, (where total energy consumption = 2243791.5 kWh) in which "small powers" = small powers + *Unmeasurable small power*). A decrease in the percentage of "lighting" and "space heating" can also be observed.

A potential solution for avoiding row energy estimations when dealing with small power in office buildings is to install sub-metering equipment in each individual appliance. This would provide detailed information about end-use energy consumption and performance [7]. However, this information comes at a high cost in terms of infrastructure, to which the installation and maintenance *time cost* also needs to be considered.

Some innovative monitoring methods, such as Non-Intrusive Appliance Load Monitoring (NIALM) have been recognized as a potential alternative for intrusive metering techniques [26]. The ability to obtain the level of information of a bottom-up technique at the infrastructure cost of a top-down one is particularly interesting for small power energy estimations. However, and although being first developed in the 1990s [27], this is still not considered a mature technology for implementation in commercial buildings [28], mainly due to the large number and heterogeneous nature of small appliances typically founded in these buildings.

A proper understanding of small power loads is crucial to determine sources of error in the audit process and improve energy estimations in office buildings. However, current energy assessment models and techniques are not sufficiently accurate to overcome the issues that entail this challenge, which has been largely unexplored by the academic community. This thesis constitutes an analysis of the different energy audit approaches for small power energy estimations, identifying weaknesses and proposing different methods and techniques to overcome them.

1.3 Problem statement, objectives and scope

1.3.1 Problem statement

The central problem addressed by this thesis is the deficiencies identified in the implementation process for quantitative energy audits in office buildings regarding small power load estimations. Figure 1.3 presents (in red) the main challenges identified in the academic literature and industrial report reviewed for the two main energy assessment approaches.

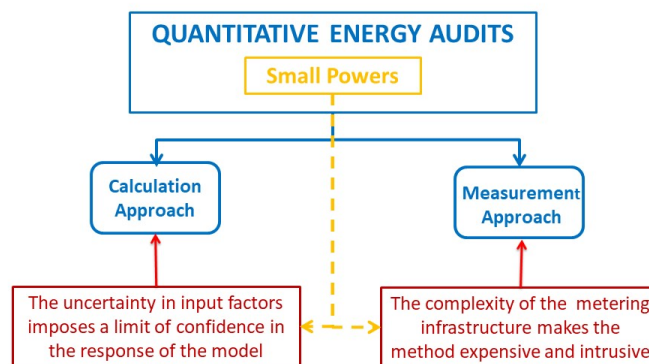


Figure 1.3: Deficiencies identified in the implementation of the two main quantitative energy audits approaches in terms of small power estimations in office buildings.

These implementation deficiencies can negatively effect not only the final small power consumption estimation, recognized as a significant part of the total energy use in buildings, but also the estimations of the rest of the building systems, resulting in poor quality of the overall energy assessment.

In order to meet the aim of the research presented in this thesis, i.e. *improve small power load estimations for quantitative energy audits in office buildings*, and after a thorough review of the

existing literature, the problem statement has been split into a number of general objectives formulated as follows.

1.3.2 Objectives

On the basis of the problem statement and the gaps in the literature highlighted above, the research objectives addressed in this thesis are the followed:

1. Create a sensitivity analysis method for calculation models to evaluate how the variation in the output of the model can be apportioned to different input factor uncertainties.
2. Conduct a comparative study to identify the most efficient meter installation strategy, i.e. bottom-up or top-down, in a typical office building for monitoring small power loads.
3. Evaluate the relationship between estimation accuracy and cost of implementation (in terms of complexity and intrusiveness) for bottom-up techniques, by relating proportional metering to total appliance load prediction.
4. Explore the use of top-down techniques for obtaining information at the individual appliance level through a practical study in an office buildings.
5. Following objective 4, analyse the disaggregation capabilities for the different signature categories ⁴, depending on the electrical nature and number of small appliances under monitoring, in order to facilitate the implementation of NIALM methods in energy audit for office building.

⁴A classification for the different categories of electrical signatures has been provided in Chapter 2.

1.3.3 Scope

The scope of the research presented in this thesis is focused on the proposition, analysis and test of different methods for improving small power energy estimation for energy audits. Further technical aspects associated with the deployment of the solution, as well as social and regulatory aspects are not within the scope of this thesis. Corresponding assumptions and justification for decisions taken during the research process are presented in the methodology sections of the chapters.

For calculation approaches, a sensitivity analysis method for ranking the input factors in order of importance is proposed. The method is not designed to quantify the input factors absolute significance as this is not considered to significantly contribute to the decision making regarding the optimal calculation model selected in an energy audit.

For metering approaches, using two different monitoring techniques, the research performs a comparison of the information quality obtained for two levels of energy analysis: individual appliances and aggregated. The comparison focuses on the monitoring hardware characteristic: sampling frequency, number of meters needed, type of data recorded, etc, but does not undertake other potential analytic variables, such as monitoring time or number of appliances under monitoring. These aspects of the monitoring process might also have an impact on the information delivered, but due to time and material constraints have not been considered in this research.

For NIALM methods, the research focuses on the third implementation stage, *electrical signature identification*, since major deficiencies in this stage have been identified as a major cause for the prevention of the extended use of NIALM methods in energy audits for commercial buildings. The other three implementation stages, *hardware installation*, *event detection*, and *load disaggregation*, also present areas for improvement, but they are not considered in this

research.

1.4 Thesis contribution

The thesis objectives presented in the previous section of this chapter are achieved through the following contributions:

1. The development of a sensitivity analysis (SA) methods for quantitative energy assessment models, evaluating the relevance of the different inputs in the energy audit process. This SA method can be used by energy auditors to select a calculation model based on the quality of information available and the appliance types in a given building in order to minimize the likely error in the calculation of small power consumption. Although the method proposed is conceived for the specific field of small power load calculations, it could be applied to other areas of energy auditing or areas of building services where a formal sensitivity analysis is required.
2. The performance of a comparative case-study for top-down and bottom-up metering techniques at different levels of energy analysis, providing new strategies for improving data analysis and proposing alternative ways for presenting and interpreting small power energy profiles.
3. The provision and testing of a statistical extrapolation method for aggregated energy estimation to calculate the relation between the number of appliances monitored and the accuracy obtained in the estimation, along with the probability of overestimates or lower estimate energy assessments, depending on the percentage of appliances monitored. This method is created to inform energy auditors about the level of metering infrastructure

needed according to the level of inaccuracy they are willing to accept for their energy estimations.

4. Testing of alternative methods for load status detection using practical case studies to demonstrate the capabilities of NIALMs and to inform about further research lines that should be followed for the efficient usage of these methods in small power energy estimations.
5. The provision of a significant contribution in the knowledge field of electrical signature with the goal of enhancing the implementation of NIALM methods in energy audits, depending on the appliances under monitoring and the signature that best identifies them.

1.4.1 Publications

The outcomes and findings of the research presented in this thesis are being disseminated through the following publications:

Peer review conference papers:

- Rodriguez, A, Potter, B, Smith, S T, Kiff, A. *Small power load disaggregation in office buildings based on electrical signature classification*, 2016 IEEE International Energy Conference (ENERGYCON). Leuven, Belgium.
- Rodriguez, A, Potter, B, Smith, S T, Kiff, A. *Sensitivity analysis for small power energy assessments under the TM22 audit framework*, CIBSE ASHRAE Technical Symposium 2017. Loughborough University, Leicestershire, UK.

Journal papers: (*In preparation for submission*)

- Rodriguez, A, Potter, B, Smith, S T. *Sensitivity analysis for small power energy assessments under the TM22 audit framework*, target journal: Energy and Buildings - *in prep* (from Chapter 3)
- Rodriguez, A, Potter, B, Smith, S T. *Comparative study of metering techniques for small power in office buildings*, target journal: Energy and Buildings - *in prep* (from Chapter 4)
- Rodriguez, A, Potter, B, Smith, S T. *NIALM performance for small load appliance identification based on electrical signature classification*, target journal: Power and Energy Technology Systems - *in prep* (from Chapter 5)

1.5 Thesis outline

The remainder of the thesis is structured as follows:

- **Chapter 2: Literature review** provides a critical evaluation of relevant literature on quantitative energy audits for office buildings with a focus on small power energy consumption and the challenges faced for its estimation. Identified gaps in the literature are stated in the conclusion of the chapter.
- **Chapter 3: Improving calculation approaches** describes the challenges coming from the information feed into the calculation models for small power energy estimations and proposes a sensitivity analysis method for overcoming and improving these sources of uncertainties.
- **Chapter 4: Improving metering approaches** tackles the challenges faced by the main monitoring techniques typically implemented in the measurement audit approach by identifying the most efficient monitoring strategy for auditing scenarios and improving

ways of analysing and presenting their information, facilitating the work of energy auditors and decision makers.

- **Chapter 5: NIALM performance for small load appliance identification** secures and describes the disaggregation capabilities that can be obtained by the different categories of electrical signatures and that could be used to create an optimal NIALM method depending on the types and number of appliances under monitoring.
- **Chapter 6: Summary and conclusions** summarises and concludes the contributions presented in this thesis and states new lines of research for future works.

Chapter 2

Literature review

This chapter provides a foundation that supports the research conducted in this thesis, it gives a critical evaluation of relevant literature on quantitative energy audits with a focus on small power energy consumption estimations in office buildings. The gaps identified in the literature are presented in the concluding section of the chapter.

2.0.1 Energy audits for buildings

The British Standard Institute (BSI) launched a publication in 2012 [29], that describes an *energy audit* as the “systematic inspection and analysis of energy use and energy consumption of a site, building, system or organization with the objective of identifying energy flows and the potential for energy efficiency improvements and reporting them”. The terms *energy audit* and *energy assessment* are being used interchangeably in this thesis because the latter is also widely accepted in the industry and appears in multiple publications and standards. In accordance with this definition, there are a wide number of energy audit/assessment methodology standards produced by different institutions and international organizations, such as: the Building Services

Research and Information Association (BSRIA) [30]; the Chartered Institution of Building Services Engineers (CIBSE) [6, 31]; the British Standards Institution (BSI) [29, 32]; the American Society of Heating, Refrigerating, and Air-Conditioning Engineers (ASHRAE) [33]; the International Standards Organization (ISO) [5]; and the British Department of Energy and Climate Change (DECC) [34].

All these standards agree that energy audits of buildings are a crucial tool to ascertain the efficiency of energy use in buildings and are the basis for any decision making for enhancing energy management. Some of them only constitute advice and guidance for undertaking audits, but others set out absolute requirements that have to be met if a user wishes to make a claim of compliance with the standard. The definitions provided by those standards for *energy audits* also vary significantly, depending of the level of detail and human skills required for their implementation. A simple preliminary audit, based on energy invoices, can be performed with basic information and little specialist knowledge about energy. An improved audit, on the other hand, often requires records of sub-meter readings and/or the performance of an on-site survey, while a full audit requires detailed information and expertise to break down energy end-use on an individual system basis [35].

The following sections critically evaluate the research efforts and applications concerning energy audit/assessment for existing buildings by focusing on two critical aspects: the assessment performance criteria; and the method used to quantify the energy use.

2.0.2 Energy performance assessment criteria for existing buildings

Environmental assessment schemes for buildings, including an assessment of the efficiency and effectiveness of the use of energy in buildings are based on *performance* and/or *feature specific* energy assessment criteria [3]. For the former, credits are awarded according to the performance

level measured against established performance indicator benchmarks and the final score graded according to the total awarded credits of all items assessed. For the latter, credits are awarded when criteria of specified features are met and the final score graded according to the total awarded credits of all items assessed [36].

Feature-specific criteria, although more easily implemented, are less realistic as the presence of the targeted features in a design does not necessarily mean that corresponding energy targets would be achieved in practice. Lombard et al. [8] provide an overview of this and others energy certification schemes issues in buildings. The use of performance-based criteria, on the other hand, is much more precise as it is based on quantifiable performance indicators that can provide the relevant information to allow improved energy performance in buildings. Poel et al. [37] conducted a number of performance-based assessment studies for existing buildings in several European countries and provided the owners with specific advice for implementing energy efficient measures.

2.0.3 Quantitative energy audit approaches

Quantitative energy performance-based assessment methods are the process of determining the amount of energy use or energy performance indicators of a given building based on the information collected. Utility bills, building audit data, end-use sub-metering systems, central monitoring systems, and computer simulations are the most common energy data sources used to quantify building energy uses in audit according to several relevant authors [8, 20, 38, 39].

Regarding the energy data source undertaken, Swan and Ugursal [3] presented a review of the research and applications of quantitative energy audits to propose a framework to classify the energy quantification assessments into three approaches: calculation-based; measurement-based; and hybrid methods, the latter being a combination of the former two. This classification

was later considered and reviewed in recent energy assessment surveys and research [4, 11, 40]. The *calculation approach* is based on algorithms that can be implemented into complicated dynamic simulations [41], or simple steady-state models [42]. All calculation models have three common implementation stages: gather the input data from the influential factors; perform the calculation algorithms; and deliver the relevant information or performance indicator [18].

Collection of adequate information, however, can at times be challenging with many sources of inaccuracy. This is because input factors are subjected to many sources of uncertainty and this imposes a limit of confidence in the response of the model. This issue is addressed in a pilot study carried out by De Wilde [21] to assess the so-called ‘performance gap’ between the actual monitored energy use and the calculation model predictions, the study highlighted how uncertainty in input data affects the accuracy of the information delivered.

In the *measurement approach* the input information is obtained by monitoring at different levels of detail and granularity, from a simple energy bill [40] to detailed end-use sub-metering [7]. Some monitoring techniques (also called *Hybrid approach*), based on energy bills or on central meters, are a low-cost combined strategies which implement a calculation model to split energy by end-uses. However, this type of break-down of energy use can be very unrealistic and, as they are based on assumptions, they involve the same type of issues as the Calculation approach. Therefore, the accuracy of disaggregated consumption at system level has a high level of uncertainty.

In contrast, sub-metering based monitoring techniques offer profuse performance information of great use to auditors and for building maintenance. However, and according to relevant literature [8, 43, 44], this techniques also comes with its own disadvantage, i.e., the complexity of the metering infrastructure as each system needs to be monitored individually and this makes the method expensive and intrusive.

2.0.3.1 Small power in quantitative energy audits, the challenge

Small power refers to any electrical device which plugs into a socket and is distributed throughout a building. This definition excludes large systems used for heating, ventilation, cooling, water heating, and lighting which are directly connected to the mains [45].

Small electrical power loads constitute a significant part of the total energy use in buildings, office equipment being the fastest growing energy use within commercial buildings [6]. As buildings become more energy efficient, small power appliances become a more significant source of energy end-use [16], accounting for more than 20% of primary energy used in commercial buildings in the U.S. This percentage is expected to increase by 40% in the next 20 years [46], and in the UK it is expected to reach up to 50% in highly efficient offices [15]. This trend makes small power loads in commercial buildings one of the fastest growing load categories [14].

Small power consumption in office building needs, therefore, to be carefully considered when performing energy audits in these buildings. However, due to their heterogeneous electrical nature and larger number they represent a challenge for both quantitative energy estimation approaches.

For the *calculation approach*, small power energy estimation relies on inputs from occupancy profiles (in [47] a model for estimating peak small power equipment loads in UK office buildings based on occupant density was suggested), and the type of activity performed (in [48] the impact of office productivity and cloud computing on energy consumption was analysed). This makes energy estimations very complex and time consuming for auditors, who will rely on assumptions based on their personal experience and benchmarks that can be outdated, which will make these estimations unreliable. Research conducted for small power energy consumption in UK office buildings highlights the deficiencies of the benchmarking provided by CIBSE Guide F [49], largely used in calculation methods.

The *measurement approach* is considered an effective strategy for estimating small power energy consumption in quantitative audits [50]. The accuracy of the metering techniques is correlated with the complexity and the level of metering granularity where high levels of metering infrastructure provide performance information of great use to auditors and for building maintenance, particularly at individual appliance level. However, large monitoring complexity usually makes the monitoring expensive, intrusive, and difficult to manage. Kamilaris et al. [13] conducted a literature review survey on the state of the art regarding work performed related to electric energy consumption for small powers in office and commercial buildings, and revealed the complexity of the current techniques used for measuring the energy consumption of office plug loads. Although the overall impact of small power loads in total energy estimations has great relevance for the assessment of energy consumption in office buildings, there is a lack of practical studies investigating the implementation of the different energy audit approaches for small power energy estimation, especially in non-domestic buildings.

2.1 Calculation models for energy audits

A typical model used to calculate building energy is comprised of three elements: inputs (influential factors); calculation algorithm; and outputs (energy performance indicators). It is the calculation algorithm used that will determine the types of inputs required and, consequently, the outputs provided. Accordingly, calculation-based models can be classified as dynamic and steady-state [20]. The former, often adopted for detailed simulations, are capable of capturing buildings' influential dynamic factors, such as thermal, systems, etc [41]. Meanwhile, in the latter models the dynamic factors are ignored or simplified by correlation factors, this greatly decreases the calculation complexity [42].

One of the primary sources of uncertainty for models which calculate building energy is the

input factor specification; this relates to the degree of uncertainty around each input parameter and is often disregarded during the audit process, particularly in the case of input factors for small power due to their variability and large number, leading to questions over the accuracy of the model outputs [51]. Different research in the field [15, 47] has conducted energy surveys in UK offices where small power equipment loads were estimated using a calculation approach. These studies concluded that the final small power calculations led to significant overestimation of the current loads and this impacts other system energy consumption estimations.

2.1.1 Sensitivity Analysis for energy audit

According to Satelli et al [52], Sensitivity Analysis (SA) is the study of how variation in the response of a model can be apportioned to different sources of variation by the information with which it is fed. In this way, a SA approach can be adopted to identify which of the uncertain input factors is more important in determining the uncertainty of the output of a model and, therefore, which input uncertainty should be chosen to reduce the most uncertainty of the output.

Modellers and practitioners from various disciplines, such as economic science [53], environmental science [54], computer science [55] and energy assessment models in building [56], have made use of some kind of sensitivity analysis method to analyse the quality of their model-based studies.

As stated by Coakley et al. [20], the built environment presents a complex challenge in terms of energy modelling and accurate prediction. Any given building is characterized by a multiplicity of parameters, including: material properties; occupancy levels; equipment schedules; plant operation; and weather conditions, among others. Such parameter diversity results in a wide range of different sources of uncertainty, however, few published case studies incorporate this work in their analyses [57–59].

For small power loads, the high dependence of energy consumption on end-use behaviour [19], makes their specific input extremely variable and case dependent. However, no practical studies have been undertaken for small power energy calculation methodologies.

2.1.1.1 Sensitivity analysis classification

The first registered science review of SA methods was undertaken by Rabitz et al. in 1989 [60], and they argued that SA tools could play an increasingly important role in understanding and finding solutions to complex, chemically based problems. A few years later, in the 1990s, Hamby et al. [61] presented a comprehensive review of more than a dozen sensitivity analysis methods. Their review was undertaken from the simplest approach, one which requires varying parameter values applied one-at-a-time to partial differentiation sensitivity techniques, along with correlation analysis used to determine relationships between independent and dependent variables. More recently, Satelli et al. [62] proposed a new taxonomy, later undertaken by other researchers [63,64], for the classification¹ of the different SA in three categories.

Local SA which examines small perturbations of the input space, typically one variable at a time (OAT), investigating the local response of the output function to variation in its input parameters. This analysis is done by computing the partial derivatives [65] (in various order) of the output with respect to that factor to obtain a sensitivity ranking. The term ‘local’ refers to the fact that all derivatives are taken at a single point, known as a ‘baseline’ or ‘nominal value’ point, from the hyperspace of the input factors. Although the method is relatively simple and well established, it does not provide insight into how the interactions between input parameters influence the output, thus it is not the best option when comparing various input factors with different magnitude ranges.

¹This classification is arbitrary and its only purpose is to provide a justified, ordered presentation of the different SA methodologies. However, alternative taxonomies can be used.

Global SA is where the input parameters are varied simultaneously and the sensitivity is measured over the entire range of the input space. Global SA methods are based on the affirmation that the exploration of a number of specific data points, judiciously chosen from the hyperspace of the input factors, is more effective, in the sense of being informative and robust, than derivative values estimated at a single data point at the centre of that space, as is the case in local SA [66].

Variance-based sensitivity analysis, also called the Sobol method [67], is a common form of global SA in which the variance of the output of the model is decomposed into fractions attributed to the different inputs. This is a good option for models where various input variables can be affected by uncertainty of different orders of magnitude, as is the case in MT22 calculation models. However, the method is more complex than local methods and comes with a larger computational cost².

Screening SA methods are based on the experience that often only a few of the input parameters have a significant effect on the model output. They are considered to be qualitative SA methods as they rank the input factors in order of importance, but do not attempt to quantify relative importance. The simplest and most common approach of screening SA is that based on an enhanced OAT methodology. The practice of reverting to the baseline point in order to compute any new effect is what makes for the poor efficiency of a typical OAT method. An improved OAT method would be one where having moved one step in one input factor, that factor is kept while the next factor is also moved, and so on until all factors have been moved one step each. This type of trajectory is presented as ‘Elementary Effects’ (EE) in Campolongo et al’s research [68], where the use of the EE analysis method is proved to work as a global analysis at the cost and complexity of a local one.

²Computational cost is defined as the number of times that the model has to be evaluated.

Morris' method is a common example of screening SA [69]. For the implementation of the method, the EE of each input factor is calculated following the OAT approach, but it randomly samples points from the whole input hyperspace. In this way the method provides an unbiased estimation of the direct impact of each factor and of their interfactor interaction by the evaluation of the mean μ and standard deviation σ of their EE distribution. The Morris method is an established SA with applications in different fields [59, 70], however, its implementation in energy audits remain limited and have not been fully analysed.

2.2 Measurement techniques for energy audits

A number of measurement techniques for energy assessment in existing building were found in the literature analysed, ranging from bill-based methods to individual plug meters to monitor methods. Such as the case study conducted by Yan et al. [71] based on two existings buildings, where the total energy consumptions from energy bills was effectively disaggregated into the consumptions of three groups of end-uses (i.e., the HVAC, internal-consumers and other-consumers). Lanzisera et al. [72], on the other side, used 455 wireless plug-load power meters, obtaining a detailed data collection of the small powers from a case study office. Other techniques use diverse levels of metering granularity, such as Menezes et al. [73] that monitored a number of typical individual small powers for obtaining an appliance type load through extrapolation; or Amenta and Tina [74], that proposed an individual load demand disaggregation method based on electrical load specific features using only a few meters, introducing the potential benefits of Non Intrusive Appliance Load Monitoring (NIALM) techniques in real scenarios. All these measurement techniques obtain their input information from monitoring at different levels of detail and granularity and can, therefore, be classified according to this.

Swan and Ugursal [75] introduced a classification for the energy consumption estimation strate-

gies of the residential sector into two main categories based on the reference to the hierarchal position of data inputs. This classification, reviewed years later by Grandjean et al. [76], established a finer segmentation of the available strategies into two categories, the *top-down* technology based and the *bottom-up* technology based. The former considers the aggregated energy consumption and then identifies the contribution of each considered end-use unit, and the latter uses input data from a lower hierarchal level and then extrapolates them to obtain the electricity consumption at a higher level. Although this classification was intended for the domestic electricity sector as a whole, Wang et al. [3] adopted this conceptual framework for measurement based quantification techniques.

The following sub-section presents the top-down/bottom-up classification applied to measurement techniques, from the simplest energy bill to the detailed end-use sub-metering and monitoring, stating their weaknesses when dealing with small power energy estimations.

2.2.1 Top-down

Top-down techniques, need to be combined with calculation models to disaggregate total energy consumption into end-use. To perform energy monitoring, dedicated hardware needs to be deployed in the main electric distribution board, in specific branches or circuits, depending on the area to be monitored. Popular commercial meters for implementing top-down monitoring are the ZEM-30 Energy Monitor from Episensor [77] and the TED Pro from TED [78].

In the top-down approach developed by Field et al. [43], the total energy bill is broken down into individual energy end-use. For the calculation of each type of end-use, input parameters, such the rated electrical load, the electrical load factor, the usage pattern, and the usage factor, were collected. A large discrepancy between the aggregated end-use calculated and the total metered consumption was found in the study, indicating larger uncertainty in the collection of

these parameters. This measurement technique offers aggregated energy profile information with a relatively low metering infrastructure complexity. However, the lack of detail regarding the energy consumption of individual end-uses eliminates the capability for the identification of key areas for improvement in the reduction of energy consumption. This problem becomes more pronounced for small powers where the input information largely depends on the usage patterns (e.g., usage factor, time schedule) which are based on assumptions and benchmarking [38] and, therefore, cannot be used to guarantee the accuracy of the breakdown estimations.

2.2.2 Bottom-up

Bottom-up techniques offer information at the individual system level by placing separate metering hardware on each relevant circuit branch or on individual equipment. Smart power outlets, or smart plugs, represent typical appliance level energy monitoring. These meters stand in between the wall socket and the electric appliances to measure their consumption and control their operation. Popular products in this category are Energy Hub Socket from Energy Hub [79], Watts-Up PRO [80] and 4-noks [81].

Ridi et al. et al. [82] carried out a survey on intrusive load monitoring. The survey consists of measuring the electricity consumption of one or a few appliances using a low-end metering device located close to the appliance that is being monitored. Their review concluded that this measurement technique has the capability to provide accurate, detailed information about energy use at the individual system level and, in doing so, can identify specific areas for improvement. However, the implementation of device-level monitoring in buildings can be very complex and intrusive, particularly when monitoring small powers, and is usually considered to be too expensive for practical application in common buildings [83].

2.3 NIALM: Alternative measurement method for energy audits in commercial buildings

Calculation approaches for small power energy come with a certain level of uncertainty associated with the input factors. The measurement approach seems to solve some of these problems to a certain degree, especially when using a large sub-metering infrastructure, however, they can be very difficult and expensive to implement due to the large degree of intrusiveness and complexity. In contrast, Non Intrusive Appliance Load Monitoring (NIALM) methods, presented in this section, constitute a simpler and less expensive alternative technology for overcoming these weaknesses, and are of particular interest in the case of small power energy estimations. NIALM methods basically apply a single, centralised hardware to monitor aggregated electricity consumption, which is then disaggregated into individual circuit/device levels from the overall signal [13]. These kind of energy disaggregation methods were first developed by George Hart [27]. In his early publications, Hart presents a method based on steady-state power metrics to describe the power draw of home appliances. The method strategy relied on the fact that when an individual appliance changed its state from off to on, the change would be unique to the mentioned appliance. Following Hart's work, many prestigious institutions and independent researchers, along with Hart's research group at the Massachusetts Institute of Technology (MIT), continued to develop non-intrusive monitoring strategies by exploring the diversity in signatures and the disaggregation methods used for identifying appliances [84–86].

Previous research in the field has mostly focused on residential buildings where NIALM methods have been reported to work well. For instance, Marceau and Zmeureanu [87] presented a NIALM method to disaggregate the total electricity consumption of a house where only the main electric entrance was monitored and three major end uses (water heater, baseboard heater,

and refrigerator) were disaggregated, obtaining an error of less than 10%. Park [88] developed a NIALM method to disaggregate the power consumption of a few typical small appliances in residential buildings based on an algorithm which includes a switching function, a truth table matrix, and a matching process. The methods obtain very good results for the appliance under monitoring, but continuous variable appliances and identical power consumption appliances were not disaggregated, possibly due to the low sampling frequency used (one minute).

Although the potential benefits of applying this monitoring strategy to commercial buildings have been recognized since the field's conception, in the commercial domain NIALM has been largely unexplored by the academic community. This is a result of the larger heterogeneity and the number of building facilities involved, particularly if small power is also to be considered. According to Batra et al. [28], most of the NIALM methods made for residential purposes cannot currently be applied to commercial buildings.

Most of the work applied to energy disaggregation in commercial buildings was completed at MIT [89, 90], where researchers have presented approaches to disaggregate a set of large end use consumers, such as chillers, fans, pumps, and different HVAC loads. However, significant research for small power disaggregation in commercial buildings has not yet been undertaken. A typical NIALM method has four stages of implementation. Firstly, a monitoring hardware installation is used to obtain a signal; secondly, an event detection algorithm is implemented to detect on/off switchings; then, signal processing techniques are used to identify and extract electric signatures; and finally, a disaggregation algorithm is used to separate individual appliance loads from the overall signal [26, 91].

The following sub-sections provide relevant background to these four stages of implementation in order to identify the main gaps and challenges that prevent the extensive use of NIALM methods in commercial buildings, and with a special interest in small power disaggregation.

2.3.1 Monitoring hardware

The role of the monitoring hardware is to acquire the aggregated load measurement at an adequate sample frequency rate to capture the key load patterns and characteristics. In [92] 260 papers and reports related to the electric energy consumption for small powers in office and commercial buildings were reviewed. The review concluded that NIALM techniques have advantages compared to intrusive sub-metering as they are easier to install and maintain and data acquisition is simpler. Also, although intrusive meters are typically based on cheaper meters, their cost scales linearly with the number of sensors. NIALM techniques constitute a cheaper alternative by applying single centralized sensing hardware for monitoring aggregated electricity consumption in a facility/area. Data gathering for NIALM methods implementation are based on top-down metering techniques, and can, therefore, use the same type of monitoring and hardware (e.g., ZEM [77], TED [78], etc). Bergues et al. [93] introduce the use of NIALM techniques for enhancing electricity audits in residential buildings and compare it with the traditional bottom-up metering techniques at the plug-level, resulting in a 14.8% error for the NIALM system when disaggregating the 17 appliances targeted in the subject home.

Several literature surveys related to NIALM methods [46, 82, 85] concluded that hardware with higher sampling frequency increases accuracy in disaggregation results as more detailed signal information is available, thereby allowing the use of frequency-based signatures that are especially useful for appliances with similar power consumption rates. However, the time and hardware to complete the processing increases with the sample rate frequency and the equipment for such systems is more costly [94].

According to the surveys reviewed, NIALM methods can be divided into two groups with regard to the monitoring hardware used for their implementation, i.e., *Low frequency hardware* and *High frequency hardware*.

Low frequency hardware installation is implemented by using inexpensive systems. This kind of hardware only allows the detection of macroscopic electrical signatures registered in the amount of power drawn and in consumption patterns. Barasli et al. [95] developed an algorithm using clustering methods and a generic algorithm that identifies appliance use by optically reading the existing domestic meters every few seconds. This algorithm needs to be run for between five to ten days to find patterns and identify individual appliances. The authors successfully detected major domestic loads, such as refrigerators and cookers, although it was left to the user to name the identified loads. However, as the electrical grid in the UK runs at a 50 Hz cycle, to capture a basic wave shape a minimum of 100 Hz sample rate would be required, according to Nyquist-Shannon theorem [96].

High frequency hardware installation (from 1 kHz up to 100 kHz) is usually more expensive than low frequency hardware, it focuses on microscopic signatures based on harmonics and waveforms. In [97] the authors develop a NIALM method to disaggregate residential appliances based on noise capture in the power line. This approach, which requires high-frequency sampling (from 100 Hz to 100 MHz), recognises devices by their spectral fingerprint. The goal of the research was to detect the event in the home, rather than to monitor energy use. The authors demonstrated an identification accuracy of 85% to 90%, although only during a single switching event, not when more than one appliance switched state simultaneously or in quick succession. According to Armel [98], 1kHz can be considered a suitable sample rate for harmonic analysis, for a higher sampling rate data transmission and storage problems are likely to occur and for frequencies higher than 15 kHz the noise captured is likely to obscure any gains in signal detection for commercial buildings.

2.3.2 Event detection

In [99] an overview of the methods used in the NIALM system is presented and categorized into event-based or non-event-based methods. The event-based method uses an edge detection algorithm on the power consumption curve to detect the appliances when a change in the curve occurs, e.g., on/off switchings. Most research works in the literature use event-based methods. Anderson et al. [100] used the power metric to select an event detection algorithm in their NIALM implementation, and Milioudis et al. [101] present an event detection novel methodology to improve the disaggregation process in NIALM methods.

Non-event-based methods, on the other hand, implement a multi-scale edge detector algorithm that continuously samples the aggregated data for inference. Few works have been conducted using non-event-based methods. The Hidden Markov Model in [102] is an example of non-event detection. The approach presents the potential to increase the efficiency of domestic electricity load identification.

Non-event -based methods have the advantage of not needing an initial training period, however, event-based methods are more computationally efficient, therefore, they are more commonly used within NIALM applications. Event-based methods allow the definition of two types of operational states: the *steady-state* and the *transient-state* [103]. The former derives from the equilibrium operational conditions between events in which the waveform is periodic, and the latter from the transitory operational event in which a short-lived burst of energy is produced during the start-up period. Some researchers focus on the identification of steady state electrical signatures [27, 104], others concentrate on the transient signatures [96, 105], while a significant number use a combination of the two [106, 107].

The steady and transient operational states can also be detected in both the *time domain* and the *frequency domain*, as stated in several related surveys [108, 109]. The former shows how a

signal changes over time, and the latter how much of this signal lies over a range of frequencies. A signal can be converted between the time and frequency domains with a pair of mathematical operators: the *Fast Fourier Transform* (FFT), which converts the time function into a sum of sine waves of different frequencies; and the *Inverse Fast Fourier Transform* (IFFT), which converts the frequency domain function back to its corresponding time function [110].

2.3.3 Electrical signature

The term *electrical signature* refers to a specific signal feature that characterises the behaviour of the load. These signatures are measurable parameters of the load that provide information about the nature of individual appliances [111]. They can be classified depending on the operating status and, among those, the domain in which they are detected.

The steady-state analysis makes use of features derived under the steady operation state of the appliances and their differences or changes with respect to the next steady state. The variations can be related to the current, the active and reactive power, the load admittance, the harmonic content, etc [108].

Hart [111], the first to develop NIALM methods, describes a method based on steady state increments in the time domain of real and reactive power signals of home appliances. The method involves the identification of real and reactive power increments between consecutive steady states. Although the method constituted an important advancement in the field of electrical signature detection, it presents some significant issues, such as its incapacity to detect load-variable appliances and distinguish between appliances that operate between similar power values.

To overcome the difficulties distinguishing between appliances that operate between similar power levels, harmonics can be used as a complementary signature to complement load identifi-

cation. Harmonic analysis can detect numerous appliances, including variable loads, however, high sample rates are required [112]. According to the Nyquist sampling theorem, the sample rate needs to be more than twice the frequency of the harmonic that is to be captured [85].

Srinivasan et al. [113] have developed a NIALM method that applies the Fast Fourier Transform algorithm (FFT) to extract current harmonics of appliances in their steady state. The method proposed by Srinivasan et al. achieved an average classification accuracy of 85%. However, a long training period is required as all possible ON/OFF operation combinations among the appliances need to be previously learned by the method. When the number of appliances increases, the combination of ON/OFF states increases exponentially and so do the training patterns needed. More recent research [114] has improved this training period by combining the analysis of the steady state current harmonics with the rate of change of the transient signal. This method, developed by Meehan et al., senses when an appliance switches *on* and *off* and uses a two-step classification algorithm to identify which appliance has caused the event. In the first step, once an event has been detected, the difference in the steady FFT harmonic amplitudes before and after the event is found, then the first three harmonics are selected for the calculation of the feature.

Several reviews [85, 108] stated that most of the appliances observed in the field have partially, or completely, repeatable transient profiles due to their unique physical characteristic(s) in terms of what transient signatures can be considered for load identification. The transient behaviour is found to have a smaller overlap in comparison to steady state signatures, their major limitation being the high sampling rate required for their capture.

The MIT group, led by Leeb and Norford, has extended the basic NIALM method proposed by Hart by the incorporation of transient signals in the time domain [90]. The researchers observed that the shape of transient events can be used as a feature for appliance detection.

Later researchers [115] have contributed to this sighting by using power spikes, or overshoots, during the transitional stage of the device as a feature for its detection.

Transient signatures in the time domain are used in many of the NIALMs methods with, or in combination with, others types of signatures. The most commonly used signatures for representing the shape of switching transients are wave spikes, these can be represented in different ways: Crest Factor ($CF = I_{peak}/I_{rms}$); Form Factor ($FF = I_{rms}/I_{avg}$) and Peak-Average Ratio ($R_{pa} = I_{peak}/I_{avg}$) [107] or the duration of the peak in time [116].

In [117], transient signals for harmonic analysis are considered for load identification. In this experimental study, the authors used the third-order harmonic content to discriminate between a computer and an incandescent bulb.

An extension to harmonics is the spectral envelope which is a collection of the first several coefficients of the short-time averages of the FFT applied on a signal [118]. However, although the spectral envelope can detect numerous appliances, including variable-load appliances, the method suffers from several drawbacks and the performance regarding accuracy on load identification has not been characterised for many practical scenarios [26].

The different electrical signatures for the event-based NIALM methods reviewed in this section can be classified under the proposed framework in Figure 5.5.

2.3.4 Machine learning techniques for load disaggregation

The last stage in a NIALM method is the implementation of a disaggregation algorithm to separate individual appliance loads from the overall signal. There are many types of disaggregation algorithm that can be clustered under the umbrella of machine learning methods. Machine learning, in the context of data mining, explores the study and construction of algorithms which

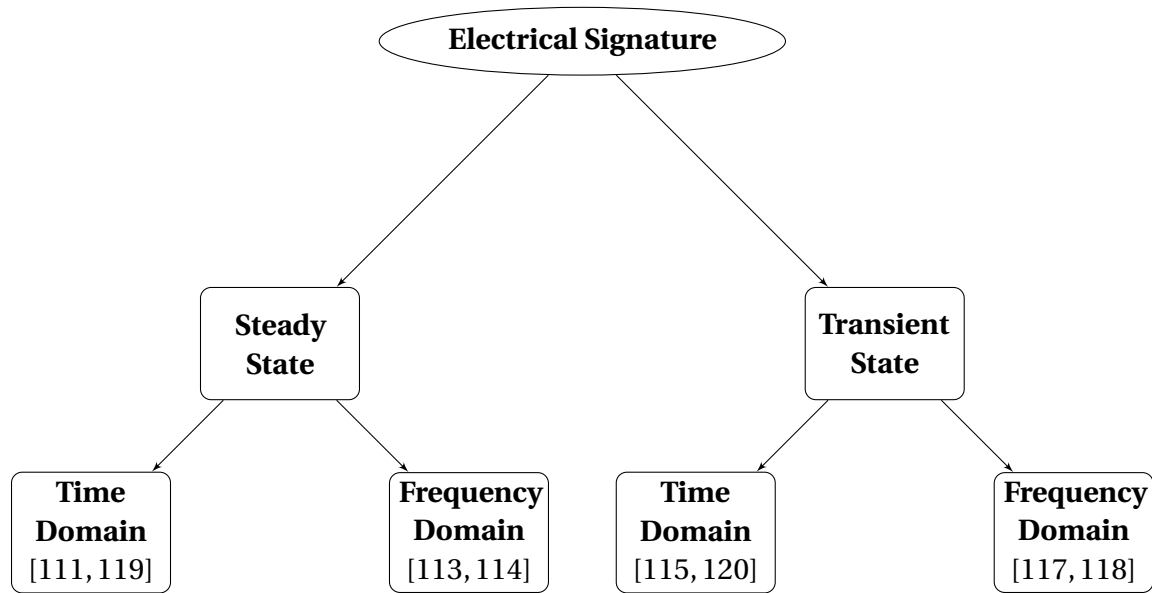


Figure 2.1: Proposed electrical signature classification

can learn from and make predictions on data. According to the literature [84, 99, 121–123], machine learning methods can be divided into two main groups, supervised and unsupervised learning techniques.

Supervised machine learning techniques require labeled data for training the classifier so that it can recognise the appliances from the aggregated data. The extracted features are matched with a database of load signatures already available in order to identify an event associated with an operation of an appliance. The goal of supervised machine learning techniques is to approximate the mapping function, $Y = f(X)$, between input variables, (x), and an output variable, (Y), so that a new input data, (x'), can be predicted from the output variable, (Y'). This prediction can be based on optimization methods which minimise the *error function*³ by systematically choosing input values or by pattern recognition methods which recognise the patterns and regularities in the input data [84].

³The *error function* defines the difference between the real and the predicted data.

Supervised learning problems can be further grouped into regression problems where the output variable is numerical or quantitative, such as the size or the temperature value and classification problems, and where the output variable is categorical, such as “yes” and “not”, or “green” and “blue”.

Unsupervised machine learning techniques, on the other hand, do not require any previous training, so the need for data training can be eliminated. Unlike most of the supervised load disaggregation approaches, the unsupervised methods are non-event-based. The goal for unsupervised learning techniques is to model the underlying structure or distribution function, $f(X)$, of the input data, but in this case without knowing the corresponding output variable, (Y) .

Unsupervised learning problems can be further grouped into clustering problems where the goal is to discover the inherent groupings in the data, such as grouping customers by purchasing behaviour and associated problems, where the goal of the rule learning is to discover rules that describe large portions of the data, such as people who buy X also tend to buy Y.

In [44], an unsupervised approach to determine the number of appliances in the household is proposed. The method creates clusters of the steady-state power consumption of the appliance changes and then employs a matching algorithm to reconstruct the original power signals using them. The method was successful when disaggregating large appliances, but presented difficulties with the small ones.

In [124] the temporal ordering implicit in on/off events of devices to uncover *motifs* (episodes) corresponding to the operation of individual devices are extracted and then subjected to a sequence of constraint checks to ensure that the resulting episodes are interpretable. The preliminary results of the study showed the capabilities of the model in distinguishing devices with multiple power levels.

There is no leading machine learning technique due to the variability of the sets of appliance

categories, the different types of measurements, sampling frequencies, and feature selections. Most machine learning approaches, nevertheless, are based on supervised techniques and few unsupervised techniques are reported for NIALM tasks. In [13] supervised and unsupervised NILM techniques are compared, results show the former to be more accurate with errors around 2-5%, while the latter are less accurate (5-15% errors). The use of unsupervised methods can, therefore, be explored for residential environments where there are usually only tens of different loads with predictable signatures, but these methods do not seem appropriate for commercial buildings.

2.3.4.1 Algorithms for supervised machine learning

Algorithms for supervised machine learning can be divided into parametric and non-parametric algorithms, according to the degree of assumptions taken in the learning process [125]. In the former, assumptions about the learning process are made and these can greatly simplify the learning process, but they can also limit what can be learned. Non-parametric machine learning algorithms, on the other hand, do not make strong assumptions as they are free to learn any functional form from the training data. Non-parametric methods are often more flexible and achieve better accuracy, but they require much more data and training time. Examples of non-parametric algorithms include Decision Trees, Naive Bayes and K-Nearest Neighbors.

The Decision Trees algorithm performs classification in two initial phases and is evaluated in a third one. The first phase is the tree building, or growth phase, in which the tree is built by recursively splitting the data into two or more branches. The value of splitting points depends upon how well separated, or “pure”, the differences are between appliance signatures [121]. In the second phase, or tree pruning phase, the algorithm keeps growing by splitting nodes as long as the new splits increase the branches “purity”. The process makes use of the training

data set for optimisation, by eliminating any leaf that increases the error rate⁴ [126]. Finally, in the performance evaluation phase, once the tree is fully grown and then pruned, the decision tree model can be used to predict the class value for new patterns. In the evaluation stage, the prediction accuracy of the decision tree classifier is evaluated using the training data set. The *10-fold cross-validation* and the *leave-one-out cross-validation* are standard validation methods [127]. Decision tree algorithms are fast at learning and making predictions and can achieve high levels of accuracy for a broad range of problems without the requirement for any special data pre-processing, thus providing high transparency within the classification process. In [128] a building energy demand predictive model, based on the decision tree method and which is able to classify and predict categorical variables, is developed. The advantage of the model over other widely used modelling techniques lies in its ability to generate accurate predictions with interpretable flowchart-like tree structures that enable users to quickly extract useful information. The method has been applied to estimate residential building energy performance indices by modelling building energy use intensity levels. The results demonstrate that the use of the decision tree method can classify building energy demand loads accurately, at 93% for training data and 92% for test data.

Naive Bayes are statistical learning algorithms for predictive modelling comprised of two types of probabilities that can be calculated directly from the training data [129], the probability of each class and the conditional probability for each class given each input value.

In [130], a naive Bayes classifier was used to detect state change and identify individual devices. The approach assumed that each device's state was completely independent of the other devices, so that devices such as TVs and DVD players, with their highly-correlated operation, were difficult to disaggregate. Naive Bayes methods are called naive because they assume that each input

⁴The error rate is a measure of the number of wrong predictions.

variable is independent, this assumption is often unrealistic for real data.

In a K-Nearest Neighbors model predictions are made for a new data point by searching through the entire training set for the most similar K instances (the neighbours) and summarizing the output variable for those K instances. Saitoh et al. [131] reported on the use of the K-Nearest Neighbors model for the identification of 35 appliances sampled at 4.4 kHz from which nine current-based features were extracted. For each feature the observed values, or input variables, were normalised using the average and standard deviation and a disaggregation accuracy of 80.5% was achieved. To determine the similarity between values the Euclidean distance between each input variable was used. However, in very high dimensions (a great number of input variables), results can negatively affect the performance of the algorithm and require much memory space to store all the data. To reduce this dimensional problem, only the most relevant variables can be used, however, this will affect the accuracy of the model predictions [132].

2.4 Conclusion and literature gaps

In this chapter, a literature review of previous research relating to different quantification approaches for energy audits in buildings has been presented. Relevant concepts in sensitivity analysis theory and NIALM methods implementation along with different calculation models and measurement techniques have been discussed with a focus on how these concepts overlap with past research on small power load disaggregation.

Among commercial buildings, and especially office buildings, energy quantification shows that small power appliances are large electricity consumers. Understanding small power loads is therefore, a crucial factor to consider in order to improve estimation. However, current energy assessment approaches are not sufficiently accurate and NIALM techniques are not mature enough to overcome the issues that entail this challenge. This conclusion is supported by recent

field studies which have demonstrated the importance of reducing small power loads in office buildings [16] and how many issues remain open in this domain [13].

The methodologies used to quantify energy use in existing buildings can be divided into two broad categories or approaches, calculation and measurement approaches. Both approaches present significant weaknesses when dealing with small power load estimations, specially in non-domestic buildings. After a review of the relevant literature on quantitative energy audits, the gaps identified are presented below.

1. For calculation approach models, there is a lack of knowledge on how the variation in the output of a model can be apportioned to different input factor uncertainties, which imposes a limit of confidence in the energy estimations. Sensitivity analysis can be used to explore this impact, however, non of these analysis has been undertaken for the use of calculation models in small power energy estimations.
2. The measurement approach can be implemented through top-down or bottom-up technologies. For the former, there are not estimations strategies that can provide details of energy consumption of individual end-uses without drawing upon the use of calculation models and their associated input inaccuracies. And for the latter, there is a lack of experimental research for reducing the complexity of bottom-up techniques for obtaining aggregated energy estimation without significantly compromising the final output accuracy.
3. The application of NIALM methods in office buildings remains immature due to the larger number and heterogeneous nature of typical office appliances. The third stage of general NIALM methods, *electrical signature identification*, has been identified as one of the main reasons for NIALM not being used extensively in office energy audits, and even so, a

study of the most suitable set of signatures, depending on the electrical appliances under disaggregation, has not been yet undertaken.

These gaps are addressed by the work presented in this thesis in order to build upon existing methods, to overcome their weaknesses, and to improve the ways in which small powers energy consumption is estimated.

Chapter 3

Improving the calculation approach

3.1 Introduction

The review of energy calculation models, presented in Chapter 2, was concluded with identification of the gaps in the literature. One of those gaps is concerned with the challenge faced by energy calculation approaches when collecting adequate input information, particularly for small power loads which are highly dependent on end-use behaviours and a large source of energy consumption in office buildings. It has been encountered in the literature that one of the primary sources of uncertainty in all building energy calculation is the input parameters specification. This relates to the degree of uncertainty in the model output and raises questions about the accuracy¹ of the calculation model. Therefore, in order to gain a proper understanding of the influence of small power on energy estimations, it is crucial to determine sources of error in the model input information. This subject is the cornerstone of the research presented in this chapter. Consequently, a Sensitivity Analysis (SA) approach has been adopted which studies

¹For this research the sensitivity is evaluated over the entire space of inputs, so that, the metric used is the accuracy.

how the variation in the output of a calculation model can be apportioned to different sources of variation in the inputs.

There are a large number of calculation models currently in use in the UK industry based on CIBSE TM22 methodology [133–135]. This methodology offers a systematic way of undertaking an energy survey, reporting the results, and calculating likely savings from changes in use, technology, or management. It was developed from energy survey techniques used in office case studies and in the Probe series of published POEs in Building Services in the CIBSE Journal [22,31]. The guide report establishes three levels of assessment, from a simple to a system specific energy breakdown, depending on the input information provided to the model; it is the third of these which is applicable to the estimation of small power loads. As such, Appendix A presents the TM22 quantitative energy assessment framework and explains the type of assessment provided at each level.

This chapter undertakes a sensitivity analysis of four calculation models for small power energy estimation following the TM22 framework. The first three models are industry established calculation procedures [31, 136, 137], and the fourth, specifically created for this study based on relevant academic literature [133, 134] and industrial energy audit reports², addresses the issue of waste energy during working hours associated with user behaviour. In order to allow comparison between these models, the Morris method [69] was implemented and simulated in Matlab (R17, Mathworks). This SA method has been adapted to incorporate a number of modifications for better alignment to the CIBSE TM22 framework.

The study provides a tool that can help auditors to decide the optimal energy calculation model for each building scenario by better understanding the significance of the input information to their final energy estimations.

²This model has not be created to improve existing ones, but for extend the test of the sensitivity analysis method proposed in this chapter. Details of its design and characteristic will are provided in the methodology section.

3.1.1 Morris method

The Morris method [69] is a *Screening* SA method comprised of individually randomised Local SA methods; it evaluates the response of output to change in one model input at a time. The sensitivity of response to the model base line is also considered, with the method designed to reduce the number of local calculations or runs needed to accurately identify the most relevant input factors. In this way, the Morris method can be considered a sudo-global method with the relative simplicity of a One at A Time (OAT) method.

The method relies on the estimation of the elementary effects (e) for each of the randomly sampled points on the input space of experimentation (Ω). Assuming a number (k) of input factors, the input space can be described as $\Omega = X_1, \dots, X_j, \dots, X_k$ with each input factor having a uniform distribution in their set of values $X_j = (0, 1/(n-1), 2/(n-1), \dots, 1)$, where n is the set size and the range is from 0 to 1. The Elementary Effect (EE) for the i -th value (x_i) of the input parameter (X_j) is given by Equation 3.1:

$$e_{ji} = \frac{y(X_1, \dots, X_j(x_i + \Delta), \dots, X_k) - y(X_1, \dots, X_j, \dots, X_k)}{\Delta} \quad (3.1)$$

where:

$(X_1, \dots, X_j, \dots, X_k)$ are the initial values, or base-case, for the input parameters and $y(X_1, \dots, X_j, \dots, X_k)$ is the model output.

$(X_1, \dots, X_j(x_i + \Delta), \dots, X_k)$ is the perturbed sample, where the single value $x_i \in X_j$ has been modified by a perturbation Δ .

And $y(X_1, \dots, X_j(x_i + \Delta), \dots, X_k)$ is the model output after the perturbation, while all other input parameters remain constant. This perturbation or variation is a multiple of $1/(n-1)$ [52].

In order to detect the linear (OAT) and non-linear (global) effects, the method implements r evaluations of the EE for each of the input parameters (X_j) which are then used to calculate the

mean μ_j (Equation 4.7) and the standard deviation σ_j (Equation 4.6) of each input. In this way, the Morris method can be considered a combination of OAT analyses, that becomes *global* when its design considers the effect of all the input iterations.

$$\mu_j = \frac{\sum_1^r Fe_j}{r} \quad (3.2)$$

$$\sigma_j = \sqrt{\frac{1}{r} \sum_1^r (Fe_j - \mu_j)^2} \quad (3.3)$$

where $Fe_j = (e_{j,1}, \dots, e_{j,i}, \dots, e_{j,r})$ is the EE distribution function for input factor X_j .

The Morris method can be classified as a screen method, as such it ranks the input factors in order of importance, but does not quantify their absolute significance. This input ranking classification uses μ and σ as its estimation factors, satisfying the purpose of the research by isolating the most important factor from among a large number that might affect the model output. The Morris method is a well-established SA, with applications in many fields [59, 70], however, its implementation in energy assessment estimation remains limited and has not been fully explored.

3.2 Methodology: The adapted SA method

This section presents the modifications incorporated to adapt the Morris method to perform SA on TM22 calculation approaches for small power loads. It also provides an implementation methodology for this adaptation, along with an explanatory example for better understanding and interpretation of the method results.

The aim is to determine which input factors contribute most to the output variability in the TM22 calculation models, those that will, therefore, require additional effort to strengthen their accuracy.

3.2.1 Refinement adaptive measures

The application of the Morris method to evaluate TM22 energy calculation models has been enhanced by a number of adaptive refinement measures.

1. *Re-scale input factor ranges*: In the original method, the input factors considered are of uniform range, between $[0, 1]$, with their values assumed in the set $(0, 1/(n-1), 2/(n-1), \dots, 1)$. In TM22 calculation models, input factor ranges have different lengths and ranges of magnitude, thus two re-scaling input ranges are used to match the corresponding small power input factor ranges to the Morris method requirements.

Discrete input range: the initial continuous input range is stratified to create the new discrete one where the single input values are equally spaced between them. To do this, each of the input factors, X_j , are assigned a uniform distribution with lower, x_{jmin} , and upper, x_{jmax} , boundaries, and the sampling stratification, or subdivision, is performed in accordance with the established degree of freedom, n , with a constant distance between values of $\gamma = (x_{jmax} - x_{jmin})/(n - 1)$. The resultant new stratified range for the input factor X_j is: $(x_{jmin}, x_{jmin} + \gamma, \dots, x_{jmin} + i\gamma, \dots, \dots, x_{jmax})$, that can be represented by: $(x_{j1}, x_{j2}, \dots, x_{ji}, \dots, x_{jn})$, where x_{ji} is the *i*th-sample point for the *discrete input range* X_j .

Normalized trajectory range: the *discrete input range* is normalised to allow the use of the Euclidean distance for the calculation of the trajectory between two points. In order to re-scale the discrete input range to the range $[0, 1]$, and maintain a constant step

$\Delta = 1/(n - 1)$ between sampling points, as is required by the Morris method, the *feature scale* process is used. According to this process, the resulting *normalised trajectory range* for the input factor X_j is: $(\frac{x_{j1} - x_{jmin}}{x_{jmax} - x_{jmin}}, \dots, \frac{x_{ji} - x_{jmin}}{x_{jmax} - x_{jmin}}, \dots, \frac{x_{jn} - x_{jmin}}{x_{jmax} - x_{jmin}})$, that can be represented by: $(t_{j1}, \dots, t_{ji}, \dots, t_{jn})$, where t_{ji} is the *ith-sample* point from the *normalised trajectory range* X_j .

2. Morris' experimental design reduces the number of model evaluations needed by performing r evaluations of the elementary effect for randomly chosen sample points for each input factor X_j , resulting in a total *design-cost* of $\mathcal{O}(r * (k + 1))$, with k being the number of input variables [69]. However, this design does not guarantee equal probability sampling for each input factor and has been shown, in some cases, to give misleading information [68].

The proposed method overcomes this problem through a systematic evaluation of all the sampled points in the input experimental space Ω . This increases the computational cost of the new experimental design to be $\mathcal{O}(n * (k + 1))$, where n is the size of input range for each input parameter (k). This extra computational cost is not of significance to the study due to the improvements in cpu operational speed since Morris' patent for "Non-Intrusive appliance monitor apparatus" in 1989 [111], and the relatively low number of input parameters under consideration. This change provides equal probability sampling for each input factor.

3. *Standardise the elementary effect*: The differences, in terms of unit and magnitude, of the small power input factors are not considered in the original Morris method and this issue can lead to misinterpretation of results. To overcome it, Sin et al. [63] proposed the use of a non-dimensional standardised elementary effect (se). For the input

X_j , $Fse_j = se_{j1}, \dots, se_{ji}, \dots, se_{jn}$. This new elementary effect is calculated by multiplying each element ee_{ji} by an standardisation factor. This factor is obtained by dividing the standard deviations of the discrete input factor range values, $X_j = x_{j1}, \dots, x_{ji}, \dots, x_{jn}$, by the standard deviations of the output values obtained for each of those inputs values, $y_j = y_{j1}(x_{j1}), \dots, y_{ji}(x_{ji}), \dots, y_{jn}(x_{jn})$. According to this, the se for the i^{th} value of the discrete input factor range, X_j , is given by Equation 3.4:

$$se_{ji} = e_{ji} \frac{\sigma_{X_j}}{\sigma_{y_j}} \quad (3.4)$$

This SEE distribution re-scaling allows for comparison of common input factors across different calculation models.

4. *The monotonicity*: The use of the estimated mean μ , as calculated in Equation 4.7 to detect the overall influence of the input factors, could be prone to failing in the identification of a factor of considerable influence on the model. If the standardised elementary effect distribution of the input factor X_j , given by $Fse_j = (se_{j,1}, \dots, se_{j,i}, \dots, se_{j,r})$, contains both positive and negative elements, i.e., if the model is non-monotonic, some effects may neutralise each other, producing a low value for μ , even for an important factor. The use of the mean in the absolute value for the Fse_j , given in Equation 3.5, addresses the immediate problem, although it introduces another by eliminating the information contained in the sign of the effect [68].

$$\mu_j^* = \frac{\sum_1^r |Fse_j|}{r} \quad (3.5)$$

To attend to this issue, a new estimation factor ($\Phi_j = |\mu_j - \mu_j^*|$) which contains the in-

formation on the sign of the effect is proposed. This enhancement measure comes at no noticeable computational cost and allows the analysis of the monotonicity of the model, i.e., if Φ has a low value, the output function is monotonic, if it has a high value this indicates non-monotonicity.

5. *The skewness*: The difference between the median and the mean of the standard elementary effect distribution also contains relevant information, indicating the degree of dispersion (spread) and skewness in the data, and pinpointing outliers. In probability statistics, skewness is a measure of the asymmetry of the probability distribution of a real-valued random variable about its mean. In accordance with the notion of non-parametric, the skew for the input X_j is given by Equation 3.26.

$$\xi_j = \frac{\mu_j - m_j}{\sigma_j} \quad (3.6)$$

where μ_j is the mean, m_j is the median, and σ_j is the standard deviation for the se_j distribution.

3.2.2 Implementation methodology

The detailed methodology for implementation of the adapted SA method and interpretation of the results are provided in this section. This methodology is implemented in three stages:

1. *Specify the starting points for the model elements*: Input value matrix (Matrix X), Trajectories matrix (Matrix T), Base-case matrix (Matrix B) and Calculation model (Function Y).
2. *Perform SA in two separate steps*: OAT analysis and Global analysis.
3. *Results interpretation*: Representative sensitivity features and SA graph.

A mathematical explanation for each step of this methodology is presented in the following subsections.

3.2.2.1 Starting points

Assuming a system with k input factors: $X_1, \dots, X_j, \dots, X_k$, the probability density function of each of those factors is considered to be a continuous uniform range bounded by their maximum and the minimum values. These assumptions simplify the code and allow the coverage of the whole potential range of the values for each input parameter, giving the same probabilistic weight to each value.

The number of discrete points n , or sampling resolution, of each input range needs to be specified to establish the experimental space dimension or the number of 'levels' over which the variable can be sampled. More points result in a higher sampling resolution and therefore, in a better accuracy, but involve more calculations.

For the first stage of the implementation methodology, three matrices are created to define what is called the input space of experimentation Ω : Matrix X , containing the discrete input ranges; Matrix T , containing the normalised trajectory ranges for each input; and Matrix B , containing n random base-case scenarios for the k input variables, and a *Function* Y defined to represent the calculation model.

Matrix X [Eq. 3.7] is generated by dividing the range of each input factor into n intervals equally spaced by $\gamma = (x_{jmax} - x_{jmin}) / (n - 1)$, where x_{jmax} and x_{jmin} are the maximum and minimum values of the input factor X_j , respectively. The $(k \times n)$ dimensional matrix represents the region of experimentation, where the row sub-index i ($i = 1, 2, \dots, n$) indicates the value within an input range set, and the column sub-index j , ($j = 1, 2, \dots, K$), the input factor itself.

$$X = \begin{bmatrix} x_{1,1} & \dots & x_{j,1} & \dots & x_{k,1} \\ \dots & \dots & \dots & \dots & \dots \\ x_{1,i} & \dots & x_{j,i} & \dots & x_{k,i} \\ \dots & \dots & \dots & \dots & \dots \\ x_{1,n} & \dots & x_{j,n} & \dots & x_{k,n} \end{bmatrix} \quad (3.7)$$

To create Matrix T [Eq. 3.8], the *feature scaling* method is implemented to rescale the range of each input parameter (each column of Matrix X 3.7) to $[0,1]$, maintaining a step size of $\Delta = 1/(n - 1)$ between each input value. This $(n \times k)$ matrix generates a Euclidean space of trajectories for all the values of Matrix X 3.7, allowing the calculation of the Euclidean trajectory, or distance, between any of those two values. Matrix T 3.8 has the same sub-index of Matrix X 3.7, but represents the position of the input values contained in Matrix X and not the magnitude values themselves.

$$T = \begin{bmatrix} t_{1,1} & \dots & t_{j,1} & \dots & t_{k,1} \\ \dots & \dots & \dots & \dots & \dots \\ t_{1,i} & \dots & t_{j,i} & \dots & t_{k,i} \\ \dots & \dots & \dots & \dots & \dots \\ t_{1,n} & \dots & t_{j,n} & \dots & t_{k,n} \end{bmatrix} \quad (3.8)$$

Matrix B [Eq. 3.9] is created with n random base-case potential scenarios and contains the position sub-index i of the input range values in Matrix 3.7.

Each row's sub-index l ($l=1,2,\dots,n$), represents one of the randomly generated scenarios and each column's sub-index j indicates the input factor ($j=1,2,\dots,k$).

$$B = \begin{bmatrix} b_{1,1} & \dots & b_{j,1} & \dots & b_{k,1} \\ \dots & \dots & \dots & \dots & \dots \\ b_{1,l} & \dots & b_{j,l} & \dots & b_{k,l} \\ \dots & \dots & \dots & \dots & \dots \\ b_{1,n} & \dots & b_{j,n} & \dots & b_{k,n} \end{bmatrix} \quad (3.9)$$

Note that Matrix B [Eq. 3.9] has the same dimensions as Matrix X [Eq. 3.7], ($k \times n$). Whilst not compulsory for the method implementation, this reduce the computational complexity of the code³.

Function Y [Eq. 3.10] represents the calculation approach model under study, and y the output variable of interest (scalar) in function of the k input parameters, with a single value for each of the n base-cases. The l -th base-case scenario ($l = 1, 2, \dots, n$), the model output, y_l , is given by Equation 3.10:

$$Y_l(X_1, \dots, X_j, \dots, X_k) = y_l \quad (3.10)$$

3.2.2.2 SA implementation

The *One-At-a-Time analysis (OAT)* is a simple and common approach in SA. The method changes one input variable at a time, all others remain at their base-case value, and analyses the effect produced on the output.

In order to undertake an OAT analysis, only the $l = 1$ row from Matrix B 3.9 is considered, array 3.11:

³The computational complexity is the amount of resources required for running the algorithm of the code.

$$B_1 = \left[b_{1,1} \quad \dots \quad b_{j,1} \quad \dots \quad b_{k,1} \right] \quad (3.11)$$

Substituting the position sub-index i in array 3.11 by the corresponding magnitude values of Matrix X [Eq. 3.7] given in this position, the first base-case is obtained, array 3.12:

$$BC_1 = \left[x_{b_{1,1}} \quad \dots \quad x_{b_{j,1}} \quad \dots \quad x_{b_{k,1}} \right] \quad (3.12)$$

Applying the BC_1 into function Y 3.10, the output $y_1(x)$ for the first base-case is obtained.

Once the base-case of our local analysis has been defined, the first input X_1 is taken as a variable and the other inputs remain fixed at their given base-case values. Function Y will now be dependent only on a single variable, moving along the input X_1 discrete range given in the first column of Matrix X (3.13), excluding the value $x_{j,i} = x_{b_{j,l}}$.

$$X_1 = \begin{bmatrix} x_{1,1} \\ \dots \\ x_{1,i} \\ \dots \\ x_{1,n} \end{bmatrix} \quad (3.13)$$

According to Morris [69], the elementary effect constitutes an estimation of the variation in the output of a model due to a perturbation taking place in one of the values of an input factor, while all the other inputs remain constant. For the input parameter X_j , the elementary effect of its i^{th} – value is given by Equation 3.14

$$e_{j,i} = \frac{y_l(\Delta_{x_{j,i}}) - y_l}{\Delta_{j,i}} \quad \forall i \neq l$$

$$e_{i,j} = 0 \quad \forall i = l$$
(3.14)

where:

y_l is the model output for the base case l ;

$x_{j,i}$ is the i -th-value of input factor X_j ;

$\Delta_{x_{j,l}}$ is the perturbation over the undertaken value; and

$\Delta_{j,i} = (t_{j,i} - t_{b_{j,i}})$ is the distance separation between the initial and the perturbed value in accordance with the normalized Euclidean trajectory space given by Matrix T 3.8

Accordingly, the elementary effects distribution for the n values of the input X_1 , excluding value $x_{1i} = x_{b_{1l}}$, is given in Equation 3.15:

$$Fe_{1,1} = \left[e_{1,1} \quad \dots \quad e_{1,i} \quad \dots \quad e_{1,n} \right]$$
(3.15)

where $Fe_{j,l} = Fe_{1,1}$ is the probability density function for X_1 and *Base – case*₁.

To allow the comparison of the input factors across different calculation models, the Standardised Elementary Effect se is calculated. For the input X_j , the Standardised Elementary Effect (SEE) is obtained by multiplying each of its element e_{ji} by the standardisation factor, this is calculated by dividing the standard deviations, σ_{X_j} , of the whole range of values of the input factor, $X_j = x_{j1}, \dots, x_{ji}, \dots, x_{jn}$, by the standard deviations, σ_{y_j} , of the whole range of values of the outputs obtained for this input factor, $y_j = y_{j1}(x_{j1}), \dots, y_{ji}(x_{ji}), \dots, y_{jn}(x_{jn})$. Accordingly, the SEE for the i^{th} value of the input, X_j , is given by equation 3.16:

$$se_{j,i} = e_{j,i} \frac{\sigma_{X_j}}{\sigma_{y_j}} \quad (3.16)$$

The probability density function of the SEE for input X_j and base-case 1 is given by Equation 3.17:

$$Fse_{j,1} = \left[se_{j,1} \quad \dots \quad se_{j,i} \quad \dots \quad se_{j,n} \right] \quad (3.17)$$

The mean of the values (μ) and the mean of the absolute values (μ^*) of the SEE probability density function of input X_j are given by equation 4.7 and 3.19, respectively:

$$\mu_j = \frac{\sum_1^n Fse_{j,1}}{n} \quad (3.18)$$

$$\mu_j^* = \frac{\sum_1^n |Fse_{j,1}|}{n} \quad (3.19)$$

where $|Fse_{j,1}| = \left[|se_{j,1}|, \dots, |se_{j,i}|, \dots, |se_{j,n}| \right]$

The absolute value of the means can be used as an estimator of the level of impact of each of the input factors over the model output. However, this local SA only considers a single base-case $l=1$, in which the impact of interaction effects between the input parameters has not been evaluated. In order to consider this impact, n base-cases, $l = 1, 2, \dots, n$, over the experimental space given by Matrix X, have been considered.

In the *Global SA*, the same procedure used for the OAT analysis for base-case $l = 1$, is implemented for the rest of the base-cases, $l = 2, \dots, n$, given in Matrix B 3.9.

Considering input X_j , Matrix M_{se_j} of dimension $(n \times (n-1))$ and containing the SEE distribution functions for all base-cases are generated. Each of the rows in Matrix M_{se_j} represents a

probability density function of the SEE for one of the n base-cases.

$$M_{se_j} = \begin{bmatrix} se_{1,1} & \dots & se_{1,i} & \dots & se_{1,n} \\ \dots & \dots & \dots & \dots & \dots \\ se_{l,1} & \dots & se_{l,i} & \dots & se_{l,n} \\ \dots & \dots & \dots & \dots & \dots \\ se_{n,1} & \dots & se_{n,i} & \dots & se_{n,n} \end{bmatrix}_j \quad (3.20)$$

The mean of the values (μ) and the mean of the absolute values (μ^*) of Matrix M_{se_j} is calculated, allowing the estimation of the grade of monotonicity for each input parameter X_j in accordance with Equation 3.21.

$$\Phi_j = |\mu_j| - |\mu^*_j| \quad (3.21)$$

where:

$$\mu_j = \frac{\sum_1^n M_{se_{j,1}}}{n} \quad (3.22)$$

$$\mu^*_j = \frac{\sum_1^n |M_{se_{j,1}}|}{n} \quad (3.23)$$

To consider the effects of the different iterations of input values in each base case, the standard deviation for each input factor X_j is calculated in accordance with Equation 4.6.

$$\sigma_j = \sqrt{\frac{1}{n^2} \sum_1^{n^2} (F(M_{se_j}) - \mu_j)^2} \quad (3.24)$$

where $F(M_{se_j})$ is the probability density function of Matrix M_{se_j} 1 values.

To analyse the behaviour of the Standardised Elementary Effects distribution, the median, or middle value, for the probability density function $G(M_{se_j})$, is calculated for each of the input factors X_j , in accordance with Equation 3.25.

$$m_j \text{ is the } \left[\frac{(n+1)}{2}\right]^{th} \text{ value of } G(M_{se_j}) \quad (3.25)$$

where $G(M_{se_j})$ is the probability density function $F(M_{se_j})$ sorted in ascending order.

Finally, the degree of skewness of the SEE distribution is calculated according to Equation 3.26.

$$\xi_j = \frac{\mu_j - m_j}{\sigma_j} \quad (3.26)$$

3.2.2.3 Results interpretation

As a result of the implementation of this method, four representative sensitivity features are identified and the information extracted is presented in the shape of graphs, this allows the ranking of the model inputs in terms of importance. The *Representative Sensitivity Features*, identified as the estimation factors for each input factor, are identified in two stages, *Primary SA* and *Secondary SA*.

The *Primary SA* provides an initial ranking of the input factors in accordance with their relative impact on the output, and is based on two sensitivity measures for each input factor X_j :

1. *Direct effect* (μ^*_j): is given by the mean of the absolute values (μ^*_j) of the SEE Matrix M_{X_j} .
The reason for considering μ^*_j instead of μ_j , as in the original Morris method, is that if the Matrix M_{X_j} contains elements of the opposite sign, which occurs when the model is non-monotonic⁴, when computing its mean some effects may cancel each other out.

⁴Some models are base-case dependent, that means that they can increase or decrease depending on the base-case considered.

Thus, a factor which is important, but whose effect on the output has an oscillating sign, may be erroneously considered as negligible. For this reason μ^*_j is considered to be better than μ_j to rank factors in order of importance. A high value of μ^*_j indicates an input factor with a significant influence on the output.

2. *Indirect effect* (σ_j): this sensitivity feature is a measure of the variation or dispersion of the SEE on Matrix M_{sej} . A low standard deviation indicates that the SEE values tend to be close to the overall mean (which indicates that the overall effect of the input factor is almost independent of the values assigned to other factors), while a high standard deviation indicates that the SEE values are spread over a wider range of values (which indicates a factor involved in interaction with other factors, or with non-linear effects).

The *Secondary SA* provides additional information about the SEE distribution sign consistency and deviations with respect to the general behavioural trend. It is based on two estimation factors, *Degree of monotonicity* and *Degree of skewness*:

1. *Degree of monotonicity* (Φ_j): the mean of the absolute values (μ^*_j) of Matrix M_{sej} provides an estimation free of any non-monotonic input to output behavior that could be present in the mean of the values (μ), thus the difference between those means (Equation 3.21) is a measure of the monotonicity of the model for the input factor. A high value of (Φ_j) indicates a model with a large degree of non-monotonicity for a specific input factor (which means the sign of the output distribution will not always be consistent with the input).
2. *Degree of skewness* ξ_j : this sensitivity feature is a measure of the asymmetry of the SEE distribution function with respect to its mean. It is calculated by comparing the mean and the median of the distribution, in accordance with Equation 3.26. If the Mean (μ_j) is greater than the median (m_j), the Elementary effects distribution is skewed to the right (i.e.,

it has a positive sign), which means there are more values greater than the mean than there are values lower for the input SEE factor distribution. If the Mean (μ_j) is lower than the median (m_j), the Elementary effects distribution is skewed to the left (i.e., has a negative sign), which means there are more values smaller than the mean than there are values greater for the input SEE factor distribution. A high value of ξ_j , on either side indicates an input factor with a large skewness Elementary Effects distribution function (i.e., there is a relatively high number of elementary effect values outside of the mean value or general trend).

The information provided by the representative sensitivity features for all the input factors, can be presented in two *SA graphs*.

The *Primary SA graph*: each of the points in Figure 3.6 correspond to one of the input parameters. The horizontal axis represents the direct effect, μ^* , on the output produced by the input, and the vertical axis represents the indirect effect, σ , created by the other inputs.

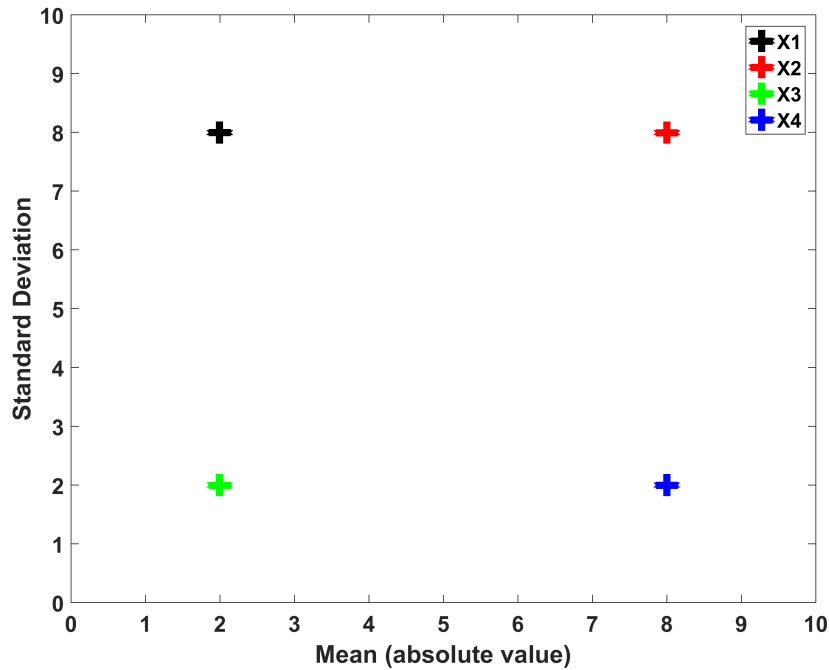


Figure 3.1: Input factors classification graph obtained from the Primary SA, based on the direct (horizontal axis) and indirect (vertical axis) effects of each input X over the model output.

Depending on the position occupied by the point, the input factor can be classified into four primary types:

1. X_1 : Low direct and high indirect impacts.
2. X_2 : High direct and high indirect impacts.
3. X_3 : Low direct and low indirect impacts.
4. X_4 : High direct and low indirect impacts.

Factors X_1 and X_3 can be neglected as their relative impact on the output value is very low. The position of factors X_2 and X_4 , on the other hand, indicates an important influence on the

output, independent of the values assigned to other factors for X_4 and largely influenced by these iterations for X_2 .

From the point of view of an energy audit, input X_2 is the factor which would require more time and effort as uncertainties in its range of values need to be reduced, not only for itself but also for the remainder of the inputs.

The *Secondary SA graph*: each of the points in Figure 3.7 correspond to one of the input parameters. The horizontal axis represents the grade of non-monotonicity, Φ , and the vertical axis the grade of skewness, ξ , of the model output for each input.

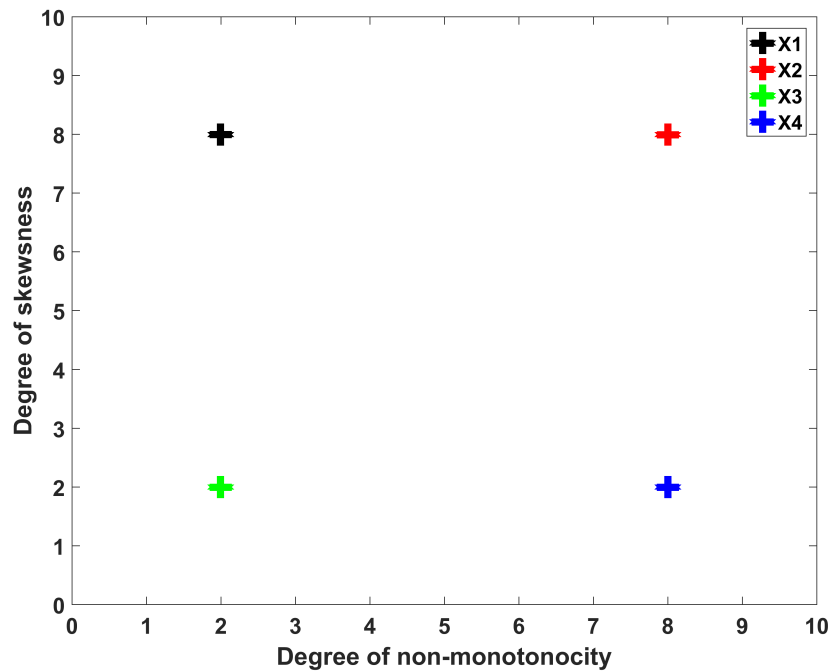


Figure 3.2: Input factors classification graph obtained from the Secondary SA, based on the degrees of non-monotonicity (horizontal axis) and skewness (vertical axis).

Depending on the position occupied by the point, the input factor can be classified into four secondary types ⁵:

⁵Note that all the inputs present a positive sign for the degree of skewness, which means that the SEE distribution

1. X_1 : Low degree of non-monotonicity and high degree of skewness.
2. X_2 : High degree of non-monotonicity and high degree of skewness.
3. X_3 : Low degree of non-monotonicity and low degree of skewness.
4. X_4 : High degree of non-monotonicity and low degree of skewness.

From the point of view of an energy audit, input X_3 will not need special requirements, for what can be neglected, as has been suggested in the Primary SA. Factor X_1 , on the other hand, although has been categorized as a negligible factor by the Primary SA, has a high degree of skewness and, therefore, some of their values can be significant for the final energy estimations. Factors X_2 and X_4 have been classified as important factors by the Primary SA. This affirmation is reinforced by the Secondary SA, which also identified them as very non-monotonic, which means the sign of the output will depend very much on the value taken by the inputs.

3.2.3 Explanatory example for the adapted SA method

To facilitate the understanding of the implementation methodology for the adapted SA method, an explanatory example is included in this section, along with some relevant graphs to aid interpretation of the results.

1. *Starting points:*

For the implementation example $k=3$, input factors, $X_1; X_2; X_3$, are considered. Table 3.1 presents the maximum and minimum values for those factors ⁶.

is skewed to the right. Negative signs mean a skewness to the left, but the same input classification will be kept.

⁶These values are aleatory and do not have any significance.

Table 3.1: Maximum and minimum values for the inputs in the explanatory example.

Input Variables	X_1	X_2	X_3
Minimum Value	10	60	20
Maximum Value	100	280	48

To simplify the example, a sample resolution of $n = 5$ has been chosen. A robust implementation of the method would require $n = 100$ or above in order to consolidate results as it is from this n -value that results begin to stabilise .

Matrix X_{ex} is generated by dividing the range of the three input factors into $n=5$ equally spaced intervals. The (5×3) dimensional matrix is given by 3.27.

$$X_{ex} = \begin{bmatrix} 10 & 60 & 20 \\ 32.5 & 115 & 27 \\ 55 & 170 & 34 \\ 77.5 & 225 & 41 \\ 100 & 280 & 48 \end{bmatrix} \quad (3.27)$$

To create *Matrix* T_{ex} , the range of each input parameter has been rescaled to $[0, 1]$, with step size $\Delta = 1/(5 - 1)$. The (5×3) dimensional matrix is given by 3.28.

$$T_{ex} = \begin{bmatrix} 0 & 0 & 0 \\ 0.25 & 0.25 & 0.25 \\ 0.50 & 0.50 & 0.50 \\ 0.75 & 0.75 & 0.75 \\ 1 & 1 & 1 \end{bmatrix} \quad (3.28)$$

Matrix B_{ex} 3.29 is the base-case matrix, containing only position sub-index i from matrix

X_{ex} 3.27.

$$B_{ex} = \begin{bmatrix} 5 & 2 & 5 \\ 3 & 4 & 3 \\ 4 & 5 & 2 \\ 2 & 3 & 1 \\ 1 & 1 & 4 \end{bmatrix} \quad (3.29)$$

For the implementation example, the calculation model given by function Y_{ex} 3.30 has been considered.

$$Y_{ex}(X_1, X_2, X_3)_l = X_1 * (150 * X_2 + X_2^2 + X_3/15) \quad (3.30)$$

This equation does not represent any energy model, it has been chosen only for explanatory purposes.

2. SA implementation:

In order to undertake an *OAT analysis*, only the row $l = 1$ row from Matrix B_{ex} 3.29 is considered:

$$B_{ex1} = \begin{bmatrix} 5 & 2 & 5 \end{bmatrix} \quad (3.31)$$

In accordance with according with Matrix X_{ex} 3.27, the input value magnitude for the first base-case is given by 3.32:

$$Base - case_{ex1} = \begin{bmatrix} x_{b1,1} & x_{b2,1} & x_{b3,1} \end{bmatrix} = \begin{bmatrix} x_{1,5} & x_{2,2} & x_{3,1} \end{bmatrix} = \begin{bmatrix} 100 & 115 & 48 \end{bmatrix} \quad (3.32)$$

Applying the *base – case*_{ex1} into function Y_{ex} 3.30 :

$$y_1(x) = 100 * (5 * 115 - 115^2 + 48/15) = 402980 \quad (3.33)$$

where $y_1(x) = 402980$ is the output for the first base-case.

Once the base-case of the OAT SA has been fully defined, the first input X_1 is taken as a variable and the remainder are keep fixed at the given base-case values: $X_2 = x_{2,2} = 115$; $X_3 = x_{3,5} = 48$. Y_{ex} will now be dependent only on a single variable.

$$y_1(x_{1,i}) = x_{1,i} * (5 * 115 - 115^2 + 48/15) \quad (3.34)$$

The value of this variable will be moved along the input X_1 discrete range, given in the first column of matrix X_{ex} , where the value $x_{b_{1,1}} = x_{1,5} = 100$ has been excluded.

$$X_{1ex} = \begin{bmatrix} 10 \\ 32.5 \\ 55 \\ 77.5 \end{bmatrix} \quad (3.35)$$

For the first value ($i = 1$) of input X_1 , the elementary effect will be given by equation 3.36:

$$e_{1,1} = \frac{40298 - 402980}{1} = -362682 \quad (3.36)$$

Where $\Delta_{1,1} = |t_{1,5} - t_{1,1}| = 1$ is the Euclidean distance between the initial and the perturbed value.

and $y(\Delta_{x_{1,1}}) = 40298$ is the output of the perturbed value $x_{1,1}$.

The EE probability density function for X_1 is given by Equation 3.37 ⁷:

$$Fee_{1,1ex} = \begin{bmatrix} -362682 & -362682 & -362682 & -362682 \end{bmatrix} \quad (3.37)$$

And the SEE probability density function for the input X_1 and base-case 1, by Equation 3.38:

$$Fsee_{1,1} = \begin{bmatrix} 12.189 & 12.189 & 12.189 & 12.189 \end{bmatrix}_1 \quad (3.38)$$

where $\sigma_{X_j} = 35.57$ and $\sigma_{y_j} = 1.0585 \cdot 10^6$.

For the other two inputs, X_2 and X_3 the distribution is given by Equations 3.39 and 3.40, respectively.

$$Fse_{2,1} = \begin{bmatrix} -45.186 & -244.006 & -343.417 & -442.827 \end{bmatrix}_1 \quad (3.39)$$

$$Fse_{3,1} = \begin{bmatrix} 0.003 & 0.003 & 0.003 & 0.003 \end{bmatrix}_1 \quad (3.40)$$

Note that $Fse_{1,1}$ and $Fse_{3,1}$ have constant SEE values, which means that the change rate in the output due to these inputs is also constant.

The mean of the values (μ_j) of Matrix M_{X_j} :

$$\mu_1 = 12.189, \mu_2 = -268.859 \text{ and } \mu_3 = 0.003 \quad (3.41)$$

⁷Note that $e_{1,5}$ is not considered as $e_{1,5} = b_{1,1}$.

and the mean of the absolute values (μ_j^*) of Matrix M_{X_j} :

$$\mu_2^* = 12.189, \mu_2^* = 268.859 \text{ and } \mu_3^* = 0.003 \quad (3.42)$$

The absolute value of the means can be used as an estimator of the level of impact of each of the input factors over the model output. However, this OAT SA only considers a single base-case $l=1$, in which the impact of the interaction effects between the input parameters has not been evaluated. In order to consider this impact, a global analysis needs to be performed. Thus, n base-cases, $l = 1, 2, \dots, n$, covering the whole experimental space given by matrix X_{ex} , have been considered.

For the *Global analysis*, the SEE matrix for inputs X_1 , X_2 and X_3 are given by Equations 3.43, 3.44 and 3.45, respectively.

$$M_{see_{x1}} = \begin{bmatrix} 12.189 & 12.189 & 12.189 & 12.189 & 0 \\ -51.032 & -51.032 & 0 & -51.032 & -51.032 \\ -110.093 & -110.093 & -110.093 & 0 & -110.093 \\ 0 & 16.346 & 16.346 & 16.346 & 16.346 \end{bmatrix}_1 \quad (3.43)$$

$$M_{see_{x2}} = \begin{bmatrix} -45.187 & 0 & -244.006 & -343.417 & -442.827 \\ -134.204 & -188.879 & -243.555 & 0 & -352.905 \\ -266.148 & -343.191 & -420.233 & -497.276 & 0 \\ -46.994 & -79.302 & 0 & -143.919 & -176.227 \\ 0 & -4.519 & -14.459 & -24.401 & -34.342 \end{bmatrix}_2 \quad (3.44)$$

$$M_{see_{ex3}} = \begin{bmatrix} 0.0026 & 0.0026 & 0.0026 & 0.0026 & 0 \\ 0.0014 & 0.0014 & 0 & 0.0014 & 0.0014 \\ 0.0020 & 0 & 0.0020 & 0.0020 & 0.0020 \\ 0 & 0.0009 & 0.0009 & 0.0009 & 0.0009 \\ 0.0003 & 0.0003 & 0.0003 & 0 & 0.0003 \end{bmatrix}_3 \quad (3.45)$$

The value $se_{l,i} = 0$ indicates the value that has been excluded from the input range in each base-case, i.e., the input values that coincide with the base-case values ($i=1$).

Note that all the elements in matrix $M_{see_{ex2}}$ and $M_{see_{ex3}}$ have the same sign, negative for the former and positive for the latter; this indicates that both inputs are monotonic, i.e., the output always decreases when X_2 decreases and increases when X_3 increases, although the latter occurs very slowly. On the other hand, each of the rows of X_1 has a different sign, which means that the input non-monotonicity is case dependent, i.e., the output increases or decreases with the input depending on the base-case.

This Global SA method has been applied to the implementation example and the representative feature parameters obtained and presented in Table 3.2. In order to obtain more robust results $n=100$ base-cases, instead of $n=5$, have been taken for the calculation of the parameters in Table 3.2 .

Table 3.2: Representative feature parameters for each input factor.

SA Parameters	X_1	X_2	X_3
Direct effect (μ^*)	132.168	202.300	0.002
Interaction effect (σ)	37.752	126.530	0.001
Monotonicity (Φ)	9.896	0.181	0
Skewness (ξ)	0.323	0.200	0

3. Result interpretation:

To better understand and interpret the numerical results from Table 3.2, a number of explanatory graphs are presented and analysed in this section.

Graphs 3.3a, 3.4a and 3.5a represent the variation (given by the SEE distribution) of the model outputs y_j against the range of values for each input X_j (for $j=1$; $j=2$ and $j=3$, respectively). Each line in the graph, plotted in a different colour, represents a different base-case.

Graphs 3.3b, 3.4b, and 3.5b represent the cumulative density frequency, where the horizontal axis is the allowable domain for the SEE distribution function and the vertical axis is the normalised probability, between zero and one. It increases from zero to one as we move from left to right on the horizontal axis. The median and the absolute value of the mean are represented by a red and a black line, respectively.

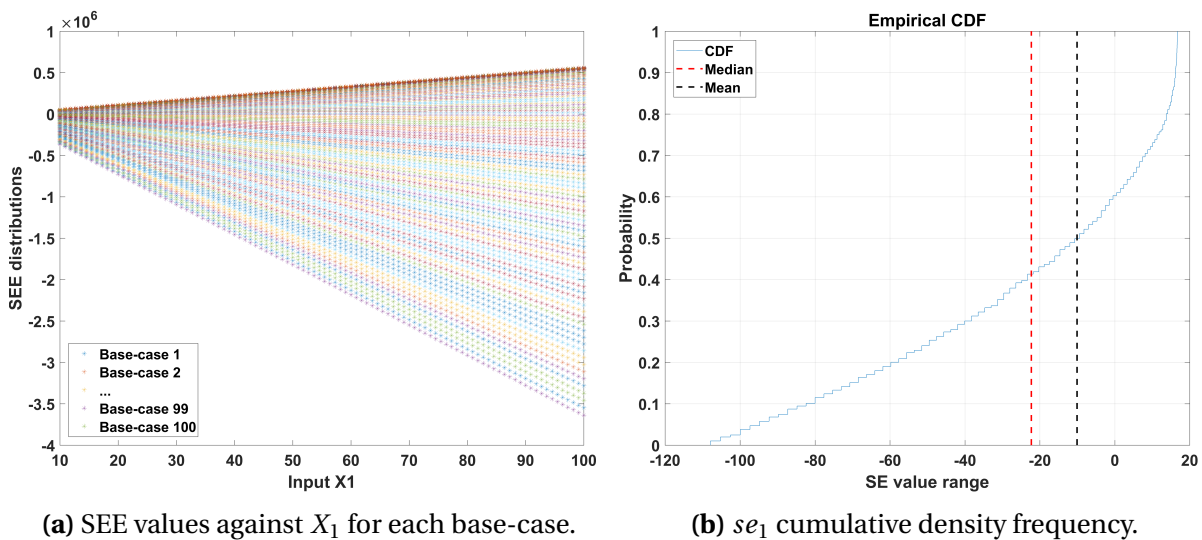


Figure 3.3: Results interpretation for the X_1 input

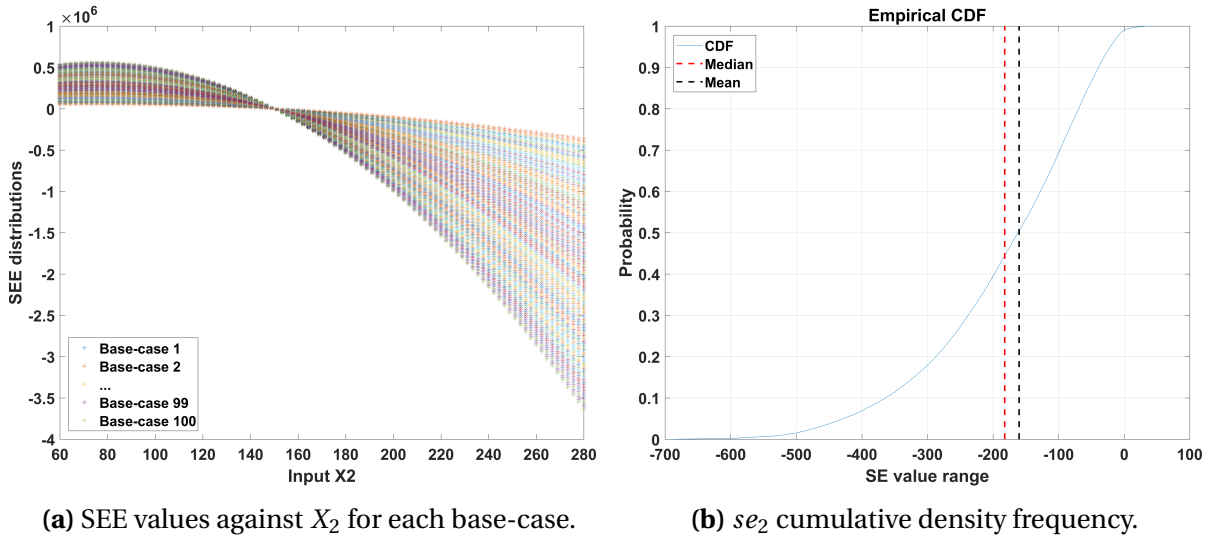


Figure 3.4: Results interpretation for the X_2 input

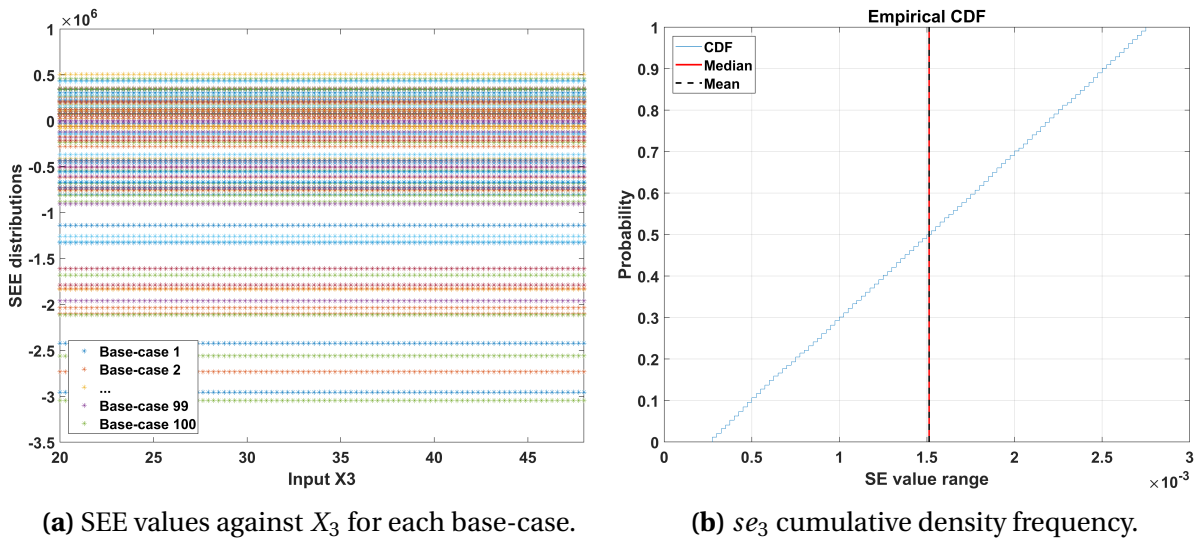


Figure 3.5: Results interpretation for the X_3 input

From the observation of the the graphs, the following findings can be obtained:

- Each line of the a-graphs contains the SEE values given for one of the rows (or base-case) of Matrix $M_{se_{ex1}}$. The steeper the slope of this line, the more significant is the

input to the output, see Graph 3.3a; and the shallower the slope, the more insignificant, see Graph 3.5a.

- Some of the lines in graph 3.3a increase with the value of the input range, and others decrease, meaning that the monotonicity of the model is base-case dependent for input X_1 . This implementation example demonstrates the importance of the use of μ^* instead of μ , to avoid the cancellation of some SEE values by others with the opposite sign ⁸.
- The horizontal axes of the b-graphs contain the range of dispersion, i.e., standard deviation, for the SEE on Matrix M_{seej} for the different input factors. Graph 3.4b presents a large plotting dispersion of approximately 600 units ⁹, indicating a wide SEE distribution function. On the other hand, Graph 3.5b shows a low dispersion of the SEE values, approximately $3e10^{-3}$, which indicates a small standard deviation value for this input.
- A graphical representation of the skewness of the model for the different inputs is also presented in the (b) graphs. This allows a comparison between the red line (median of the elementary effect distribution) and the black line (mean of the absolute value of the distribution). For Graphs 3.3b and 3.4b, the mean is smaller than the median, which means there are more values greater than the mean than there are smaller for these input factors X_1 and X_2 , especially for the former. In Graph 3.5b both lines are superposed, this indicates a Gaussian distribution shape for the elementary effect distribution function.

The SA method provides an easier way to present these results and the findings for the

⁸It is important to remember that μ^* and μ are calculated for the whole value distribution given in Matrix M_{see1}

⁹This unit will be determined by the magnitude of the input factor.

three input factors into two single graphs:

Primary analysis:

Each of the points in Figure 3.6 correspond to one of the input parameters. The horizontal axis represents the direct effect, μ^* , on the output produced by the input, and the vertical axis represents the interaction effect, σ , created by the others inputs.

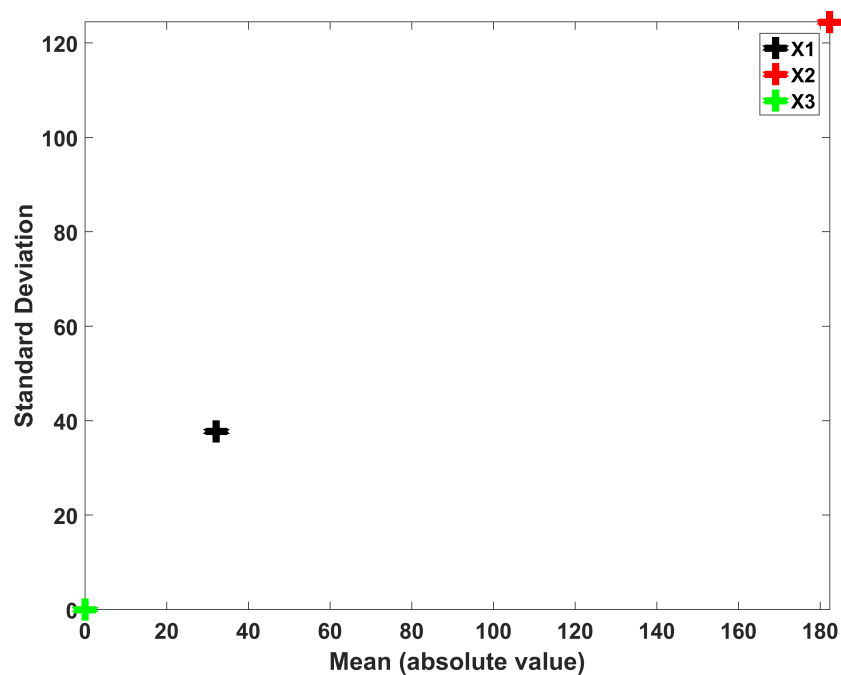


Figure 3.6: Primary SA

According to Figure 3.6, X_2 is the most relevant input, with a large value for μ^* and σ , followed by X_1 and finally by X_3 , which can be considered as having negligible influence.

Secondary analysis:

Each of the points in Figure 3.7 correspond to one of the input parameters. The horizontal axis presents the grade of monotonicity, Φ , of the model for each input and the vertical

axis the grade of skewness, ξ .

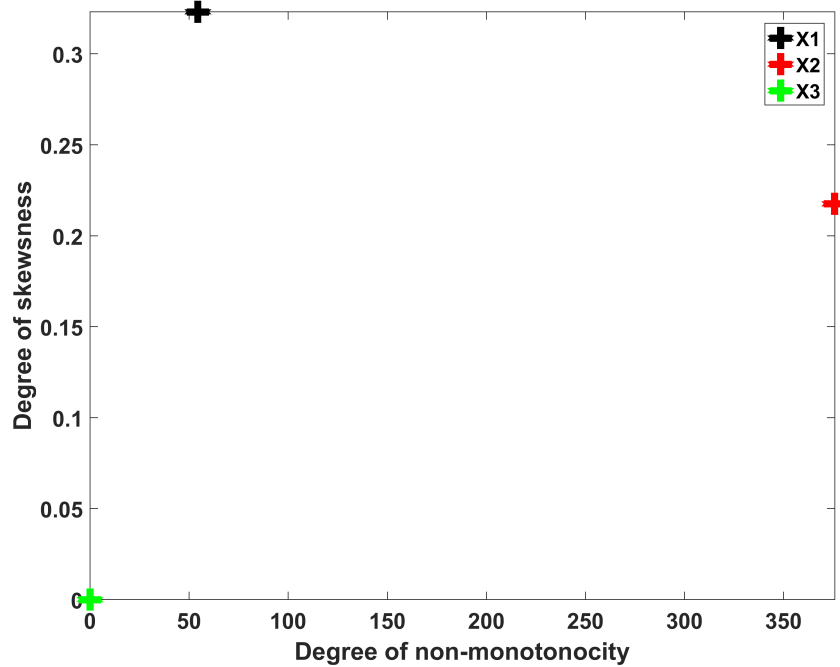


Figure 3.7: Secondary SA

According to Figure 3.7, X_2 has the most asymmetric elementary effect distribution, with the larger non-monotonic and positive skewness behaviour. Factor X_1 , has a relatively low degree of non-monotonicity, but with a high skewness compared with the rest of the inputs, while factor X_3 , has presented none of those behaviours.

Finally, taking into account both Primary and Secondary results, input X_2 seems to be the most relevant, thus effort should be made to reduce uncertainties in its range of values during the auditing process. Input factor X_1 has, in general, less impact on the output than X_2 , however, its behaviour is significantly asymmetric¹⁰, which means that some specific values of X_1 can

¹⁰More values greater than the mean of the distribution than there are lower.

outweigh X_2 in terms of influential impact on the output, therefore, special care is advised when information is collected for this input.

Both analyses show that X_3 is the lowest significant input to the output, and therefore less audit time should be spent in qualifying its values.

3.3 Case-study

3.3.1 Calculation models

For this case-study the adapted methods have been applied to four different energy calculation methods. The first three models are well established within industry and the fourth was specifically created for this case-study.

Model A. CIBSE TM22 software:

As part of the TM22 guidance, CIBSE provides a Microsoft Excel spreadsheet that can be used for estimation of energy consumption within buildings by end use [22, 31]. The total annual small power energy usage, E_T , is calculated by Equation 3.46 :

$$E_T = U_n * P_L * F_L * O_h * (F_{ON}^* + (8760 - O_h) * F_w^* / O_h) \quad (3.46)$$

where:

E_T is the total annual energy consumption;

U_n is the number of installed units;

P_L is the nameplate load;

F_L is the load factor;

O_h is the operational hours;

F_{ON}^* is the ON load factor;

F_w^* is the wastage load factor; and

8760 is the number of hours in a year.

*Asterisked data are optional, which means the model can still be implemented if this information is not available.

Model B. CIBSE TM54:

The CIBSE TM54 Technical calculation model [136] is based on the use of dynamic simulation modelling to calculate energy loads within the building, however, calculation estimates for certain types of consumption are required, with small power loads being one such example. The model was initially introduced for the design stage, but it also provides a reasonable approach for estimation of energy use in an occupied building. The total annual small power energy usage, E_T , is calculated using Equation 3.47:

$$E_T = U_n * ((P_{ON} * O_h) + (P_w^* * (8760 - O_h))) \quad (3.47)$$

where:

E_T is the total annual energy consumption;

U_n is the number of installed units;

P_{ON} is the average ON power;

P_w^* is the average waste power;

O_h is the operational hours; and

8760 is the number of hours in a year.

*Asterisked data are optional, which means the model can still be implemented if this information is not available.

Model C. Energy Consumption Guide 35:

This model provides an alternative approach for estimating the number of units installed based on the occupancy density and the kind of appliance, it assumes that small power demand per unit floor area is closely related to occupancy density. Energy Consumption Guide 35 [137], published by BRESCU and BSRIA in 1995, was the first guide to use this approach to calculate energy efficiency in offices. This strong correlation between the small power load demand and the occupant density has also been corroborated by recent practical studies on office buildings, such as the Welsh School of Architecture [47]. The total annual small power energy usage, E_T , is calculated by Equation 3.48:

$$E_T = O_d * P_r * P_L * F_L * O_h \quad (3.48)$$

where:

E_T is the total annual energy consumption;

O_d is the annual averaged occupancy density;

P_r is the annual total number of persons;

P_L is the nameplate load;

F_L is the load factor; and

O_h is the operational hours.

Model D. Consumption behaviour:

Recent studies involving surveys in commercial buildings have shown the large impact of occupant behaviour on small power energy waste [133, 134]. Defining *waste energy* as the energy consumed consumed which is not associated with specific occupant activity, this calculation model is proposed in this thesis as a method to address the lack of energy awareness of building users.

The proposed model incorporates a new input parameter, the “Waste Time Factor” (T_w) that accounts for the portion of time, in hours, that the appliances are wasting energy, i.e., consuming energy without being used for work or other occupant activity. In this way, the new model considers three operational modes: *ON* (when appliances are consuming energy that is used only to produce work), *OFF* (when appliances are not consuming any energy), and *Waste* (when appliances are consuming energy but they are not producing any work: sleep mode, stand-by mode, appliances left ON but not being used, etc). The total number of hours in a year (8760 hours) is divided into those three modes and the total annual small power energy usage, E_T , is calculated according with that to the Equation 3.49:

$$E_T = U_n * P_L * O_h * (F_{ON} + F_W * T_w) \quad (3.49)$$

where:

E_T is the total annual energy consumption;

U_n is the number of installed units;

P_L is the nameplate load;

F_{ON} is the ON load factor;

F_W is the Waste load factor¹¹;

O_h is the operational hours; and,

T_w is the waste time factor.

During the remaining portion of time, $8760 - O_h * (1 + T_w)$, the appliances are considered to be in OFF mode and not consuming any energy.

¹¹Note that $F_W = 0$ only if there is not any energy wastage, otherwise $F_W \neq 0$

3.3.1.1 Calculation models input parameters

Within the calculation models considered in the study, some input parameters are common and others are model specific. In order to facilitate comparison and analysis of the models, Table 3.3 has been created to present a classification of all the input parameters in accordance with *Level III* of the TM22 methodological framework presented in the literature review, along with their description and an indication of the model in which they are used.

Table 3.3: Description table for input data to energy models

Input	Description	Model			
Number of Units					
Units: U_n	Number of individual appliances installed	A		C	D
Occupancy Density O_d (Person/Unit)	Number of persons per Unit		B		
Persons: P_r	Total number of people		B		
Power Consumption					
Nameplate Load : P_L (W)	Nominal power rate per unit	A		C	D
*Average ON Power: P_{ON} (W)	Average power consumed during operational hours		B		
**Averaged Waste Power: P_w (W)	Average waste power		B		
***Load Factor: F_L (%)	Percentage of the actual load used with respect to the name-plate (NP) Load	A	B		
*ON Load Factor: F_{ON} (%)	Ratio of load used with respect to the NP during operational hours	A			D
**Waste Load Factor: F_w (%)	Percentage of waste load used with respect to the NP during non-operational hours	A			D
Hours per Year					
Operation Hours: O_h (h)	Productive hours in a year (different from the occupancy hours)	A	B	C	D
Management Factor					
Waste Time Factor: T_w (h)	Number of hours in a year that the appliance is consuming waste energy				D

3.3.2 Information sources

To demonstrate the benefits of the approach in the evaluation of post-occupancy calculation models for office buildings, two case study open space offices of 30 m^2 of conditioned floor area with five types of small power equipment (PCs, laptops, screens, printers, and fridges) has been considered. The first one, a typical office with a fix number of staffs performing administrative work and the second one, a co-working space with a fluctuating number of staffs from different backgrounds and companies sharing workspace.

In order to replicate a standard preliminary audit process, the range in *Number of Units*, *Occupational Density*, *Nameplate Load*, *Average ON Power*, and *Average Waste Power* values for the different small power equipment types, has been obtained from established industrial benchmarking sources [15, 138, 139].

The range in *Number of Units*, *Occupational Density*, *Nameplate Load*, *Average ON Power*, and *Average Waste Power* values for the different small power equipment types are based on benchmarking [15, 138, 139].

Based on previous audits, the *Operational hours* range for PCs, laptops, and screens has been assumed to be from 1040 hours (equivalent to operating 4 hours/day, 5 days/week) to 3120 hours (equivalent to operating 10 hours/day, 6 days/week) for the typical office and from 624 hours (equivalent to operating 4 hours/day, 3 days/week) to 7280 hours (equivalent to operating 20 hours/day, 7 days/week) for the co-working office. Except for fridges, that have been assumed to be operating the whole year (8760 hours) and for printers, where benchmarking in [138] has been used.

The *Waste Time Factor* range has been considered to go from 0 hours to $(8760 - \min(O_h))$ for each of the small powers, except for the fridge which is assumed to operate constantly without waste.

The three load factors, as calculated in Equation 3.50¹², are used for the different small powers except the fridge which uses $F_w = 0$ and $F_l = F_{on}$ (and therefore $P_v = P_{on}$).

$$F_l = P_v * 100/P_l; F_{on} = P_{on} * 100/P_l \text{ and } F_w = P_w * 100/P_l \quad (3.50)$$

According to this information, Table 3.4 for the typical office and Table 3.5 for the co-working office, have been created. These tables do not intend to constitute a benchmark for small powers, rather they provide a set of input parameter values for the current case studies. The range in values for input factors in a real energy audit would depend on the specific building scenario (i.e., information available) and the auditor criteria.

¹²Where P_v is the averaged actual power rate and the remaining variables are described in Table 3.3.

Table 3.4: Value ranges for the input parameters presented in Table 3.3 for a typical office.

Equipment	U_n	P_l	P_v	P_{on}	P_w	F_l	F_{on}	F_w	O_h	T_w	O_d	P_r
	-	(W)	(W)	(W)	(W)	(%)	(%)	(%)	(%)	(h)	-	-
PC	10	480	48	52	1	4	5	0	1040	0	0.5	19
	25	1200	97	120	53	20	25	11	3120	7720	1	25
Laptop	10	50	12	30	1	9	23	1	1040	0	0.5	19
	25	130	36	40	20	72	80	40	3120	7720	1	25
Screen 15"-21"	19	240	20	25	0	8	10	0	1040	0	1	19
	50	260	36	45	1	15	20	0.5	3120	7720	2	25
Printer Multi-use	1	1440	550	600	260	30	32	14	260	0	20	19
	2	1850	1060	1400	350	74	82	21	520	8240	30	25
Fridge Small	1	100	90	90	0	25	25	0	8760	0	20	19
	2	300	120	120	0	85	85	0	8760	0	30	25

Table 3.5: Value ranges for the input parameters presented in Table 3.3 for a co-working office.

Equipment	U_n	P_l	P_v	P_{on}	P_w	F_l	F_{on}	F_w	O_h	T_w	O_d	P_r
	-	(W)	(W)	(W)	(W)	(%)	(%)	(%)	(%)	(h)	-	-
PC	8	480	48	52	1	4	5	0	624	0	0.8	10
	30	1200	300	600	150	30	35	22	7280	8136	1	30
Laptop	8	50	12	30	1	9	23	1	624	0	0.8	10
	30	130	90	100	50	85	90	50	7280	8136	1	30
Screen 15"-21"	8	240	20	25	0	8	10	0	624	0	0.8	10
	50	260	40	53	10	30	40	1	7280	8136	1.7	30
Printer Multi-use	1	440	140	250	30	20	25	10	130	0	10	10
	4	1850	1250	1600	250	75	85	28	1400	8136	40	30
Fridge Small	1	65	55	55	0	12	12	0	8760	0	10	10
	4	300	250	250	0	95	95	0	8760	0	40	30

3.3.3 Results

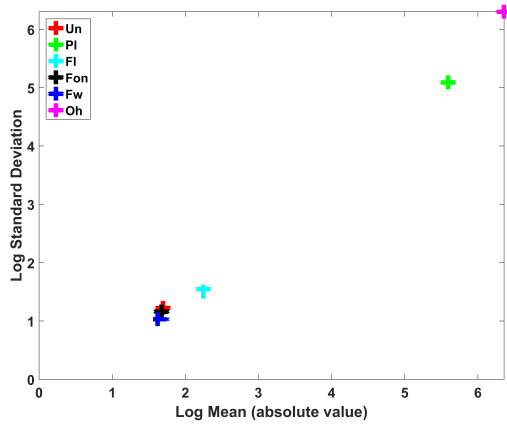
The *Adapted SA* has been implemented on the four calculation models presented in section 1.2.1. of this chapter, using the ranges of input factor values provided in Table 3.4 and Table 3.5.

As an example of the method implementation, the Primary (Figure 3.8) and Secondary (Figure 3.9) graphs obtained for the PCs from the first case study have been presented and analysed in this section .

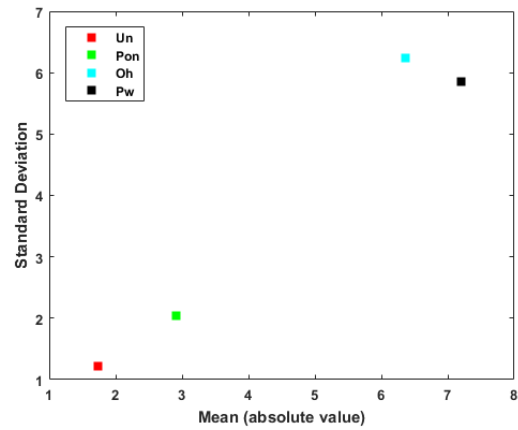
Primary SA:

Sub-Figures 3.8a, 3.8b, 3.8c, and 3.8d, show the graphical results obtained from the implementa-

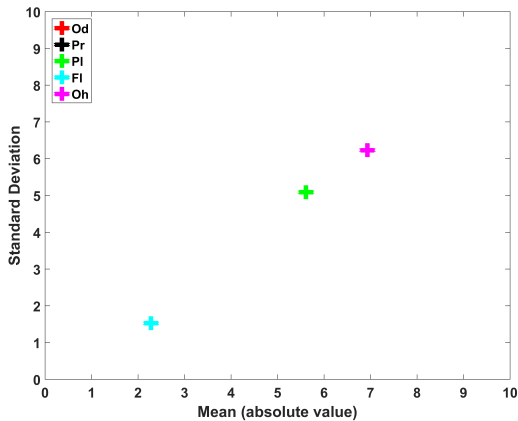
tion of the Primary SA method to models A, B, C, and D, respectively. Each point in the graphs corresponds to one of the PC input parameters (presented and described in table 3.3), represented with respect to the absolute value of the mean, μ^* (x-axis), and the standard deviation, σ (y-axis). Logarithmic values have been used to represent those sensitivity features in order to make small distances between points visually perceptible.



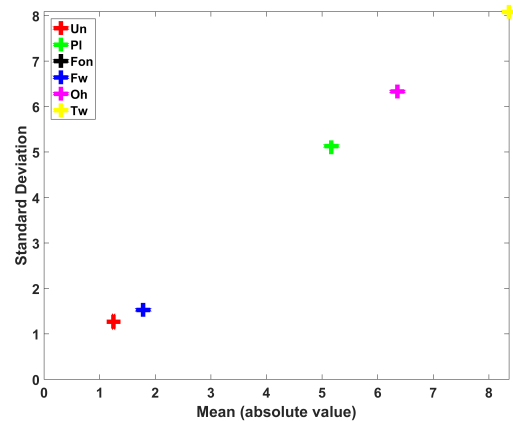
(a) Model A applied on PCs



(b) Model B applied on PCs



(c) Model C applied on PCs



(d) Model D applied on PCs

Figure 3.8: Primary SA graphs: Estimated mean (μ^*) of the absolute values and standard deviation (σ) of the different input factors of the four case-study models (applied on PCs' energy estimation)

Considering the position (or values of μ^* and σ) of the input factor points on the four graphs

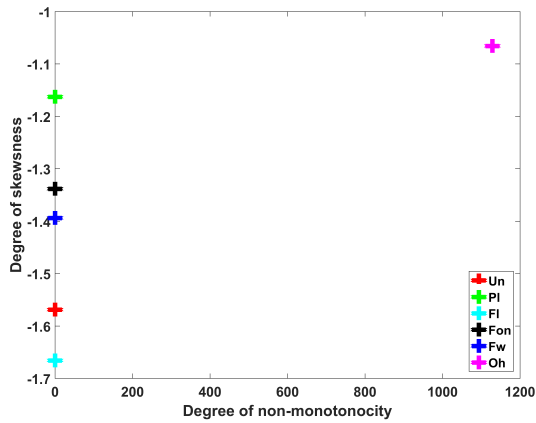
in Figure 3.8, and in accordance with the classification Figure 3.6, the input factors for the four models under study can be analysed and compared to obtain the following relevant findings:

- The *Waste Time factor (Tw)* from model D is the most relevant input parameter, as it has the highest μ^* and σ values. In model B, *Average Waste Power (Pw)* also presents a high value for the measurement parameters, indicating that models B and D should not be used if there is great uncertainty associated with waste energy related inputs. The analysis reveals the high levels of uncertainty associated with the "Waste" related factors, thus direct monitoring of these factors would be recommended with the exception of the *Wastage Load factor (Fw)*, which shows a relatively low relevance for both models A and D.
- For models A and C *Operational Hours (Oh)* and *Nameplate Load (Pl)* are the most influential factors. The effect of these two input factors shows approximately constant values across the different models in which they are contained, A, C, and D. This means that model B would be an option to be considered in the case of great uncertainties associated with those factors.
- There are inputs with a very low impact on output, some do not even appear in the figures due to their low values. *Units* and *Occupancy Density* are the least influential factors among the models, benchmarks and assumptions can be used for these inputs.
- Large values of μ^* are associated with high values of σ . This makes sense as large influential inputs have more weight over the model output and, therefore, minimal variation in their effects due to external variations will be translated into large impacts in the model output.

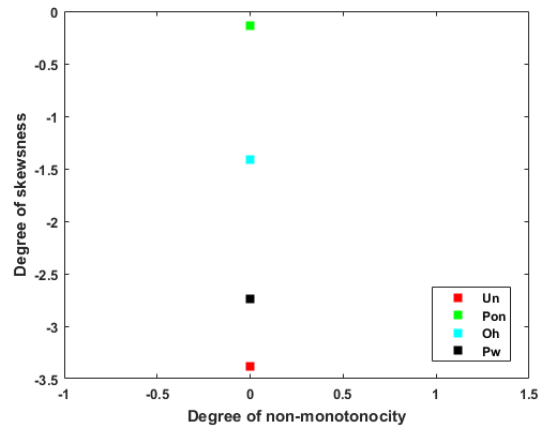
Secondary SA:

Sub-figures 3.9a, 3.9b, 3.9c, and 3.9d, show the graphical results obtained from the implementation of the Secondary SA method to models A, B, C, and D, respectively. Each point in the

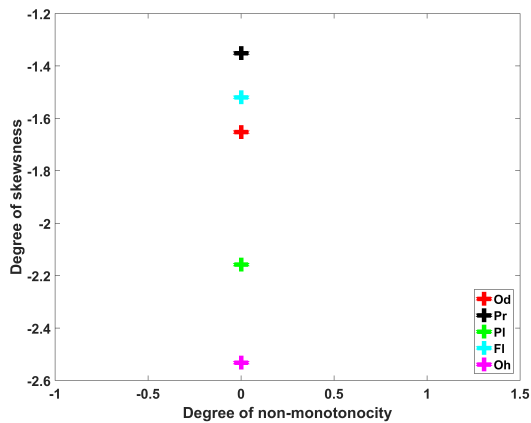
figures corresponds to one of the PC input parameters, represented with respect to the grade of non-monotonicity, Φ (x-axis), and the grade of skewness, Sk (y-axis). Logarithmic values have been used to represent those sensitivity features in order to make small distances between points visually perceptible ¹³.



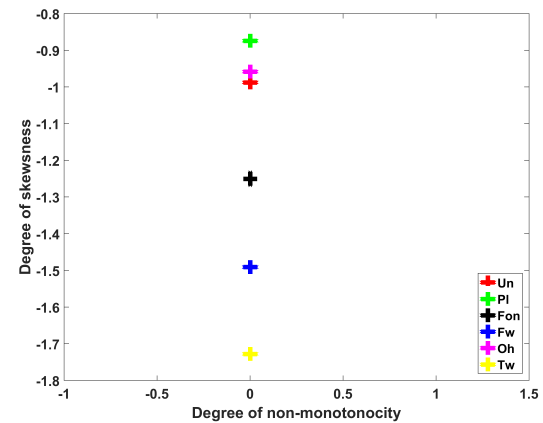
(a) Model A applied on PCs



(b) Model B applied on PCs



(c) Model C applied on PCs



(d) Model D applied on PCs

Figure 3.9: Secondary SA graphs: Estimated degree of non-monotonicity (Φ) and degree of skewness (ξ) of the different input factors of the four case-study models (applied on PCs' energy estimation)

Considering the position (or values of Φ and ξ) of the input factor points on the four graphs in

¹³Note that the logarithmic value for a numbers n : $0 < n < 1$ is negative.

Figure 3.9 and according to the classification Figure 3.7, the input factors for the four models under study can be analysed and compared between them, obtaining the following relevant findings:

- Models B, C, and D are monotonic for all their input factors. This facilitates the energy audit process as it ensures the output sign is consistent with the input (i.e., it always increases or decreases with the input). In model A, all inputs follow the same pattern with the exception of the *Operational Hours (Oh)*. This last input is the only one that presents a certain degree of non-monotonicity, that is, does not maintain the same sign in its input-output relation for the whole set of base cases considered (i.e., it sometimes increases and sometimes decreases with the input).
- None of the input factors have a symmetric SEE distribution function, which means there is not an equally partitioned number of values on both sides of the mean. Almost all inputs have a negative sign for the degree of skewness, which means that there are more values on the left of the SEE distribution than on the right. Only the *Nameplate Load (Pl)* in model B presents the opposite trend with a negative value.
- The *Units (Un)* factor from model B, classified as a low impact factor by the Primary SA, is the most asymmetrical. Regarding the value of *Un* for this model, and according to Equation 3.26, the Mean (μ_j) is much greater than the median (m_j), which means there are a large number of SEE values greater than the mean, or the general behaviour trend.
- In a similar way, factors *Un* and *Fon* for model A, also classified as low impact factors in the Primary SA, have a relatively high degree of skewness, and therefore, especial effort needs to be taken to reduce uncertainties in their value ranges as some of those values (deflected from the mean trend) can have a large impact on the output.

Taking into account the Primary and Secondary SA, Table 3.6 has been created to rank the importance of input factors with respect to the output results. It highlights (in bold) the relevance of some factors that, although considered negligible in the Primary SA, can contain specific high impact values.

Table 3.6: Input factor impact ranking for PCs from the *typical office* case study.

Input factors	High Impact	Low Impact
Model A	Pl; Oh	Fw; Fon; Un
Model B	Oh; Pw	Pon; Un
Model C	Pl; Oh	Pr; Od
Model D	Oh; Tw	Fon; Fw ; Un

Factors classified as *High Impact*, where the associated uncertainties will largely affect the output, need to be prioritised when collecting information for energy audits, and for *Low Impact* factors, where the associated uncertainties will not significantly affect the output, benchmarking and assumptions can be taken without risk of affecting the energy estimation, except for highlighted factors that, due to their complex (asymmetric or non-monotonic) behaviour, can contain specific values that can largely affect final energy estimations.

The proposed SA method categorizes the sensitivity of the model output to the uncertainties associated to the different inputs. Table 3.6 can be used to identify where will be more efficient reduce uncertainties for the improvement of the final model estimation.

3.3.3.1 Visual result representation

To incorporate the remaining small appliances considered in each case study and easily enable interpretation of the data, the results obtained from the Primary and Secondary SA have been reformed into *chrome maps* and presented in Figures 3.10 and 3.12, for the first case study, and Figures 3.11 and 3.13, for the second case study. These maps provide a visual indicator of the

performance of the model depending on the kind of appliances considered in the assessment and the initial information available (Tables 3.4 and 3.5) for each of the calculation models. The colour bar at the right of each map indicates the mapping of data values into the *chrome maps*, by a monotonically increasing color scale that goes from the minimum to the maximum numeric values of the map.

Primary SA:

The relative impact of the input factors for each model is indicated through the colour tonality of the Primary chrome maps, Figures 3.10 and 3.11, and quantified in the colour bar at the right of each map. This colour variable is calculated for each appliance's Primary SA graph (e.g. Figure 3.9 for the PCs) as the Euclidean distance from the origin of the graph to the corresponding input factor point (Equation 3.51). Logarithmic values of d_1 have been used to allow visual recognition of the results in the graphical representation.

$$d_1 = \sqrt{\mu^{*2} + \sigma^2} \quad (3.51)$$

The Primary SA chrome maps can be used to identify the most suitable calculation model and relevant input information for an audit depending on the scenario or the case study. For the first case study, the *typical office*, the following four Primary SA chrome maps were obtained, one for each calculation model considered.

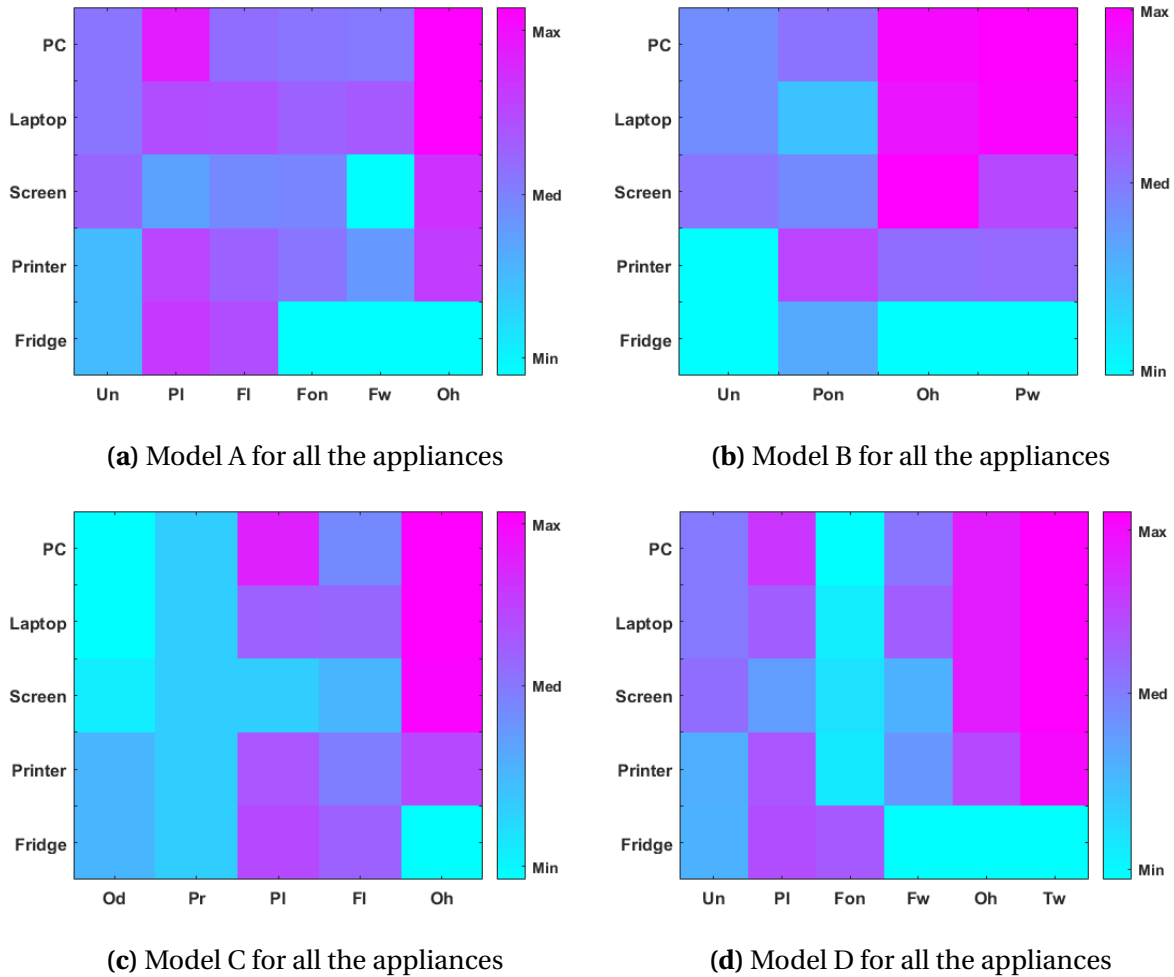


Figure 3.10: Primary SA chrome maps: impact of the different input factors (x-axis) for each of the small power considered in the typical office case study (y-axis)

The analysis of Figure 3.10 resulted in the several relevant findings.

- Regarding the appliances targeted in the study: PCs and laptops have the major relevance in the final outputs across the four calculation models. Fridges, by contrast, are not very relevant in any of the model calculations, specially in model B.
- In terms of the different input factors feeding the calculation models: The number of *Operational Hours*, *Oh*, maintains a high impact in the energy estimation of the four

models. Others high impact factors are the nominal power rates Pl for models A, C and D and the energy wastage related inputs, Pw and Tw , for models B and D.

And the less influential input factors are, the number of *Units*, Un , for model A and B and the *Occupancy density*, Od , and number of *Persons*, Pr , for models C; and the *ON Load factor*, Fon , for model D.

For the second case study, the *co-working office*, the following four Primary SA chrome maps were obtained, one for each calculation model considered.

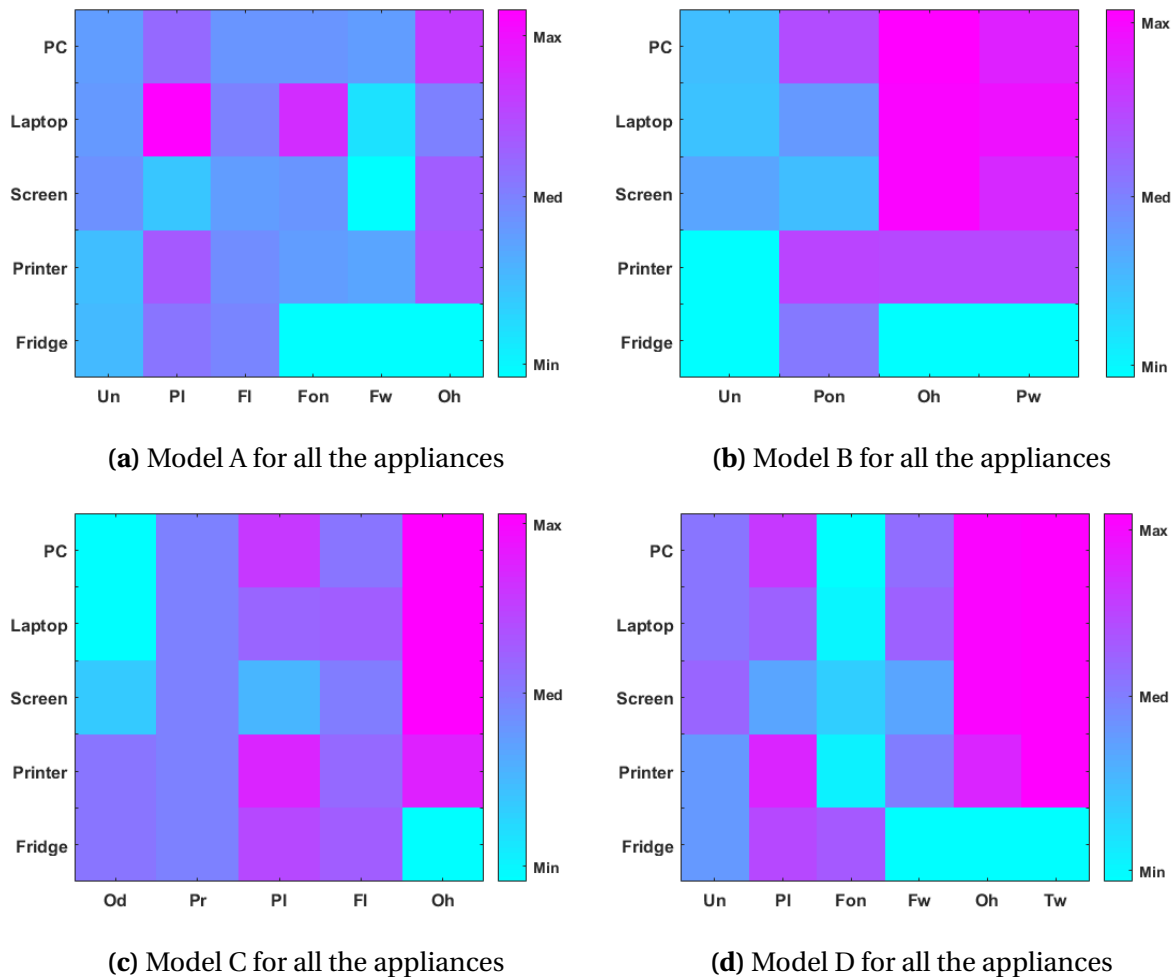


Figure 3.11: Primary SA chrome maps: impact of the different input factors (x-axis) for each of the small power considered in the co-working office case study (y-axis)

Although each chrome-map presents a case dependent input ranking for each specific calculation model, i.e. they cannot be directly compared between them, the contrast of Figures 3.10 and 3.11 provides an overview of the models sensibility depending on the case studies. Being model A the most sensible and D the less affected by the change of scenario.

The analysis of Figure 3.11 and its contrast with Figure 3.10 resulted in the several relevant findings.

- Regarding the appliances targeted in the study: PCs and laptops continue to have a major relevance in the final outputs across the four calculation models, closely followed by the Printers. Again, Fridges are the less relevant across models, although this impact has notably increased for model C.
- In terms of the different input factors feeding the calculation models: the number of *Operational Hours, Oh*, continues to have a high impact over the four models, slightly decreasing for model A and increasing for model B. The energy wastage related inputs, *Pw* and *Tw*, remains as high impact factors for models B and D and the nominal power rates, *Pl*, impact slightly decrease for models A and C.

The less influential input factors continue to be the *ON Load factor, Fon*, for model D and the number of *Units, Un*, for model A and B, although the impact of this last factor has slightly decreased. For model C, only the *Occupancy density, Od*, remains as a low influential input factors, since the relative impact of the number of *Persons, Pr*, has notably increased.

Secondary SA:

The relative complexity (e.i., the degree of non-monotonicity and deflection from the mean trend) of the input factors for each model is indicated through the colour tonality in the Secondary chrome maps, Figures 3.12 and 3.13, and quantified in the colour bar at the right of each map. This colour variable is calculated for each appliance's secondary SA graph, as the Euclidean distance from the origin of the graph to corresponding input factor point (Equation 3.52). Logarithmic values of d_2 have been used to allow visual recognition of the results in the graphical representation.

$$d_2 = \sqrt{\Phi^{*2} + Sk^2} \quad (3.52)$$

For the first case study, the *typical office*, the following four Secondary SA chrome maps were obtained, one for each calculation model considered.

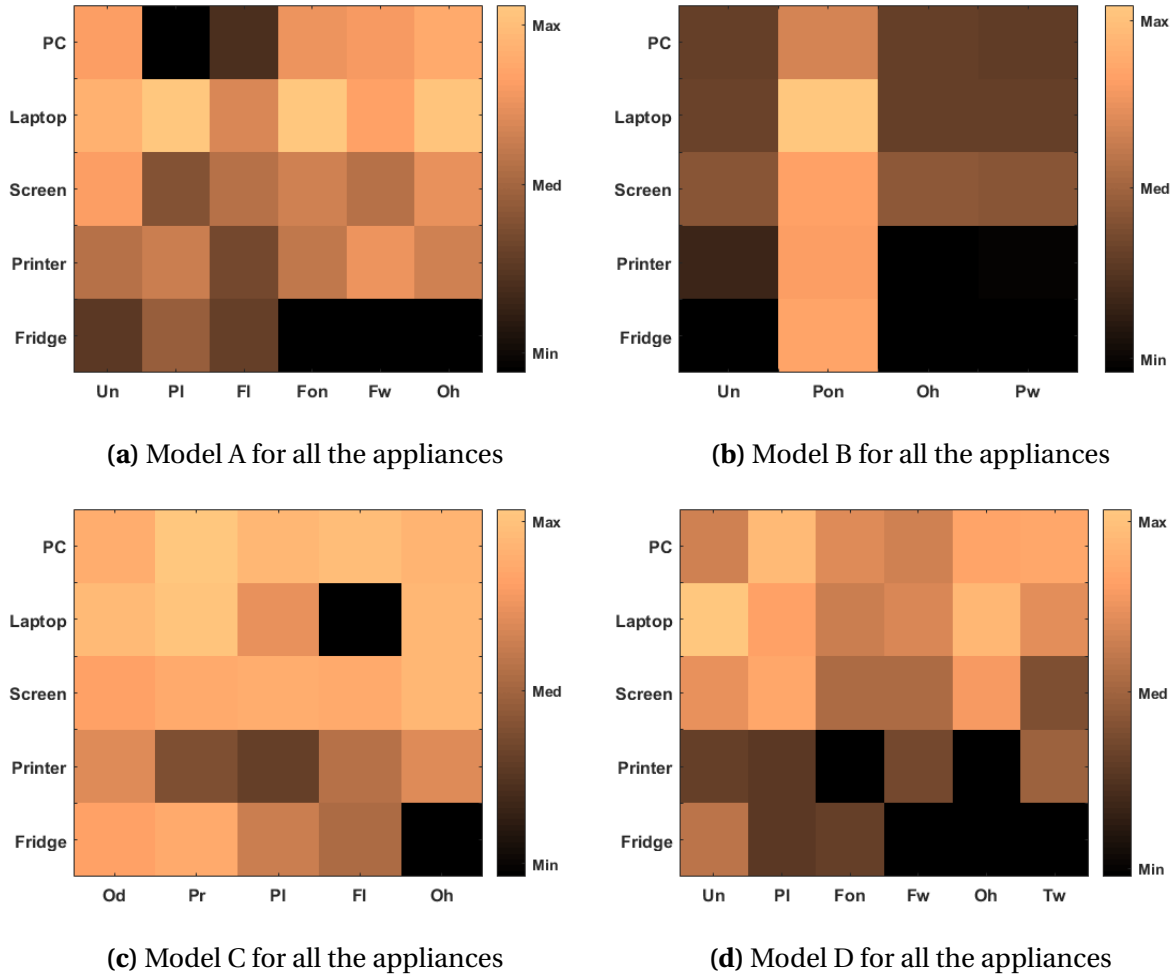


Figure 3.12: Secondary SA chrome maps: complexity of the different input factors (x-axis) for each of the small power considered in the typical office case study (y-axis)

Once the most influential inputs have been detected through the Primary SA method, the Secondary SA chrome maps in Figure 3.12 can be used to detect additional information regarding asymmetries on the output due to the input effects. This helps to understand the significance of the different input factors on the final energy estimations, as stated in some of the relevant

findings below.

- PCs, laptops and screens have the most general asymmetric behavior and fridges the most symmetric behavior across the four calculation models.
- Regarding the input factor impact on the asymmetric of the model response: the *Averaged ON Power, Pon*, have the higher impact for model B; the *Occupancy Density, Od*, and the *Number of Persons, Pr*, for model C; and the *Number of Units, Un*, for model D. The asymmetric behaviour is distributed between the different input factors for model A.

For the second case study, the *co-working office*, the following four Secondary SA chrome maps were obtained, one for each calculation model considered.

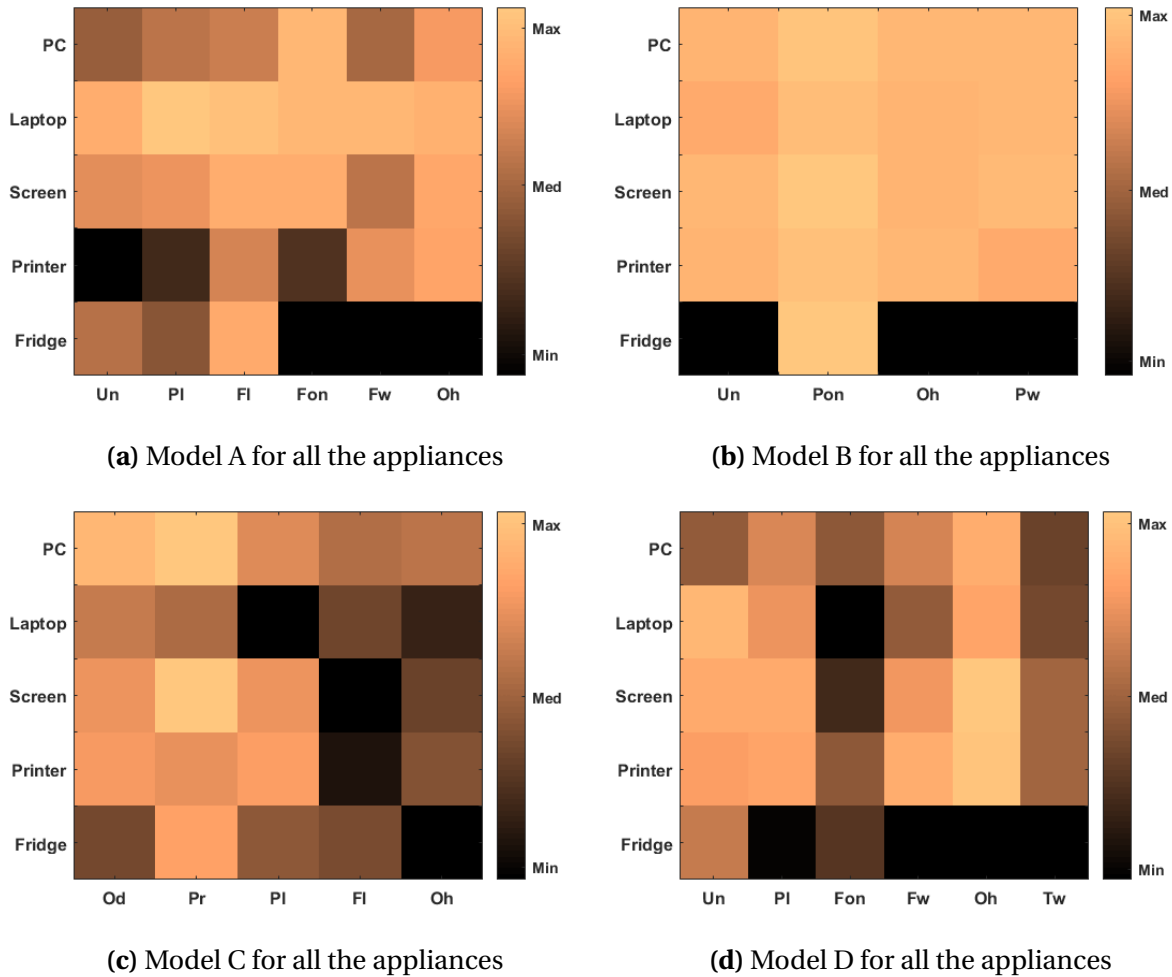


Figure 3.13: Secondary SA chrome maps: complexity of the different input factors (x-axis) for each of the small power considered in co-working office case study (y-axis)

The analysis of Figure 3.13 and its contrast with Figure 3.12 resulted in the several relevant findings. Regarding the appliances targeted in the study:

- PCs, laptops and screens continue to have a high asymmetric behavior models A and B, but this behaviour has notably decreased for model C and D.
- The low asymmetric behavior of the fridge across the four calculation models has decreased even more.

Regarding the input factor impact on the asymmetric of the model response: the *Averaged ON Power, Pon*, has the higher impact for model B; the *Occupancy Density, Od*, and the *Number of Persons, Pr*, for model C; and the *Number of Units, Un*, for model D. The asymmetric behaviour is distributed between the different input factors for model A.

- Regarding the input factor impact on the asymmetric of the model response: the high impact of *Averaged ON Power, Pon*, for model B has notably increased, as well as the impact of the *Load factor, Fl*, for model A and the impact of the *Number of Units, Un* for model D. The *Occupancy Density, Od*, and the *Number of Persons, Pr*, remain with similar high impact for model C.

3.4 Summary and discussion

Previous work documented the effectiveness of SA methods for the evaluation of calculation models in several fields [53–55], including energy calculation models in buildings [56]. However, these studies have not focused on small powers, even though these types of power are considered to be a major source of uncertainty for energy audits. In this chapter, a SA method for evaluating the influence of small power on energy estimations has been defined and tested by two case studies, a detailed methodology of the process and relevant results have also been presented.

To create the new SA method, the established Morris method has been modified through a number of adaptive refinement measures in order to overcome the deficiencies of this last SA method when implemented in calculation approaches for small power loads. These adaptive refinement measures related to what was called the *space of experimentation*: re-scaling the input factors' value ranges for homogenising the space and performing a systematic evaluation of all its points; and also to the *elementary effect distributions* of each input: standardising their

estimation factors, incorporating an additional analysis of the symmetry of the distribution, and providing a visual representation of the results in the shape of chrome-maps.

The resulting adapted method provides two levels of analysis. Firstly, the *Primary SA* creates an initial ranking of the input factors according to the overall significance of the input over the output. Secondly, the *Secondary SA* supplies additional information about the monotonicity and skewness on the output value distribution due to each input. Through these two levels of analysis, the method helps to determine the input factors that contribute most to the output variability and to determine the calculation model that best works for a specific energy audit scenario, depending on the appliances and information sources available.

To test the practicability of the new SA method, a case study has been proposed. For this, four different calculation models, operating under the CIBSE TM22 methodology umbrella, were chosen and a range of input values for a set of small powers obtained from established industrial benchmarking sources and assumptions based on previous audits for two different case studies or scenarios: a typical office with a fix number of staffs performing administrative work and a co-working space with a fluctuating number of stuffs from different backgrounds and companies sharing work-space.

Chrome-maps obtained from the implementation of the Primary SA highlighted the appliances with a major relevance in the final estimation output; data from these appliances should be made a priority during the audit, such as the PC and laptop, and the appliances that, by contrast, are not very relevant and simple benchmarking can be used, such as the fridges, across the four evaluated calculation models for both case studies.

This intial SA also identify a number of *High Impact* inputs , such as the number of operational hours and the energy wastage related inputs for models B and D, which means more effort is required to reduce uncertainty in their value ranges in both case studies whichever model is

chosen for the audit.

The Secondary SA chrome maps can be used to identified input factors that, although classified as *Low Impact* by the Primary SA, contain specific values that can have a complex impact on the output, i.e., they may deflect from the mean trend. As the number of Units in model A and the Occupancy Density in model C, for the first case study, and the number of Persons in model C, for the second case study. Special care needs to be taken for these factors when selecting the individual values for their input range as they can largely affect final energy estimations.

These improvements extends those proposed by Campolongo et al. [68] and of Sin et al. [63] on the generalization of Morris method, allowing it implementation for the analysis of calculation models operating under the CIBSE methodology. The improved method provides a classification of the different input factor depending on their relevance for the final model estimation, allowing to identify which input uncertainty should be chosen to reduce the most uncertainty of the model output and thereby, helping to optimize the auditors' time management and the overall audit process.

The present paper contains the first study to undertake small powers as the specific target for the SA. However, although the method was originally conceived for the specific field of small power load calculations, it could be applied to other areas of energy auditing, or areas of building services, where a formal sensitivity analysis is required. Further studies should be conducted to determine the effectiveness of extending the method to these new areas of implementation.

Chapter 4

Improving the measurement approach

4.1 Introduction

The previous chapter described the challenges related to the uncertainty associated with the information fed into the models used in the calculation approach for small power energy estimations. Moreover, it proposed a sensitivity analysis method for the identification and ranking of these sources of uncertainties which is dependent on their relation to the model output. This chapter tackles the challenges related to uncertainties associated with the metering techniques used in the measurement approach introduced in the Literature Review chapter of this thesis. The measurement approach involves some degree of monitoring. This approach offers accurate performance information to auditors and those involved in building maintenance [140]. According to Carrel et al. [7], residential energy savings that are a result of direct monitoring at the appliance level can account for up to 12 % savings of a building's overall consumption. This approach can be complex of implement, especially considering small power loads. In office buildings, small power loads account for more than 20 % of the total energy used [141], and up to 50 % in highly efficient buildings [15]. However, few practical studies about the benefits derived

from the use of direct monitoring of small power loads in office buildings have been conducted. This chapter assesses the two main measurement techniques categories, *bottom-up* and *top-down*, presented in the literature review chapter [3, 75, 76]. In the bottom-up techniques, each item is monitored individually and then summed up for the estimation of total energy consumption. Top-down techniques use the aggregated energy consumption monitored from a single central meter which is then broken down into individual items or systems, using calculation models. These last techniques offer detailed information about aggregated energy profiles with a relatively low complexity of metering infrastructure. However, break-down energy strategies for the top-down technique are based on assumptions about appliance use profiles, and therefore, increase the uncertainty of their small power energy estimations [38]. Bottom-up techniques, on the other hand, offer information at the individual system level, but these techniques can be expensive and intrusive [83]. It becomes crucial to understand the particularities of these two metering techniques, to identify the most efficient monitoring strategy for auditing different office scenarios, and to improve ways to analyse and present their information.

In order to compare these two measurement approaches, *bottom-up* and *top-down* techniques, the findings from a case study of an office building in which they are implemented are analysed. This allows identification of the benefits and disadvantages of each category and proposes further lines of research which involve alternative measurement strategies along with an study of the uncertainties associated to this new strategies.

4.2 Methodology: metering techniques for small power loads

This section presents the hardware installation used for the implementation of the two metering techniques evaluated in this chapter, along with the comparison of the corresponding data sets

obtained. To do this, two offices at the University of Reading¹ were considered for a case study. The total area, approximately 30m², is divided into two office-rooms; office A is occupied by the University's energy management team, and office B is occupied by the University's cleaning management team. Within these two rooms a total of 16 appliances were targeted for the study. Four are shared or common user appliances, made up of: one small refrigerator, two multi-use printers, and one shredder. And the remaining twelve are individual user appliances, made up of twelve desks (eight PC-based and four laptop-based). Appendix B presents a summary table with relevant information for the appliances monitored (i.e., plug meter connected, appliance type, manufacture and power rate for operative and sleep mode) and specifications for the experimental design. The appliances were monitored using two different metering techniques over a period of five non-consecutive weeks (from 18th August to 4th September, 2017; 2nd to 11th October, 2017; 6th to 13th November, 2017 and 24th November to 3rd December, 2017)

4.2.1 Monitoring hardware

To obtain the individual appliance energy consumption data, a wireless, pass-through socket monitoring system (4-noks smart plugs kit [81]) was used to monitor each targeted appliance. The power consumption data from the 16 individual appliances data are collected using individual smart plugs and sent via a gateway to a PC configured to retrieve active power averaged data every 10 seconds using a Modbus master simulator. This sample rate has been chosen due to the amount of data traffic created by the smart plugs used in the monitoring. Login intervals of less than 10 seconds have been tested, resulting in issues of data transmission. Figure 4.1 presents the topology of the 4-noks metering system experimental set-up, and Appendix C shows the schematic layout of the smart plugs distribution over the two offices case study area.

¹The selection of the monitored area was subjected to availability and suitability for the metering system connection.

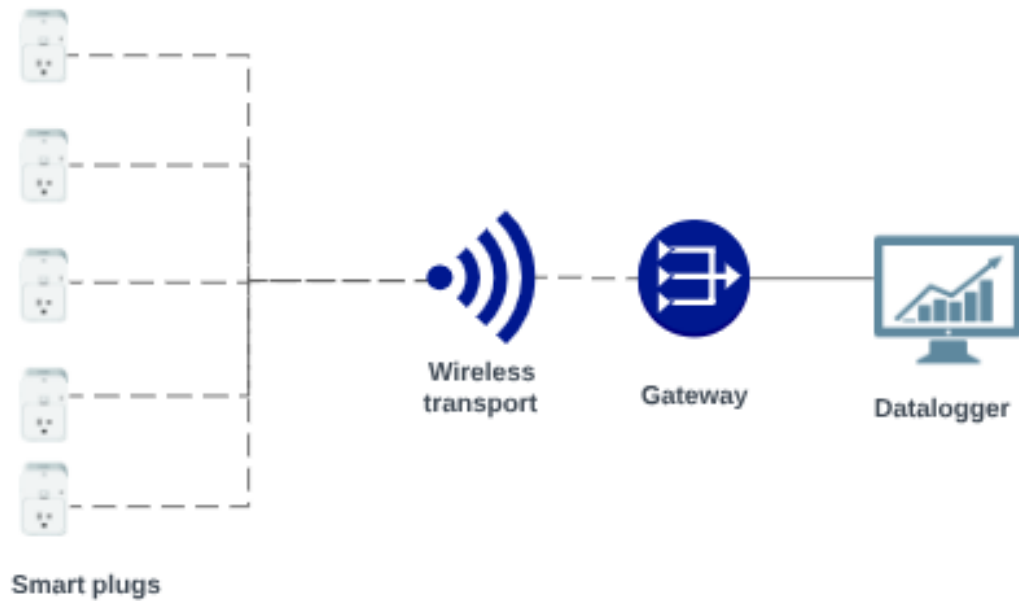


Figure 4.1: 4-noks metering system experimental set-up

The monitored appliances are fed by three separate electrical circuits (6L1 connected to phase I, 6L3 connected to phase III, and 8L1 connected to phase I) on the local distribution board that are exclusive to the case study office space. To obtain the small power aggregated load, the instantaneous active power feeding each circuit is monitored using a Measuring Transmitting Unit (MTU) manufactured by TED [78] (see Figure 4.2b). For that, current data are collected through three current transformer² (CTs) connected around each of the three electrical circuits and instantaneous voltage data from the corresponding phase (Figure 4.2a).

²The current transformer measure alternating current by producing a current in its secondary which is proportional to the current in its primary.



(a) MTU circuit and phase connectors.

(b) MTU installation in the unit board.

Figure 4.2: MTU monitoring equipment and installation.

The MTU is connected via Ethernet to a data-logger that stored the instantaneous active power readings from each of the three electrical circuits every 10 seconds³. These three datasets are

³Lower sampling frequencies showed issues in data transmission.

summed up to obtain the total energy consumed by the small powers. Table 4.1 presents the MTU monitoring layout (e.i., the wire, phase, CT connector and the appliances fed for each circuit).

Table 4.1: MTU monitoring layout explanation.

Wires	Phase*	CTs	Circuit	Appliances
Black	I	A	6L1-office A kitchen	Small fridge and instant boiler.
Red	III	B	6L3-office A right wall and office B	5 Desks, 2 printers, 1 shredder
Blue	I	C	8L1 office A main wall	7 Desks**

* From the three-phase electric power distribution system. ** Desktop computer or PC.

4.3 Result analysis

In this section, the databases obtained by each technique are compared, to establish the measure(s) of "truth" that will be used to evaluate uncertainties, along with the information provided at two different levels of analysis, the aggregated total load level and the individual appliance load level. The aim is to analyse the information provided by each metering technique and propose ways to expand it.

4.3.1 Data meter comparison

The consumption data gathered by the two metering techniques during the 43 monitored days provided two databases: one containing the 16 individual energy consumption profiles (one for each appliance targeted); and a second one with the aggregated energy consumption of all the small power feeds by the three electrical circuits under monitoring. Table 4.2 present the two

databases used to analyse the metering techniques under study.

Table 4.2: Case study data bases

Database	Data packages	Description	Meter
I	16 datasets	Individual appliances energy consumption profiles	16 Smart plugs
II	3 datasets	Aggregated appliances energy consumption profile	MTU

Both databases from Table 4.2 are compared to obtain the *profile errors* ε' (Equation 4.1) and ε'' (Equation 4.2), defined as the difference, in kWh, between the two databases total energy read, considering Database I and Database II as the "True" value, respectively.

$$\varepsilon' = \left| \frac{kWh_I - kWh_{II}}{kWh_I} \right| * 100 \quad (4.1)$$

$$\varepsilon'' = \left| \frac{kWh_{II} - kWh_I}{kWh_{II}} \right| * 100 \quad (4.2)$$

Where power kWh_I is the aggregated energy from the 16 appliance profiles of Database I and kWh_{II} from the three circuit profiles of Database II. The major sources, or cause, of these "error" during the monitoring period have been experimentally identified and are presented below:

1. Singular communication issues in the MTU causing the signal to drop to zero value.
2. An instant water boiler rated 2400W and directly connected to the mains that has only been monitored by the the MTU meter, along with other unidentified temporary small appliances (e.g., mobile phone chargers, small desk fans, etc).
3. The MTU and the smart plugs monitoring system are not exactly synchronized, i.e., their data are not continually harmonized over time.

4. Differences in the sampling procedure of both meters: the MTU sampling active power instantaneous values every 10 seconds and the Smart Plugs averaged values over a 10 second period. This difference between meter readings become more noticeable for appliances with fast active power fluctuates. Figure 4.3 presents the printer profile comparisons of the two meters during a thirty-minute period (blue for the MTU profile and red for the smart plug) as an example of this reading mismatching.

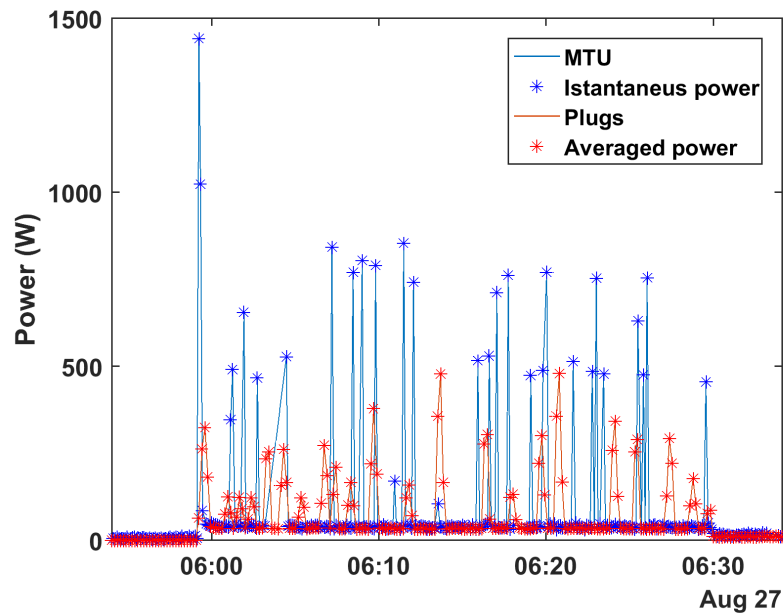


Figure 4.3: Comparisons of the MTU and Plugs power profile reads for the printer.

These differences in the readings are due to the monitoring sampling frequency restrictions that, according to the Nyquist Theorem, must be at least twice the highest analogue frequency component of the signal, which means that with a sample rate of 0.1Hz it is not possible to accurately monitor signals with frequency contents higher than 0.2Hz (profile changes happening within 20 second periods), as is the case for printers, PCs, and laptops. Individual consumption profiles for these appliances, using 100Hz sample

rate, are presented in Appendix D. According to these profiles, printers are the appliance most affected by the fourth identified error cause with sharp fluctuations of nearly 1000 W magnitude and a time interval between them of approximately eight to 20 milliseconds.

Compensation measures have been implemented for each of the identified causes of profile error. These measures do not necessarily improve the accuracy of either of the two meters, rather they reduce the differences between their readings to allow comparison between them.

1. The zero values in the MTU profiles, which are due to singular communication issues, are identified and averaged with the previous and later value. This measure assumes the average of the two closest neighbour values provides a better estimation than the zero value.
2. Peaks bigger than 200W are assumed to be caused by the instant water boiler as the remaining appliances have lower power rate nameplates. These peaks are identified in the MTU profile and removed through signal processing techniques.
3. To synchronize the monitor readings, curve fitting techniques have been used. A linear interpolation has been implemented to synchronize MTU values with those of the smart plugs. These new interpolations of the MTU values are estimations of the original readings, some degree of accuracy in the MTU profile can be lost with the implementation of this measure.

The resulting “compensated errors” during the whole 43-days monitoring period, for the minimum, maximum and averaged values after the implementation of the compensation measures, are provided in Table 4.3).

Table 4.3: Compensated errors band vales for ε'_k and ε''_k .

Error band	Minimum	Maximum	Averaged
ε'_k (%)	4.1	15.3	9.6
ε''_k (%)	3.9	13.3	9.3

In the following section the information extracted in the field of small power energy by the bottom-up (Database I) and the top-down (Database II) metering techniques at both levels, i.e., individual appliance and total energy consumption performance, is analysed and methods to expand them proposed. The different uncertainties associated with those methods considered and their energy estimation validated in accordance with the correspondent "compensated error".

4.3.2 Energy audit benefits obtained from aggregated appliances energy use data

An accurate estimation of the total energy consumed by the aggregated small powers can provide a significant improvement to the energy audit process. The performance of large office building systems, such as mechanical ventilation, heating, cooling, and lighting, are usually centrally controlled and monitored, and thus their performance parameters can be relatively easily obtained. Information relevant to small power energy performance, by contrast, is more complex to obtain. This is a result of their heterogeneous nature and high dependency on occupancy consumption behaviours. In typical audits, energy estimations are made for large systems (either using calculation models or direct monitoring), and the remaining energy is attributed to small power loads, often leading to over-estimations, and thereby causing errors for the rest of the systems energy assessed, e.g., the oversize of the air conditioning load [6]. Thus, aggregated

small power energy estimations need to be considered to ensure accurate energy audits.

Relevant existing top-down techniques are presented and discussed in the followed subsections and an alternative bottom-up method for the monitoring of aggregated appliances energy use data proposed and tested.

4.3.2.1 Analysis of top-down existing techniques

In a typical energy audit that undertakes a measurement approach, aggregated energy consumption is collected by top-down techniques and consumption profiles are usually presented in two ways, as either power consumption profiles (W), or as energy consumption profiles (kWh), the latter usually averaged per hour, day, week, etc.

Figure 4.4 shows these typical profile shapes for the MTU reading, using dataset II from Table 4.2, during two consecutive weeks (21st August to 3rd September). The top profile provides detailed information about energy consumption behaviour, i.e., when energy is being used. For a normal working day, energy consumption starts around 0430 becoming higher from 0800 to 1700, coinciding with occupancy hours. The bottom profile reports the amount of energy consumed per day, allowing an easy direct comparison between days, weeks, etc. For example, during the second weekend (2nd – 3rd September) around 1.5 kWh/day more was consumed than during the first weekend (26th – 27th August). Moreover, comparing Monday 21st (a normal working day) with Monday 28th August (an unoccupied day⁴) it can be seen than the former consumed about the double kWh energy of the latter.

⁴August bank holiday in UK.

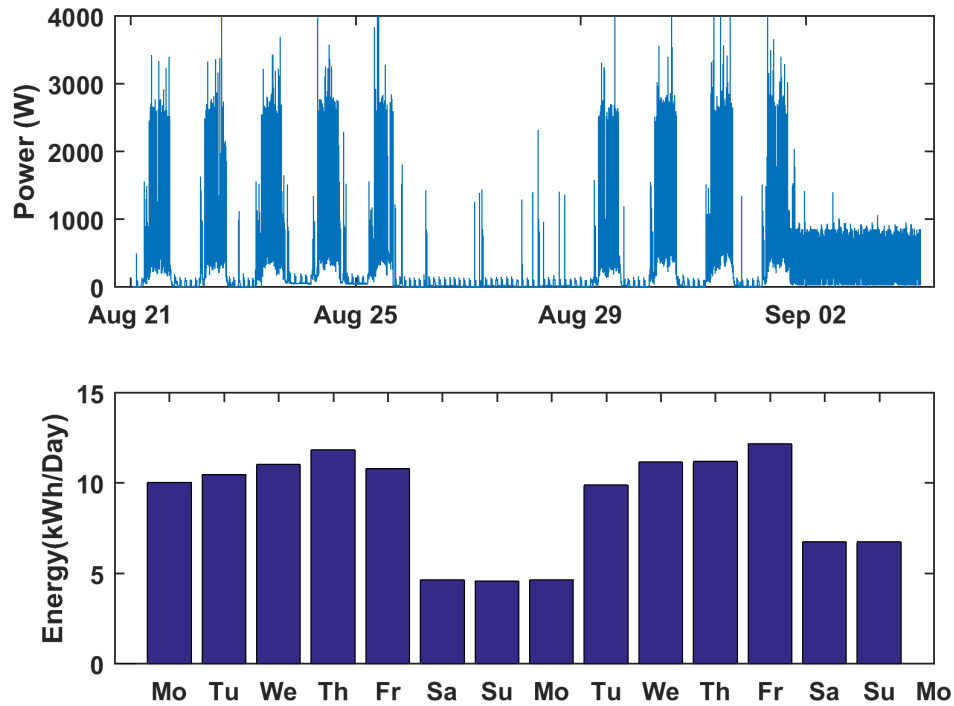


Figure 4.4: Power and energy consumption profiles from 21st August to 3rd September.

The analysis of the power and energy profiles presented in Figure 4.4 is an extended technique in energy audits and presents a useful tool to better understand energy demand and general consumption behaviours. However, they can be complex and difficult to interpret, particularly for highly variable systems such as small powers.

An alternative way to present aggregated energy profilers is the use of chromo-maps, where data magnitudes are represented by different colour intensities. These maps can be very useful for providing a picture of the overall energy performance, making occupancy pattern data visible and understandable at a glance.

Three consecutive weeks of data (from the 21st August to the 10th September)⁵ are presented

⁵This typical holiday period was chosen to evidence the influence of occupancy profiles.

in Figure 4.5, using both profile representations, power consumption lines (at the top) and a chromo-map (at the bottom). In the chromo-map graph the horizontal axis contains the 24 hours of the day, the vertical axis the days of the week stacked for three individual weekly power profiles (at 10 second sampling rate). The colour-bar at the right of the map relates the logarithmic value of the power with this color intensity scale, from maximum to minimum values, making it easier to identify peaks and base lines.

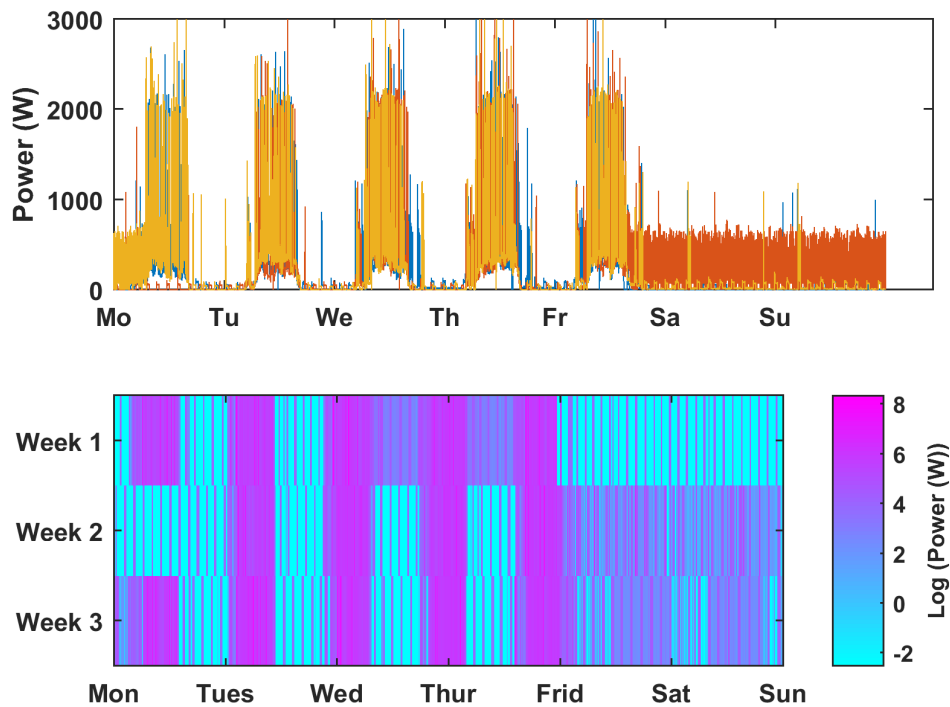


Figure 4.5: Power consumption profiles from the 21st August to the 10th September 2017

In accordance with Figure 4.5, the chromo-map representation (at the bottom) makes easier the identification of unoccupied days (e.g. Monday 28th August) and the detection of increments in the base-load energy consumption (e.g., Wednesday 23rd and Thursday 24th August, and the weekend from Friday 1st to Monday 4th September), in comparisons with the power

consumption lines representation (at the top), which makes very difficult to identify this information. Chromo-maps are, then, considered as the best visual tool for comparing weekly power consumption profiles in this case study.

Figure 4.6 presents the plot of the seven individual daily power profiles (at 10 second sampling rate) for the week of the 21st to the 27th August. Again, with both profiles, power consumption lines (at the top) and a chromo-map (at the bottom).

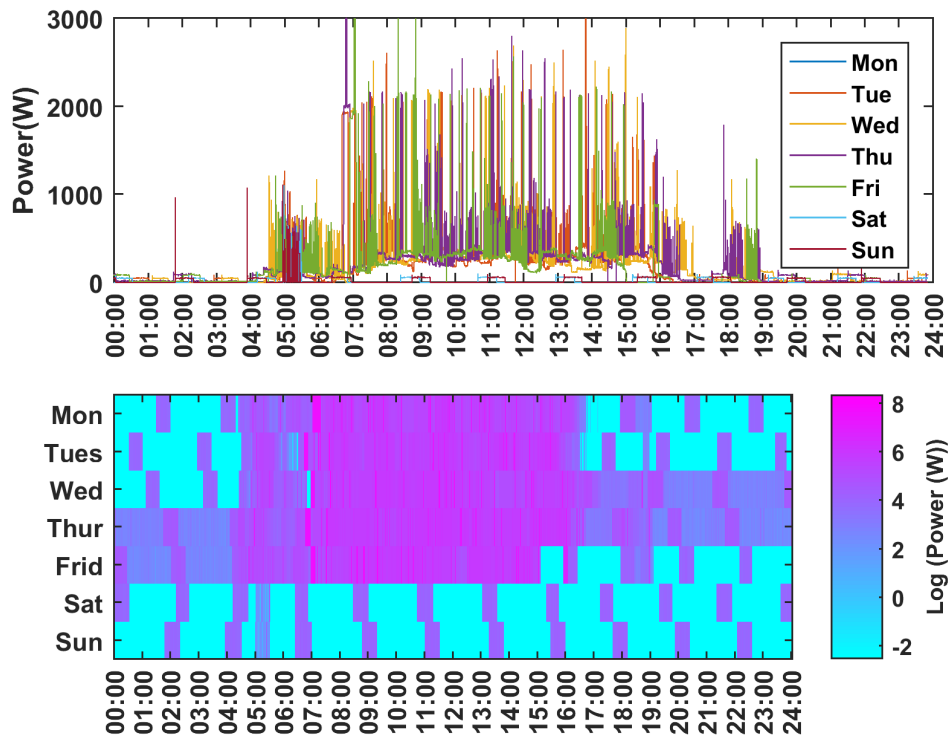


Figure 4.6: Power consumption profiles from the 21st to the 27th of August.

In contrast with Figure 4.5, the daily power consumption behavior can be observed on both profiles in Figure 4.6. The shape of these profiles indicate occupancy hours to be around 0700 to 1630, during this hours the power consumption profile is very oscillating, with a base line

of around 400 W^6 and during no occupied hours the power consumption base load, when the fridge is switched-off, is nearly null 7 .

Using the chromo-map profile irregularities such as difference between occupancy hours, e.g. a detected finish time on Friday of 1500, are easy to spot. However, for identifying the reason of unusual behaviour, such as the consumption increase of 50 W registered during the nights of Wednesday to Friday as a result of one of the hot desks being left on in room A, individual consumption profiles are needed (Figure 4.7 presents the hot desk individual power profile during 23^{rd} to 24^{th} of August monitored by a smart plug.).

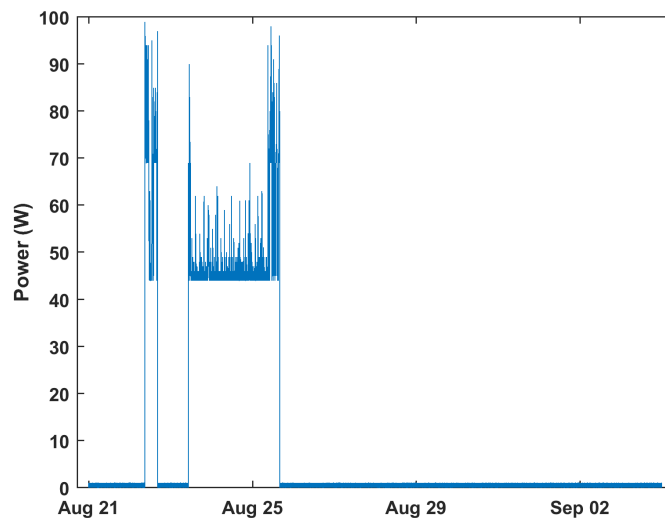


Figure 4.7: Hot desk leaved on from 23^{rd} to 24^{th} of August

4.3.2.2 Use of bottom-up techniques at the aggregated level

An important issue for bottom-up techniques, and one which has not been tackled by the literature reviewed, is the relation between the percentage of appliances monitored and the

⁶ $\log(400) \approx 6$

⁷ $\log(0.1) \approx -2$

accuracy obtained in the estimation of the aggregated energy consumed by the small power loads. To address this, an extrapolation method that provides accurate estimations of the total energy consumed for each of the possible permutations of an individual meter has been proposed. The method is implemented in four stages:

1. In the first stage, the aggregated energy collected by each of the individual meters during the monitoring period is calculated, creating a set of energy values 4.3:

$$e = \{e_i\} \quad (4.3)$$

where:

i is the meter counter ($i=1,2,\dots,n$);

n is the total number of individual meters considered;

and e_i is the total aggregated energy, in kWh, monitored by meter i during the period t .

2. In order to consider all the possibilities for the metering granularity, in the second stage of the method all of the possible permutations of the n elements from set e are obtained and the values of their elements summed up, resulting in n -sets of aggregated permuted energy values:

$$p_k = \{p_j\}_k = \left\{ \sum_1^{m_k} e_i \right\}_k \quad (4.4)$$

where:

k represents the numbers of meters considered in the permutations ($k=1,2,\dots,n$);

m_k the length of each k -permutation set, given by:

- $m_k = n! / ((n - i) i!)$; for $i < n$
- $m_n = n$; for $i = n$

and j is the value counter for the elements of the sets ($j=1,2,\dots,m_k$).

3. In the third stage, each of the previous n -sets are extrapolated for estimating the energy that would be consumed if all the 12 meters were considered, this obtained n -sets of estimated total energy values:

$$E_k = \{E_j\}_k = \{p_j * (n/k)\}_k \quad (4.5)$$

4. In the fourth and final stage, the uncertainty⁸ is expressed as a standard deviation of the dispersion of each set E_k , in accordance with Equation 4.6:

$$\sigma_k = \sqrt{\frac{1}{m_k} \sum_1^{m_k} (E_j - \mu_k)^2} \quad (4.6)$$

where μ_k is the mean of the the set E_k , and is given by Equation 4.7;

$$\mu_k = \frac{\sum_1^{m_k} E_j}{m_k} \quad (4.7)$$

and the *relative standard uncertainty percentage* (RUP) is given by Equation 4.8.

$$RUP_k = \frac{\sigma_k}{\mu_k} * 100 \quad (4.8)$$

⁸In accordance with the *EURACHEM/CITAC Guide Quantifying Uncertainty in Analytical Measurement*. [142], when the uncertainty component is evaluated experimentally, it can be expressed as a standard deviation of the dispersion of repeated measurements.

Once defined, the new proposed extrapolation method is tested by its implementation on the 12 individual desk profiles from Database I (Table 4.2)⁹. Figure 4.8 presents the RUP_k obtained for the permutations of 11 meters¹⁰.

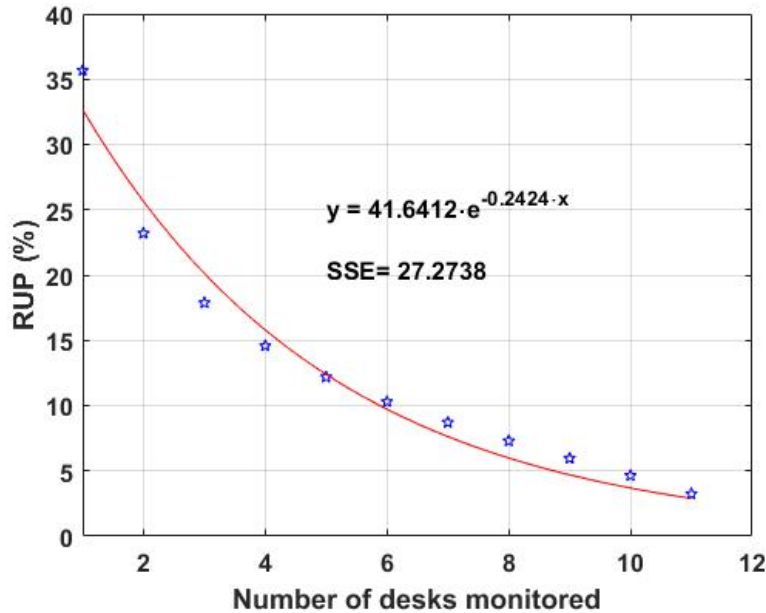


Figure 4.8: RUP of the aggregated desk energy estimation depending on the number k of meter used

In Figure 4.8, each RUP_k value is represented by a blue star and the exponential regression fitting line in red (i.e., given by the equation $y = b_1^{a_1 x}$). The fitting line shows relatively small squared errors of prediction (SSE), which means a good fit of the model to the data. The graph presents an exponential decay shape where the RUP values decay exponentially with k , a large initial value is followed by an abrupt collapse which approaches the $RUP=0$ value asymptotically. Plotting the data on a logarithmic scale rearranged them into a linear regression line, as shown in Figure 4.9.

⁹The shared appliance profiles (fridge, printers, and shredder) are considered separately.

¹⁰Note that $k=12$ is excluded from the implementation of the extrapolation method because to include it would mean monitoring the complete set of desks.

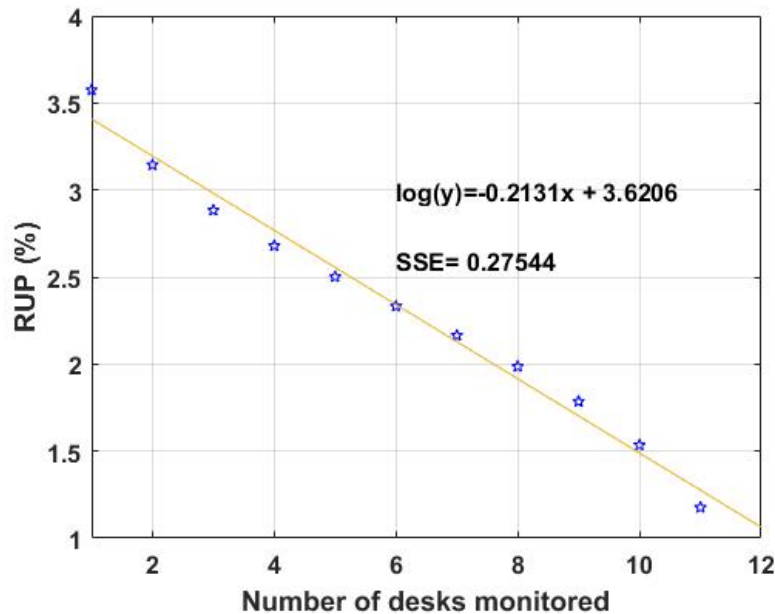


Figure 4.9: RUP logarithmic values of the aggregated desk energy estimation depending on the number k of meter used

In Figure 4.9, each RUP_k logarithmic value is represented by a blue star and the new regression fitting line is shown in yellow (i.e., given by the equation $\log(y) = a_2x + b_2$), with a similar SSE value to the exponential one. Both equations maintain the exponential-logarithmic relationship (i.e., $a_1 \approx a_2$ and $b_1 \approx \log(b_2)$). This relationship between RUP percentage and the number of meters used means that the variation between consecutive values of RUP is greater for low values of k and decreases dramatically when the number of meters used increases. Translated to the present case study, this means that, for instance, increasing the number of meters from $k=1$ to $k=6$ will achieve a reduction in the RUP of nearly 25%, but the addition of more meters would only improve the prediction by a maximum of 10%.

The study of the range in values for the different numbers of monitored appliances also provides significant additional information relevant to the statistical analysis. In Figure 4.10 each blue box represents the variation in samples of one set E_k , and offers a visual presentation of the degree of

dispersion of the different sets which, as shown in the graph, decreases with the increase in the number of meters. On each box, the central red mark indicates the normalised median (M_k)¹¹ for each of the correspondent number of desks monitored, given by the middle value separating the greater and lesser halves of the data set, the bottom and top edges of the box indicate the 25th and 75th percentiles, respectively, and the whiskers extend to the most extreme data points without considering outliers, which are plotted individually using the '+' symbol. The last "box" appears as a single line because the set E_{12} contains only one energy estimation value.

The confidence interval limits for each set E_k are defined by Equation 4.9.

$$CI_k = \mu_k \pm t_{1-\alpha/2, m_k-1} \frac{\sigma_k}{\sqrt{m_k}} \quad (4.9)$$

where μ_k is the mean (considered as the "true" value by the method), σ_k the standard deviation and m_k the size of each set E_k ; and α is the desired significance level, that defines the confidence coefficient $1 - \alpha$. The upper and lower limits for each mean μ_k provided by a 95% two-sided confidence interval are also represented in Figure 4.10 by a green and pink asterisk respectively.

¹¹Each median value is divided by its correspondent mean value.

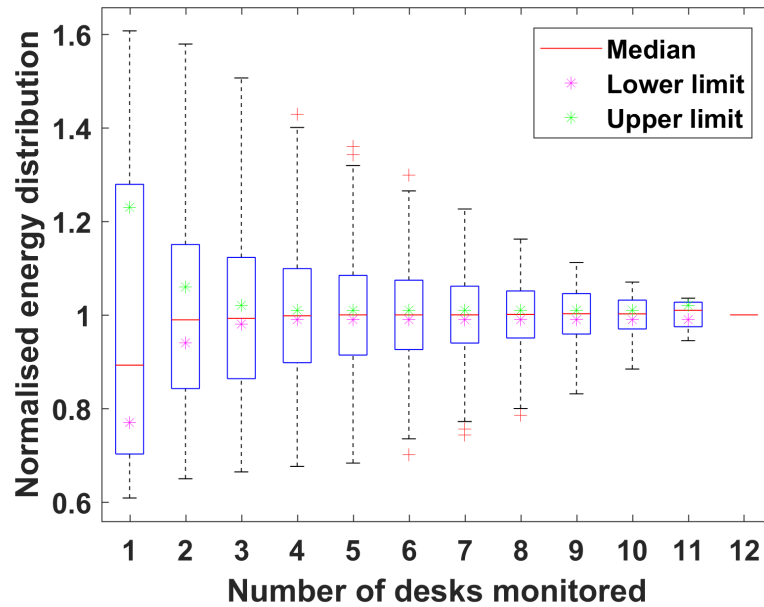


Figure 4.10: Box plot graphical of the normalised energy distribution against the number of desks monitored.

The confidence interval is an indication of how much uncertainty there is in the method estimation of the "true" value (defined as the mean of the distribution). A low number of desks monitored in Figure 4.10 provides wider confidence intervals, meaning more uncertainty in the method estimation.

The skewness of the E_k set distribution can be also analysed, as a measure of the asymmetry, or more precisely, the lack of symmetry of the data around the sample mean. This magnitude contains relevant information, indicating the degree of dispersion and existing outlier values in the data, which are values behaving outside general. If the skewness is negative, the data are spread out more to the left of the mean than to the right. If it is positive, the data are spread out more to the right, zero representing a normal distribution. The skewness percentage S_k of each energy estimated set E_k is defined by Equation 4.10.

$$S_k = \frac{\frac{1}{m_k} \sum_1^{m_k} (E_j - \mu_k)^3}{\left(\sqrt{\frac{1}{m_k} \sum_1^{m_k} (E_j - \mu_k)^2} \right)^3} * 100 \quad (4.10)$$

Figure 4.11 represents the skewness percentages for each E_k against the number of meters used.

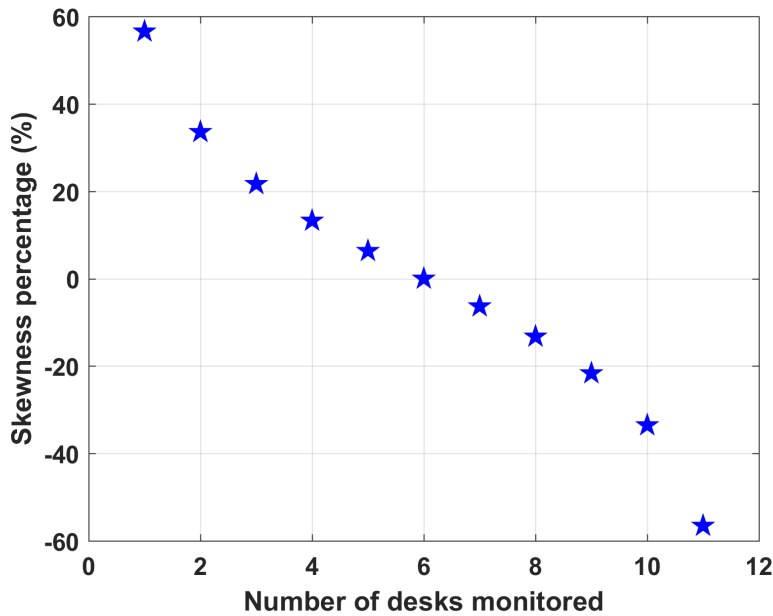


Figure 4.11: Skewness percentage of the energy distribution set against the number of meter.

In accordance with Figure 4.11, only the set E_6 has a normal distribution, i.e. the possibilities of over-estimated or lower-estimated the results are 50%-50%. The use of more meters will result in the probability of over-estimate the total energy consumption values up to nearly 60% for $k=1$ (right skewness of the distribution); and the use of fewer meters will result in the probability of an under-estimation of these values down to nearly 60% for $k=11$ (left skewness of the distribution).

4.3.2.3 Bottom-up method validation

The aggregated energy consumed by the four shared appliance profiles from Database I (i.e., one fridge, two printers, and one shredder) is subtracted from the MTU total energy read (Database II) and this new energy value divided by the mean μ_{12} (from Equation 4.7), obtaining a normalised MTU energy value (KWh_{II-Sh}). This new value is compared with each of the median (M_k) estimated by the extrapolation method in accordance with Equation 4.11.

$$\varepsilon'_k = \left| \frac{KWh_{II-Sh} - M_k}{KWh_{II-Sh}} \right| * 100 \quad (4.11)$$

Where ε'_k is the *error*, or difference, between the MTU energy read and the extrapolation method estimations. The relative error ε'_k for each of the twelve method estimations during the monitored period is given by Table 4.4.

Table 4.4: Relative error for each of the extrapolation method estimations

Desk	1	2	3	4	5	6	7	8	9	10	11
M_k	0.892	0.989	0.993	0.998	1.000	1.000	1.000	1.001	1.002	1.002	1.010
ε'_k (%)	23.0	14.7	14.4	13.9	13.8	13.8	13.8	13.7	13.6	13.6	12.9

This comparative value goes from 12.9% to 23%, with all the estimated values, except the one corresponding to $k=1$, below the maximum bound of ε' (15.3%) provided by the boundary Table 4.3.

The proposed extrapolation method provides a way of understanding the uncertainties associated with the proportion of the total appliances monitored. In this way, the method can serve energy auditors to decide the level of meter infrastructure needed depending on the grade of uncertainty they are willing to accept for their final energy estimations. However, further research

work should be designed for a more robust validation of the method through a comprehensive coverage of appliance loads, a larger database incorporating other classes of appliance.

4.3.3 Energy audit benefits obtained from individual appliance energy use data

Typically, end-use energy estimations in audits have been restricted to large systems and used to spot possible malfunctions and misuses, and to identify energy efficient measures, e.g., refurbishment of the system or investment in a more efficient one. Small powers, due both to their dependence on consumption behaviour and their large number, present a challenge for collecting data consumption at the individual level, for what, when monitored in energy audits, small power loads are typically considered as a unique aggregated system (i.e., miscellaneous items, office equipment, etc). However, the decrease in energy consumption of the large system in highly efficient buildings is increasing the relevance of individual small powers. This makes the identification of specific consumption behaviour (such as campaigns to switch off computers during non-occupied hours), or the replacement of high energy consumer appliances (such as old printers or fridges) efficient energy measures to consider.

The information extracted from the use of currently used bottom-up techniques are analysed, and an alternative top-down method for the monitoring of individual appliance energy use data explored and tested.

4.3.3.1 Analysis of bottom-up existing techniques

The infrastructure for bottom-up monitoring techniques is more intrusive and complex than that for top-down techniques. However, in return they provide more detailed information about consumption behaviour for individual appliances, and thus allow the identification of potential

malfunctions or inefficient appliance usage. This section explores the information collected by these techniques through a classification of the appliances into different categories based on their energy consumption profiles.

As for total aggregated energy estimations, the most popular way of presenting the consumption profiles for the different appliance types is through profiles of both power consumption (W) and energy consumption (kWh). This section presents the profiles of three different appliance types monitored during two consecutive weeks, from 18th August to 4th September, 2017, during which period the consumption behaviour and occupancy profile of the office staff was observed and registered.

Figure 4.12 presents the individual power consumption profile of the fridge in office A.

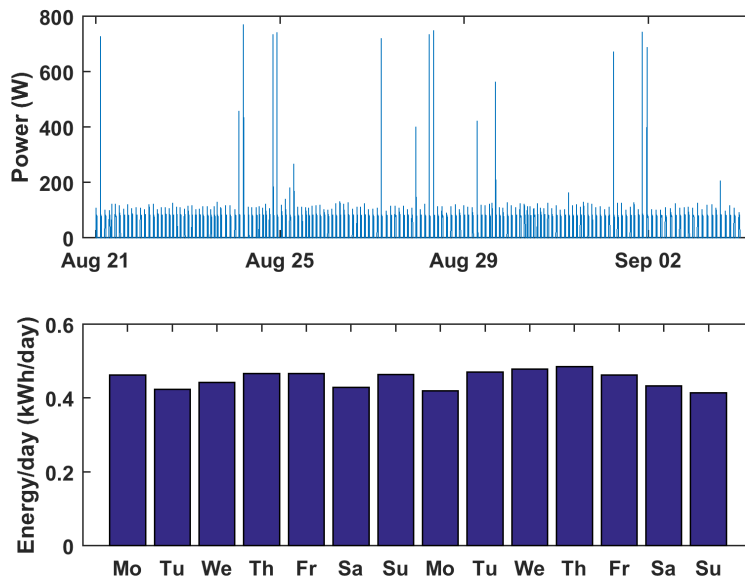


Figure 4.12: Fridge power and energy consumption profiles from 18th August to 4th September, 2017.

The profile in Figure 4.12 presents a regular shape, relatively constant during the evaluation period with a daily base line energy consumption of around 0.45 kWh. The power profile for

the fridge is also very regular. It shows a cyclical behaviour of 1 hour 36 minutes 32 seconds, comprised of one ON-period of 23 minutes 30 seconds maintaining an average power of 80 W, and one OFF-period of 1 hour 13 minutes 2 seconds, which allows the energy consumption of the fridge to be estimated at 18 Wh of constant energy consumption, or 4.3kWh per day (24 hours). The remaining difference ($0.45-0.43=0.002\text{kWh}$) is caused by the energy peaks which appear at the beginning of some ON-periods and which are due to the fridge's compressor cycle. These peaks last for a very short period of time, around 10 to 20 seconds, and have variable lengths between 100 to 800 W, which means the resolution of the meters, 10 seconds, is not enough to properly register these power peaks. The flat profile shape of the fridge evidences its low dependency on the occupancy profile, and thus benchmarking and/or calculation models can be used without a high impact on the final energy estimation for this appliance. However, there will be a risk of missing failures and/or unexpected usages.

Figure 4.13 presents the profile of a PC and a laptop based desk.

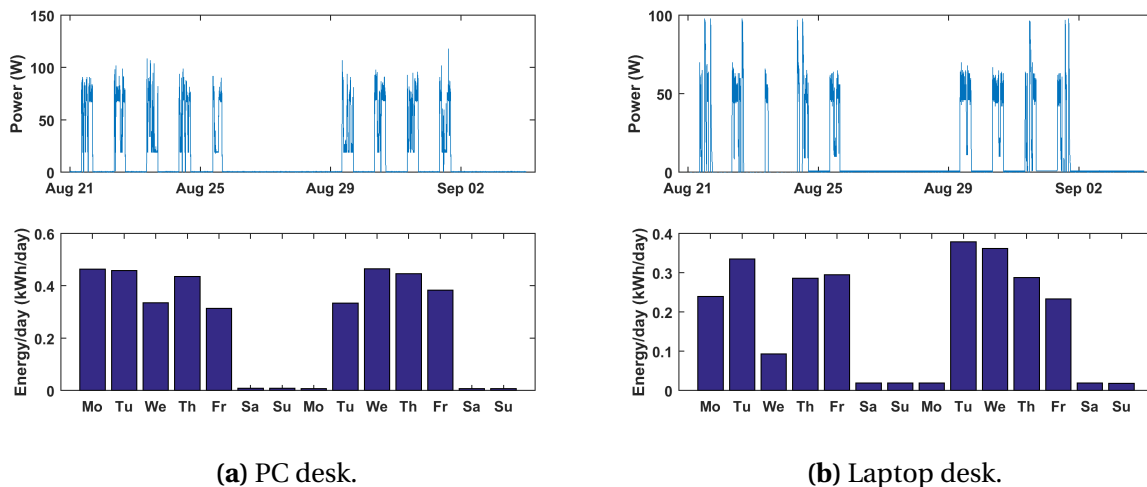


Figure 4.13: Desks power and energy consumption profiles from 18th August to 4th

Figure 4.13 presents a clear link between the desk energy profiles and the occupancy profiles.

It demonstrates a typical office hours profile, starting around 08:30 and finishing about 17:00, with null energy consumption during nights, weekends, and unoccupied days (eg., Monday 28th August). In general, the PC-based desk (see Figure 4.13a) has a higher power rate consumption and daily energy consumption than the laptop-based desk (see Figure 4.13b), although the latter has a higher continuous base line that can be observed during unoccupied days. The strong link with occupancy profiles suggests that calculation approaches can be used for this type of appliance if there is good knowledge of the occupancy times of the office (e.g., the implementation of the approximation method proposed in Section 4.3.2.2. of this chapter).

Figure 4.14 presents the profiles of the printers in offices A and B.

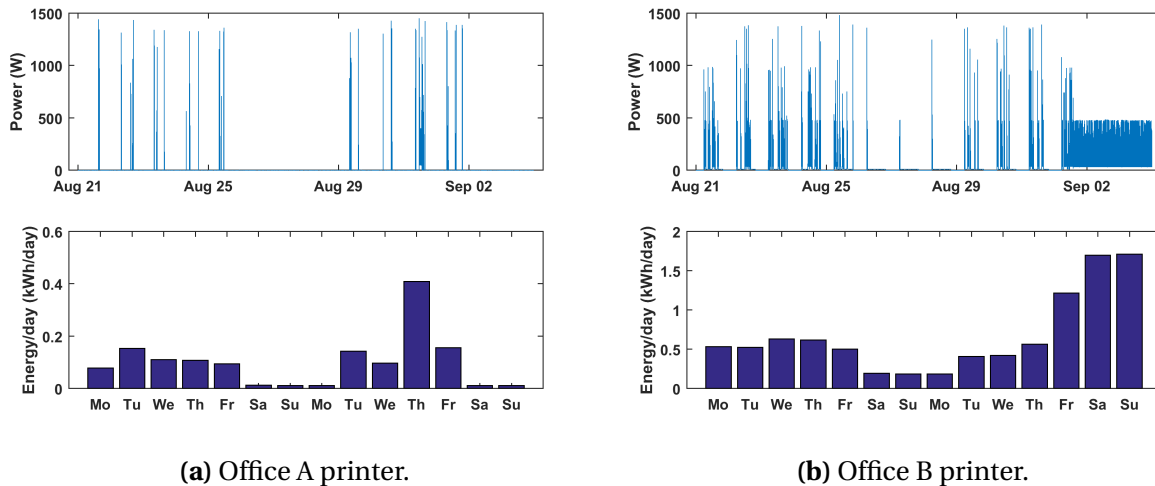
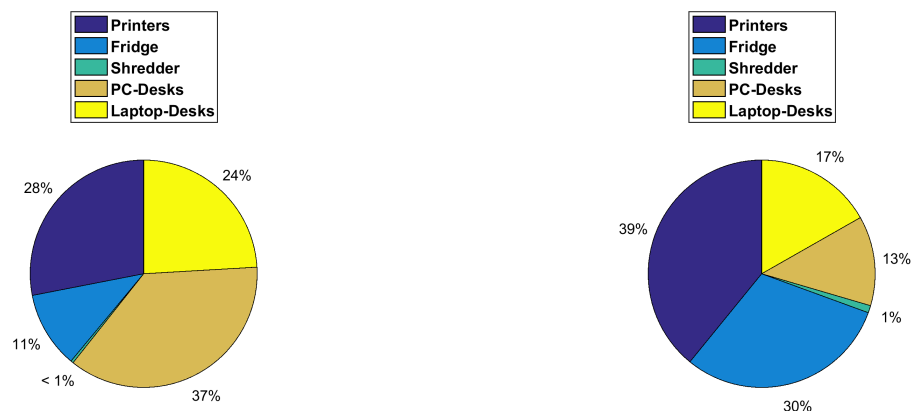


Figure 4.14: Printer power and energy consumption profiles from 18th August to 4th

The highly variable profiles, presented in Figure 4.14, for both printers suggest their energy consumption is highly dependent not only on the occupancy profiles, but also on the consumption behaviour of staff. There is no clear pattern, thus the use of benchmarking for this type of appliance can lead to a high degree of inaccuracy (e.g., during the two week period, both printers present a difference of 2.45 kWh). Figure 4.14b indicates high usage of the printer in office B

during the second weekend of monitoring, this was due to a failure in the appliance operation. Such unexpected behaviours can only be spotted through individual appliance monitoring. Bottom-up techniques can be also used to provide an overall estimation of the percentage of energy consumption by appliance type and help identify in which areas it would be more valuable to implement energy efficient measures.



(a) Energy percentage per appliance type (b) Average energy percentage per appliance unit

Figure 4.15: Energy consumption percentage classification representations.

Figure 4.15 shows two different ways of presenting the energy consumption percentage classification for the different types of appliances monitored. The first Pie chart (see Figure 4.15a), the most common representation used in energy audits, shows the energy percentage for each appliance type over the total small power consumption. According to this chart, PC desks are the most energy demanding, followed by the printer and the laptop desks. However, this ranking classification changes when the second Pie chart is considered (see Figure 4.15b) as it shows percentages according to the number of appliances in each category. According to this last classification, the printers consume the most energy, followed by the fridge. It is also interesting to note that the laptop-based desks consume more energy than the PC-based desks, even though

their power nameplates are lower, as a result of their more intense use. These analyses can be valuable for the efficient implementation of energy measures (e.g., a sensible investment regarding a possible appliance renovation would be to replace the printers.).

4.3.3.2 Use of top-down techniques at the individual appliance level

Traditional top-down end use energy break-down techniques provide an assessment for systems and equipment in energy audits, however, they need to be combined with calculation methods and, therefore, rely on assumptions that cannot guarantee the accuracy of the energy estimations [20]. Against these assumption-based energy break-down techniques, Non-Intrusive Appliance Monitoring (NIALM) techniques provide the energy consumption of the individual loads using a purely metering strategy. The method suggested by Hart [27] relies on the identification of variations in the consumption of power to detect the status (ON or OFF) of loads¹². This section proposes and implements a load status detection algorithm over the aggregated load readings collected through the MTU meter (Database II from Table 4.2), using the information from smart plugs (Database I from Table 4.2) for verification, to understand the potential capabilities of NIALM techniques in office building environments with a large number of variable loads (e.g., printers, PCs, etc), allowing research lines for further studies in the field. The event detection identification algorithms are based on Meehan et al's method [114]. In accordance with this method, a moving window of M samples from the MTU power consumption signal is used for the event detection, two conditions must be met for an event to be identified.

1. *The first condition* is that the absolute magnitude of the power signal should be greater than a certain threshold value during the established moving window.

For $S = s_1, s_2, \dots, s_i, \dots, s_n$, being n the length of the power signal, an *event* i occur when:

¹²Though more information is required to identify some kinds of loads.

$$\left| \frac{1}{M} \sum_{k=0}^{M-1} P_{RMS_{s_{i+1}}} - \frac{1}{M} \sum_{k=0}^{M-1} P_{RMS_{s_i}} \right| > \alpha \quad (4.12)$$

where P_{MTU} is the power consumption signal and α is the fixed positive threshold value for this signal, above which an event, $i \in \mathbb{N}$, is considered to have occurred; 75% of the smallest appliance's nameplate power rate has been chosen for the establishment of this parameter¹³.

2. *The second condition* that must be fulfilled is that the previous event detected must not have occurred during the threshold period T , in accordance with Equation 5.3.

$$\exists i \in \mathbb{N} \mid |t_{RMS_{event\ i}} - t_{RMS_{event\ (i+1)}}| > T \quad (4.13)$$

Where $T = (p \cdot \Delta t)$ seconds, Δt being the sampling time period and p the number of samples for establishing the threshold period.

This threshold established the steady and the transient sequences for each event, and therefore, it needs to be considered when identifying all the appliance categories presented in this chapter. For the present case study, due to the relatively large sample rate period (10 seconds), $p=1$ sample has been chosen¹⁴. Nevertheless, there remains the limitation that events that occur within the 10 second sampling period will not all be identified correctly.

If the two previous conditions are met, an event is detected and can be labeled ON or OFF depending on the direction of the change in magnitude.

For testing the potential of NIALM as an alternative top-down disaggregation method, the detection algorithm was implemented, for a few hours, over the three CT MTU input power

¹³Based on empirical tests and the Meehan et al. method [114].

¹⁴Any transient period lower than 10 seconds has been registered for the targeted appliances.

readings (Table 4.1) during the morning of the 21st of August, 2017. Figure 4.16 presents the event detection on the profile readings from circuit 6L1 which feeds the fridge and instant water boiler¹⁵.

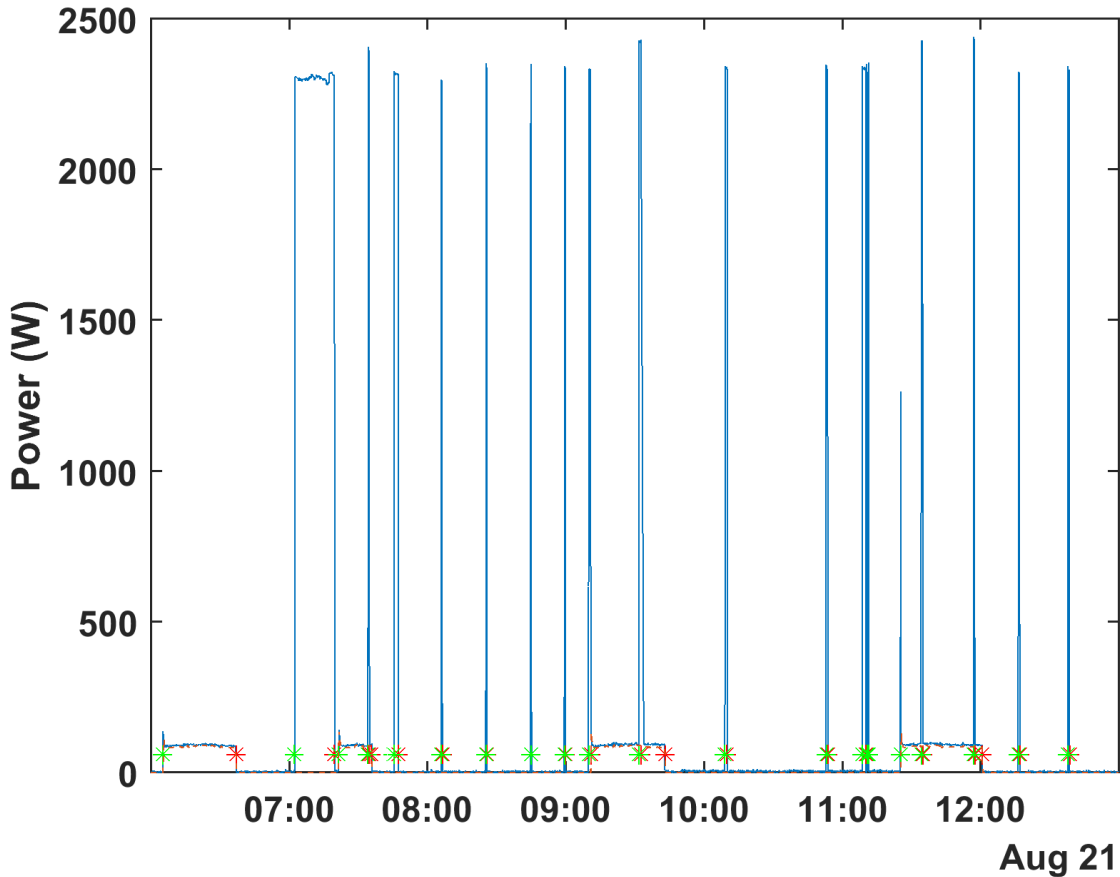


Figure 4.16: CT-A power reading event detection, for the morning of the 21st of August 2017

The electrical circuit 6L1 monitored by CT-A is the less complex in terms of disaggregation as it only contains two distinguishable appliances with large fluctuation periods in comparison to the 10 second sample rate of the meter. With this configuration, a high degree of event detection can be seen in Figure 4.16, where the MTU profile reading is presented in blue and the fridge

¹⁵The instant water boiler is only monitored by the MTU.

smart plugs in red, and switching ON and OFF events are marked with green and red asterisks, respectively.

Figure 4.17 presents the event detection on the MTU (in blue) and the individual smart plugs (red for the printer) profile readings from circuit 6L3, feeding the right wall of office A and the whole office B, with five desks, two printers, one shredder.

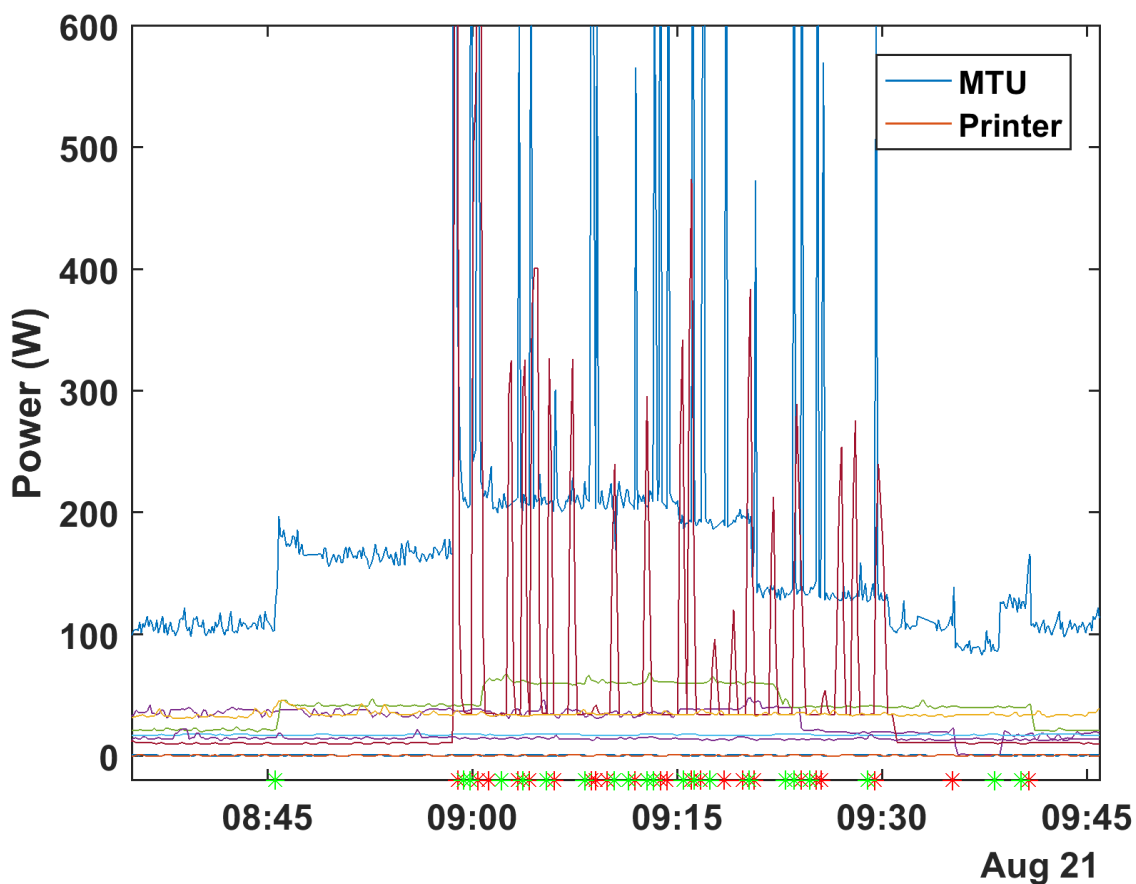


Figure 4.17: CT-B power reading event detection, for the morning of the 21st of August 2017

Much more complexity for the event detection scenario can be observed in Figure 4.17 for the electrical circuit 6L3 monitored by CT-B. This is not only due to the larger number of appliances, but also to the high operational variability of their consumption profiles. Although some degree

of event detection is achieved for the desks (before 09:00 and after 09:30), the high variability of the appliances, especially the printer (red curve) which fluctuates with a higher frequency than the meter sample reading (as explained in Appendix D), makes the process of event identification highly inaccurate when printers are operating. This can be seen in Figure 4.17 which shows the hours from 09:00 to 09:30.

Figure 4.18 presents the event detection on the profile readings from circuit 8L1 which feeds the seven desks.

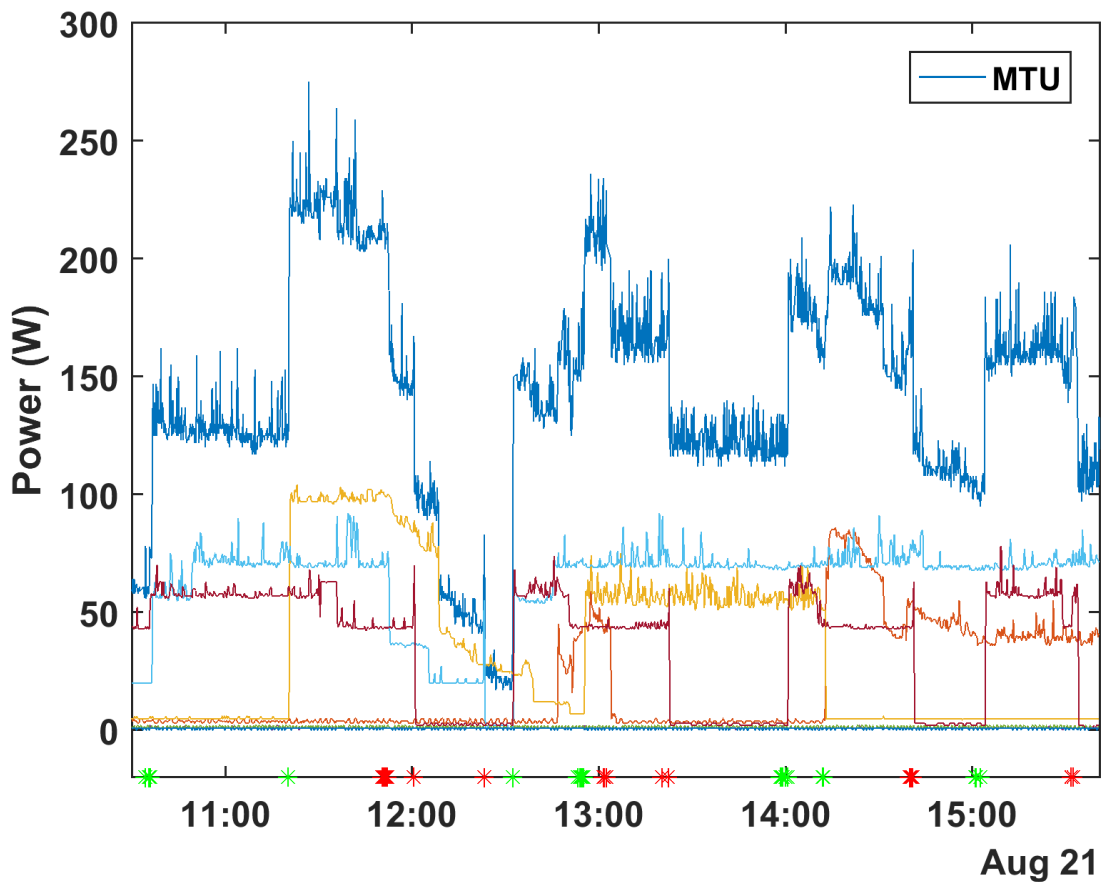


Figure 4.18: CT-C power reading event detection, for the morning of the 21st of August 2017

A larger degree of event detection with respect the previous scenarios can be also obtained for

the electrical circuit 8L1 monitored by the CT-C current clamp, as seen in Figure 4.18, where MTU reading are presented in blue and the individual smart plugs readings in different colours. This is because although desks have a high fluctuation variability, (around 200 millisecond period) these fluctuations are relatively small when compared with their averaged power rate magnitudes (around 20 W), as explained in Appendix D. Therefore, fluctuations do not interfere with the power threshold given the first condition of the proposed event detection method. However, there is the issue of event overlapping, as can be observed between 12:00 and 13:00, where some events are not being detected due to their proximity to each other in time (i.e, lower than the time threshold T given in the second condition of the proposed event method).

4.3.3.3 Top-down method validation

For the method validation, the seven desks fed by the electrical circuit 8L1 and monitored by the CT-C current clamp have been considered. The aggregated number of operational ,or *ON-status*, hours of the desks have been identified by the load status detection algorithm during the week from 21st to 28th of August (138.66 hours assuming there is not event overlapping) and multiplied by an averaged desk power consumption (82W¹⁶ assumed to be constant for all desks). Figure 4.19 shows the switching on (green dots) and off (red circles) events detected by the algorithm during the validation period.

¹⁶Average power consumption for PCs, laptops and monitors from CIBSE Guide F [143].

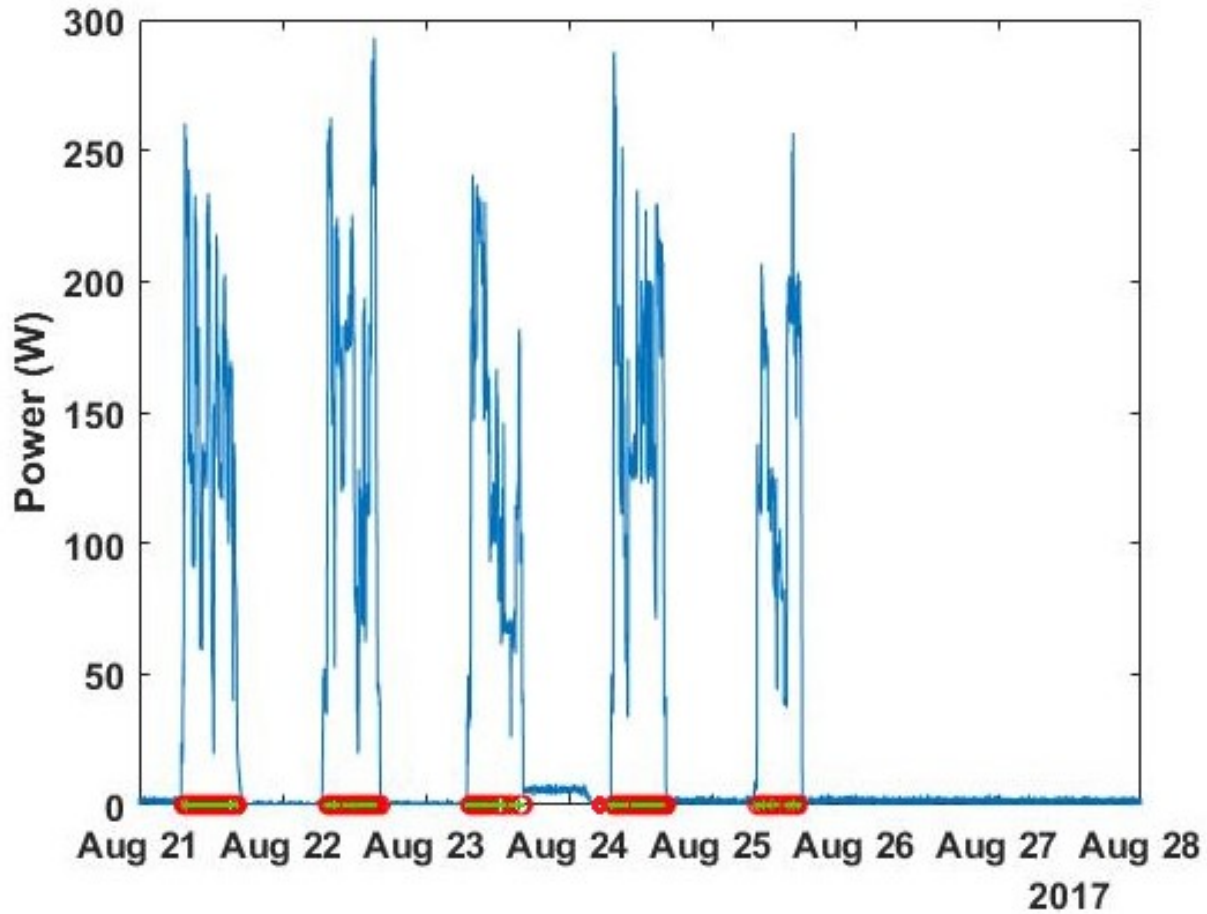


Figure 4.19: Detected switching on and off events in circuit 6L3 from 21st to 28th of August.

Assuming an equitable consumption, the energy estimated for each desk will be $KWh_{NIALM, j} = 1.57kWh$. This estimation is compared with the total energy monitored by each of the seven correspondent plug meters ($KWh_{plug j}$ from Database I), in accordance with Equation 4.14.

$$\varepsilon_j'' = \left| \frac{KWh_{plug j} - KWh_{NIALM}}{KWh_{plug j}} \right| * 100 \quad (4.14)$$

Where ε_j'' is the *error*, or difference, between each of the individual plug meter energy read and the NIALM method estimations. The relative error ε_j'' for each of the seven desk monitored is

provide by Table 4.5.

Table 4.5: Relative error for each of the NIALM method estimations.

Desk	1	2	3	4	5	6	7
$KWh_{plug, j}$	1.34	1.46	2.07	1.44	1.49	1.59	1.16
ϵ_j'' (%)	17.2	7.5	24.1	9.0	5.4	1.2	35.3

This comparative value goes from 1.2% to 35.3%, with an averaged percentage error of 14.2%, nearly coinciding with the maximum bound of ϵ'' (13.3%) provided by the boundary Table 4.3. A relative low error in the estimations, considering the assumptions made about the appliances power rates and the issues of event overlaps.

This practical implementation does not constitute a rigorous validation of the NIALM method, rather it presents an example of the potential capabilities of this techniques and a visual indication of some of the issues raised by this implementation in a real case. It also informs further research lines that should be followed to properly implement NIALM techniques for small power disaggregation.

4.4 Summary and discussion

The implementation of measurement techniques for small power monitoring currently face a number of challenges concerning metering infrastructure and interpretation of the collected data. The overall energy contribution of small appliances, especially for office areas, has been recognised, however, a rigorous study for better understanding and overcoming the challenges has still not been undertaken.

In this chapter, two common measurement techniques first introduced in the literature review, bottom-up and top-down, have been implemented in a case study office using two different

monitoring systems: a set of smart plugs for bottom-up techniques; and a centralised meter directly connected to the mains for the top-down techniques. The corresponding databases obtained for each technique have been analysed and compared in order to understand the causes for their differences. These causes are associated with the different technologies used in the meters and in the implementation of the infrastructure (e.g., synchronization, sampling frequency, appliances that can be monitored only by the central meter, etc). Once identified, a number of compensation measures have been proposed to neutralize these differences, establishing a set of error boundary values for allowing comparison and methods validation. The information extracted in the field of small power by these two monitoring techniques and the potential benefits derived from their use have been explored and compared. This analysis has been done at two monitoring levels, the aggregated and the individual appliance energy end-use. Regarding small power energy assessment at the aggregated level, a number of graphical tools were implemented to present and analyse the centralised meter's data (i.e., the top-down technique's data), including a comparison of typical energy profile representations and chromo-maps. The benefits of the latter graphic representation for providing a better picture of the overall energy performance have been recognised (e.g. occupancy patterns and irregular data are visible at a glance and easier to interpret and compare). The benefits of the use of bottom-up techniques at this monitoring level have also been explored. For that, the relation between the number of appliances monitored and the accuracy obtained in the estimation of the total energy consumption have been considered. To facilitate this, a statistical extrapolation method was created and implemented in a practical study. The method provides a statistical technique to calculate this relation and inform the probability of over- or under-estimations of energy use depending on the percentage of appliances monitored. This method informs auditors about the level of monitoring granularity needed to achieve the required accuracy standards for their energy consumption

estimations.

Regarding small power energy assessment at the individual level, the energy profiles from the smart plugs readings (i.e., the bottom-up technique) have been classified based on occupancy and energy consumption behaviour, considering the impact of substituting the use of direct metering by benchmarking and calculation models. Accordingly, for appliances such as fridges, which have continuous cyclical profiles, direct monitoring can be substituted by benchmarking without greatly affecting energy consumption estimations. For others, such as those associated with an individual user, like PCs and laptops, calculation approaches are suitable if occupancy profiles are well known. However, individual monitoring would be advisable for shared appliances, such as printers, which are highly dependent on consumption behaviours. It is, nevertheless, important for auditors to consider that the use of benchmarking and/or calculation models carries the risk of missing information regarding the identification of mis-usage and any irregular performance of specific appliances. To explore the use of top-down techniques at this individual level, a method for load status detection is proposed and implemented in a case study. The method, based on two detection conditions, constituted the first step for NIALM implementation. The NIALM technique has the benefits of the bottom-up approach, but with the low level of infrastructure and intrusiveness of the top-down approach. Visual examples, from the case study are provided which demonstrate the capabilities of NIALM techniques and, although the study does not constitute a rigorous validation for the method, it informs further research lines that should be followed for the efficient implementation of NIALM techniques in small power disaggregation. Some important practical issues have also been highlighted, such as the need for a high sampling frequency rate for small power disaggregation.

From the analysis of the two measurement techniques implemented in this research study, two novel contributions have been obtained: the formulation of an extrapolation method, using

bottom-up techniques at the aggregated level, and the exploration of NIALM method capabilities, using top-down techniques at the individual level. These two contributions constitute a notable improvement in the field of data analysis and energy auditing, since they pursue the same information which is achieved when monitoring at individual appliance level, but propose a lower metering infrastructure configuration than traditional measurement techniques. Both methods were implementing for the case study, including an analysis of the uncertainties associated with their energy estimations and a validation assessment based on the error boundaries established at the beginning of the chapter. Limitations which should direct future research for both method have also been described, such as the convenience for a more comprehensive coverage of appliance loads for the extrapolation method and the need for more robust signature values for NIALM methods implementation. This last issue constitutes the central research topic of the next chapter.

Chapter 5

NIALM performance for small load appliance identification

5.1 Introduction

The previous chapter tackled the challenges faced by classical measurement techniques, analyzing the benefits and drawbacks of their implementation at two levels of appliance load monitoring: aggregated and individual. For the latter, the potential capabilities of NIALM techniques for load disaggregation have been proved along with the identification of a number of factors that prevent them to be extensively implemented in energy audits. Further research work has been suggested for this specific area. This chapter undertakes this this line of research and delves into those factors, as well as into the uncertainty associated with NIALM techniques for small power load disaggregation in offices.

The benefits of NIALM techniques for the disaggregation of small power in domestic buildings has also been tested by a number of researchers [88, 97] since the technique was first introduced

in 1989 [111], and this has led to the development of numerous NIALM methods. However, the implementation of these methods is limited to the domestic sector with its smaller number of loads in comparison to those of commercial buildings. Despite the fact that the potential benefits of applying this technology to commercial buildings have been recognized from the field's foundation [144], most NIALM methods are not directly applied to commercial buildings [28]. According to Hart [27], electrical signatures are defined as the characteristic features extracted from the current and voltage signal that can be resolved to separate individual appliance loads and so provide information about the activity of individual appliances. This chapter considers that the lack of understanding of the optimal electrical signatures combination in the disaggregation process is a fundamental reason for not extending the use of NIALMs to the commercial sector. In order to tackle this issue, a typical generic NIALM method is considered and implemented using a set of electrical signatures under the classification framework suggested in the literature review section of this thesis. Under the hypothesis that a better understanding of the signatures electrical characteristics would provide the necessary information for successfully implement NIALM methods in energy audits, experiments which recreate residential and office environments have been conducted to compare the disaggregation capabilities of each signature category dependent on the types and number of appliances under monitoring. The novel contribution of this chapter, therefore, is not in the implementation of the NIALM method itself, but in the analysis of the disaggregation capabilities of the different combinations of signature categories.

The findings described in this chapter outline the aspects which most influence the effectiveness of existing NIALM method regarding the electrical signatures combination used and constitute a knowledge contribution to the field of NIALM methods implementation in energy audits for office buildings.

5.2 Methodology

The most commonly used NIALM methods have several principle stages: firstly, the use of a monitoring system to obtain the consumption signal; secondly, implementation of an ON/OFF event detection algorithm; thirdly, the extraction of a specific electrical signature; and finally, the implementation of a disaggregation algorithm which is first trained, using an individual appliance profiles database, and then used to separate individual appliance loads from the overall signal.

In order to establish a generic method, this section covers the four stages of a common NIALM method, presented in Figure 5.1. A detailed explanation of each of the stages justifies the decisions made for the method establishment, including the selection of the different electrical signatures, a fundamental part of this study.

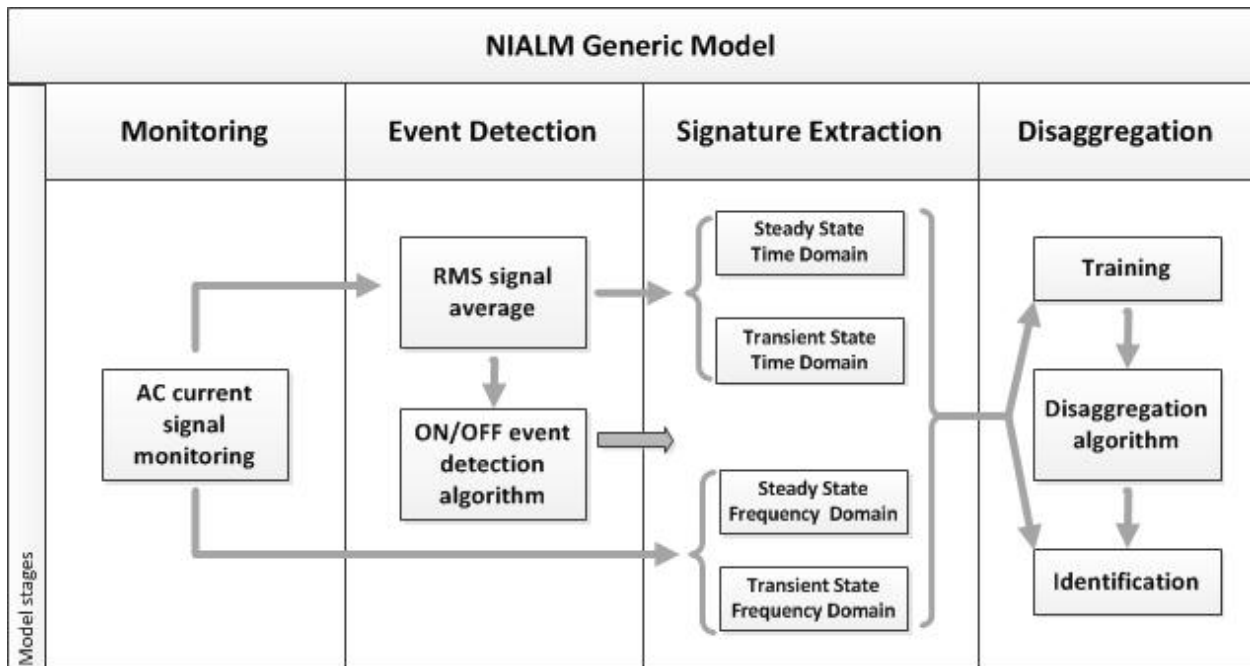


Figure 5.1: NIALM model work flow

Once the generic NIALM method is established and the experimental data set up, the model is implemented for individual appliance identification and in an experimental case study which recreates a house and an office area.

5.2.1 First NIALM stage: Monitoring system installation

The first step in the implementation of a typical NIALM method is the selection of an appropriate monitoring system (sensor and raw data acquisition hardware). This allows the acquisition of aggregated load data at an adequate sample frequency rate and resolution to identify distinctive load patterns and electrical characteristics. Prior to the selection of the monitoring system, a number of technical requirements need to be considered. These are discussed in the following section.

5.2.1.1 Monitoring equipment considerations

There are a wide variety of data acquisition systems on the market which are designed to measure the aggregated load of a building [91]. In order to choose the most suitable monitoring device for small power disaggregation in office buildings, a number of technical requirements and constraints need to be considered:

- the resolution of the hardware should supersede the value of the magnitude under monitoring. The closer the magnitude value to the error, the lower the accuracy of the method;
- the electrical grid in the UK runs at a 50Hz cycle (period of 0.02 seconds), so according to the NyquistShannon theorem [96], a minimum of 100 Hz sample rate (a period of 0.01 seconds) is needed for an analysis of wave shape and signal changes;
- another sampling frequency issue to consider is the probability of event simultaneity,

the probability of which increases with the number of appliances on the network being monitored, or when a short-cycle appliance is in operation;

- with regard to the sampling frequency, the 1 to 15 kHz range is of particular interest (although little work has been done in these frequencies), since this is where harmonics would begin to become available. The noise captured using frequencies higher than 15 kHz is likely to obscure any gains in signal detection for commercial buildings [98], and so sets a maximum sample rate;
- medium-high frequency metering equipment is more expensive than low frequency sampling meters. There are a large number of commercially available 1 Hz meters, these are considered to be medium-high frequency, [98]; and
- there are hardware limitation issues, e.g., data gathering traffic, storage capacity, data streaming, etc, which increase with the sample frequency.

The 1 kHz sample rate range is, then, of particular interest since it is at this frequency that transient features begin to be captured with no excessive high frequency noise.

According to these considerations, a high-resolution monitoring system, which collects at a sample rate of 1 millisecond, has been chosen for the experimental set up of the present study, ensuring quality of information at low data management complexity. The monitoring system consists of a 15 A extension cord to which the different appliances were plugged. For safety reasons, no direct connections were made to the wires of the cord, instead a security box was created to house a current transformer, thereby allowing safe data collection. For this, a Pico current [145] data logger¹ is connected to a portion of the live cable line separated from the extension cord and extracted outside the box, creating a short loop. The live conductor cable loop

¹The logger has 2% of vertical resolution over the total reading.

is protected by heat shrink sleeving so that the entire assembly is safely and doubly insulated. The current data logger is used in combination with a 2204 PicoScope [11] that collects, and then stores, current data at a sample rate of 1 millisecond. These data can be accessed via USB for subsequent analysis. The different components of the high-resolution monitoring system are presented in Figure 5.2.

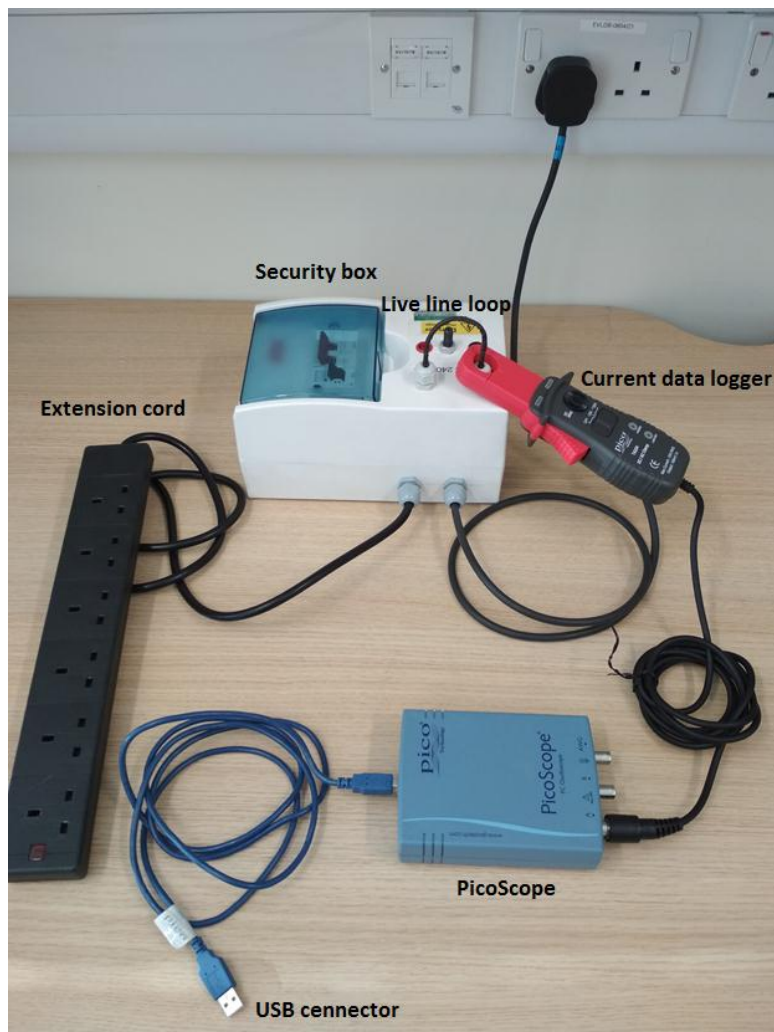


Figure 5.2: Different components of the high-resolution monitoring system.

5.2.2 Second NIALM stage: Event detection

NIALM methods can be categorised into event-based or non-event-based methods. The former uses an edge detection algorithm on the power consumption curve to detect which appliances record a change in the curve, and the latter continuously samples the aggregated data for inference.

For the case study, event-based methods have been chosen since they are more computationally efficient than the non-event based methods, and therefore, are more commonly used within typical NIALM applications [99].

5.2.2.1 Signal preprocessing

To facilitate the event detection stage, the root mean square (RMS) averaged over several cycles of the current signal is calculated. This average is an extended signal preprocessing technique, that provides a better measure of the current than the alternating current (AC) signal which continually changes from zero up to the positive peak, and so facilitates the implementation of the detection event algorithm.

A graphical representation of a small portion of the AC signal is presented in Figure 5.3, where the crossing points of the signal with the horizontal axis of the representative coordinate system can be visually identified. Three consecutive zero crossing points correspond to a whole cycle of the wave, which lasts for approximately 20 milliseconds.

The Root Meter Square (RMS) of the current signal over a given number m of wave cycles is calculated using Equation 5.1:

$$I_{RMS} = \left(\frac{I}{\sqrt{2}} \right)_{m \cdot cycle} \quad (5.1)$$

where I is the monitored current signal and $m \cdot cycle$ the averaged periods.

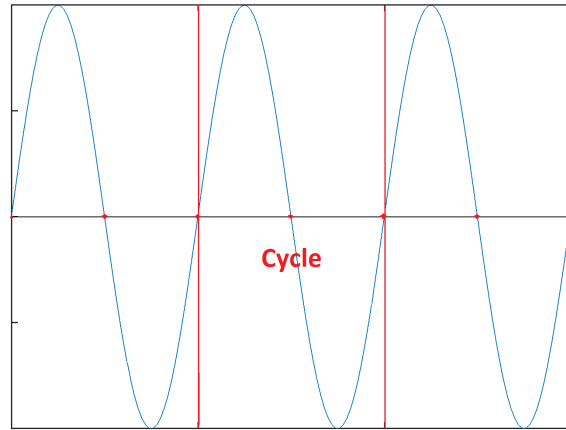


Figure 5.3: Zero crossing points in a wave cycle.

This signal transformation reduces the sample rate of the new signal, but also makes the event detection process easier for what is the most common operational mode for commercial meters.

5.2.2.2 Event detection algorithm

The event detection algorithm, based on Meehan et al's method [114], is the same as that proposed in Chapter 4. The method uses a moving window of M samples of the RMS current signal to identify changes in its amplitude and requires two conditions in order for an event to be identified. The first condition requires that the absolute magnitude of the RMS current signal should be greater than a certain threshold value during the established moving window.

For $S = s_1, s_2, \dots, s_i, \dots, s_n$, being n the length of the RMS current signal, an *event* i occur when:

$$\left| \frac{1}{M} \sum_{k=0}^{M-1} I_{RMS_{s_{i+1}}} - \frac{1}{M} \sum_{k=0}^{M-1} I_{RMS_{s_i}} \right| > \alpha \quad (5.2)$$

where α is the fixed positive threshold value of I_{RMS} , above which an event, $i \in \mathbb{N}$, is considered to have occurred.

The second condition that must be fulfilled is that the previous event detected must not have

occurred during the last p samples, in accordance with Equation 5.3.

$$\exists i \in \mathbb{N} \mid |t_{RMS_{event\ i}} - t_{RMS_{event\ (i+1)}}| > T \quad (5.3)$$

Where $T = (p \cdot m \cdot cycle)$ seconds and each cycle takes approximately 0.02 seconds.

This last condition allows the appliances enough time to settle into the steady state, and thereby prevents parts of the same transient signal being detected as spurious events. However, it also adds the limitation that events that occur within this period T will not all be identified correctly. This second condition also established the steady and the transient sequences for each event, as is graphically represented in Figure 5.4.

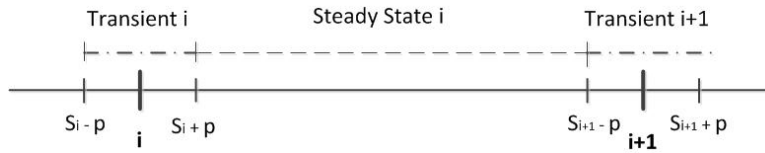


Figure 5.4: Steady state and transient segment wave definition.

This method assumes that the load is switched and that there is a steady state from which it is moving, therefore, it will not work with constantly varying loads (e.g., automatic dimming lighting or variable speed pumps). However, this restriction is not applicable to general small power office loads and will not be considered in this research.

According to Figure 5.4, the following definitions can be applied to describe an RMS current signal:

- $S_i = s_{i_1}, s_{i_2}, \dots, s_{i_j}, \dots, s_{i_{n_i}}$, is the RMS signal segment between the consecutive events i and $i+1$ and n_i is the length of the segment ($s_{i_{n_i}} = s_{i+1}$).
- $S_{i\ steady} = s_{i_1 + p}, \dots, s_{i_j}, \dots, s_{i_{n_i}} - p$ is the RMS steady state signal segment after event i .

- $S_{i \text{ transient}} = s_{i_1} - p, \dots, s_{i_1} + p$ is the RMS transient state signal segment during event i .²

Extrapolating these definitions to the original monitored current signal gives:

- $S_i^* = s_{i_1}^*, s_{i_2}^*, \dots, s_{i_j}^*, \dots, s_{i_{n_i}^*}$ is the monitored signal segment between the consecutive events i and $i+1$ and n_i^* is the length of the segment.
- $S_{i \text{ steady}}^* = s_{i_1}^* + p^*, \dots, s_{i_j}^*, \dots, s_{i_{n_i}^*}^* - p^*$ is the monitored steady state signal segment after event i .
- $S_{i \text{ transient}}^* = s_{i_1}^* - p^*, \dots, s_{i_j}^*, \dots, s_{i_1}^* + p^*$ is the monitored transient state signal segment during event i .³

5.2.3 Third NIALM stage: Electrical signatures extraction

In the third stage of the NIALM method, once steady state and transient state have been established for the monitored signal, characteristic electrical signatures are identified and extracted. In order to cover a systematic review of the most common identified signatures types, which are presented in Figure 5.5, and a study of their disaggregation capabilities, the literature review offers a comprehensive classification of types.

²Note that while a fixed length has been defined for transient state, steady states have a variable length by definition.

³There are $m \cdot 20$ s^* samples of the original monitored signal between two consecutive samples of the RMS averaged signal.

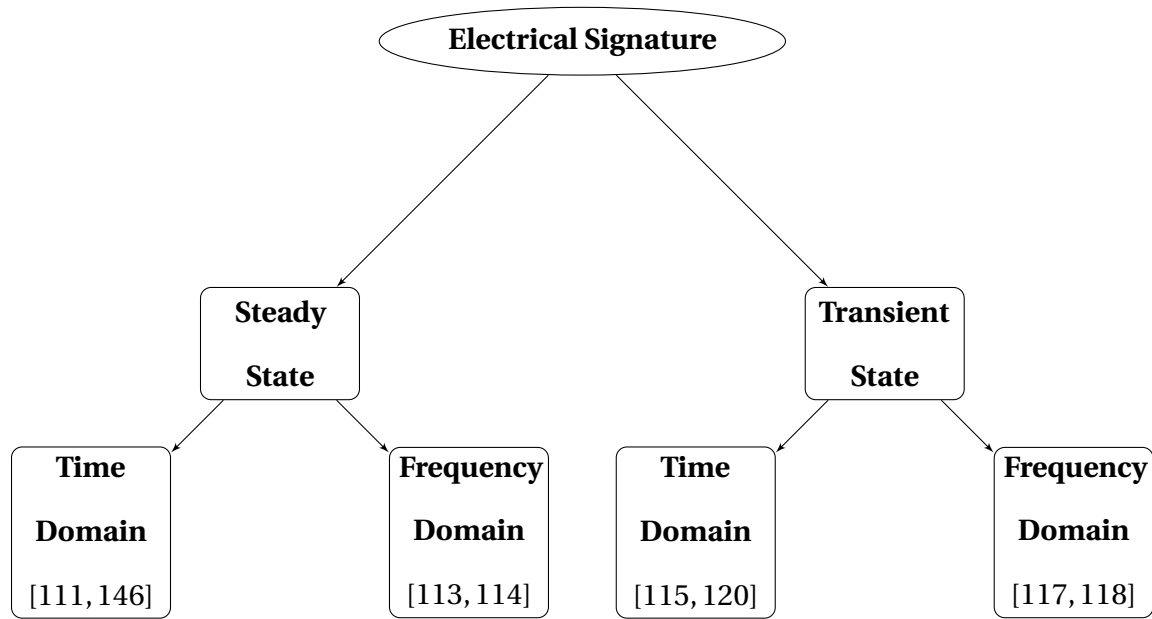


Figure 5.5: Proposed electrical signature classification

One representative signature for each of the proposed categories is chosen for the experimental part of the study, this provides a study of the information and requirements associated with each of these categories. The selection of the representative signatures takes into account the monitoring system’s technical specifications and capabilities.

5.2.3.1 Steady- state in time domain signature

RMS current increment (Ψ_i), used in the first NIALM method developed by Hart in the 1980s, has been chosen as the representative steady- state/time domain signature. This signature can be used to identify the device causing the load when the current draw of the devices is distinct and well known ⁴.

To extract the current *RMS Increment* signature, the I_{RMS} average value between consecutive events is calculated. For each event i the *RMS Increment* between these averaged intervals is

⁴To implement this method and initial “on” operational state has been assumed for all the appliances.

calculated in accordance with Equation 5.4.

$$\Psi_i = \left| \overline{I_{RMS_{i+1}}} - \overline{I_{RMS_i}} \right| \quad (5.4)$$

where $\overline{I_{RMS_i}}$ is the average value of the $I_{RMS}(S_{i \text{ steady}})$ calculated between the event i and $i+1$, and $\overline{I_{RMS_{i+1}}}$ is the average value of the $I_{RMS}(S_{i+1 \text{ steady}})$ calculated between the event $i+1$ and $i+2$.

The *RMS Increment* _{i} signature Ψ_i , is identified as an On event for positive values and an Off event for negatives.

5.2.3.2 Steady-state in frequency domain signature

The disaggregation method used by Meehan et al. [114], based on steady state current harmonics for a similar set of small power systems, analyses the current signal steady state in frequency domain, obtaining good results. According to this method, the third odd harmonics of the spectrum gives a sufficient approximation of the signal and distinguishes each appliance.

To extract the current *Steady Harmonic Increments* (Sh_3) signature, the Discrete Fast Fourier Transform (DFFT), $I_i(e^{jw})$ of the steady state monitored signal segment after each event i , $I(S_{i \text{ steady}}^*)$, is calculated, according to Equation 5.5.

$$I_{Steady_i}(e^{jw}) = \sum_1^{n_i^* - 2p^*} I(S_{i \text{ steady}}^*) e^{-jw} \quad (5.5)$$

where $I_{Steady_i}(e^{jw})$ is a complex function of the angular frequency w of the steady segment of the signal between event i and event $i+1$. This complex function can be also expressed as:

$$I_{Steady_i}(e^{jw}) = \left| I_{Steady_i}(e^{jw}) \right| e^{j\theta(w)} \quad (5.6)$$

where $|I_{Steady i}(e^{jw})|$ is called the *magnitude function* and $\theta_{I_{Steady i}(w)}$ the *phase function*.

The third odd harmonic amplitude is extracted from the signal before and after an event i and the absolute value of the difference of these two magnitudes calculated and expressed as a percentage of the fundamental harmonic amplitude, corresponding to $w=50\text{Hz}$, as presented in Equation 5.7.

$$Sh_3 = \frac{|I_{Steady(i-1)}(e^{150j})| - |I_{Steady i}(e^{150j})|}{|I_{Steady i}(e^{50j})|} * 100 \quad (5.7)$$

5.2.3.3 Transient signatures in time domain signature

Crest Factor coefficient (CF) The *Crest Factor coefficient (CF)* is the measure of the ratio of the signal peak to its effective value, and is a good indicator of how extreme the peaks are in the waveform. It is, therefore, a very common transient signature used in a large number of NIALM methods [107, 131, 147, 148].

The Crest factor coefficient signature for the signal transient segment i , is calculated by Equation 5.8:

$$CF_i = \frac{Max(|I_{RMS}(S_i \text{ transient})|)}{\Psi_i} \quad (5.8)$$

where $Max I_{RMS}(S_i \text{ transient})$ is the maximum absolute value of the RMS segment signal during the transient i and Ψ_i is the *Increment* signature value after event i .

5.2.3.4 Transient signatures in frequency domain signature

For identification of a representative transient signature in the frequency domain, the third harmonics of the signal during the transient period is extracted and its relative amplitude compared to the fundamental frequency.

The *Transient Harmonic Increments* (Th_3) signature is calculated in a similar way to the *Steady FFT Harmonic Increments*, except that the DFFT is calculated for the steady state monitored signal segment previous to an event i , Equation 5.9, and for the transient state monitored signal segment during the event i , Equation 5.10.

$$I_{Steady(i-1)}(e^{jw}) = \left| I_{Steady(i-1)}(e^{jw}) \right| e^{j\theta(w)} \quad (5.9)$$

$$I_{Transient i}(e^{jw}) = \left| I_{Transient i}(e^{jw}) \right| e^{j\theta(w)} \quad (5.10)$$

The relative amplitude of the third harmonics steady-transient increment, compared to the fundamental frequency amplitude of the transient, is calculated in accordance with Equation 5.11.

$$Th_3 = \frac{\left| I_{Steady(i-1)}(e^{150j}) \right| - \left| I_{Transient i}(e^{150j}) \right|}{\left| I_{Transient i}(e^{50j}) \right|} * 100 \quad (5.11)$$

The first two odd harmonics, which correspond to 50 Hz and 150Hz, are extracted for the corresponding *magnitude function*, $\left| I_{Steady i}(e^{jw}) \right|$ and $\left| I_{Transient (i-1)}(e^{jw}) \right|$, the absolute difference of the harmonic amplitude is calculated and the third harmonic increment, Th_3 , is expressed as a percentage of the input current at the first.

5.2.4 Fourth NIALM stage: The disaggregation algorithm implementation

Once the signatures have been extracted from the electrical wave, a disaggregation algorithm is used to separate individual appliance loads from the overall signal. Supervised learning techniques, as reported in the literature review, are more convenient for the present case study as they obtain a higher accuracy for appliance identification [149]. Since the aim of this thesis is to

investigate the disaggregation capabilities of different sets of electrical signatures, it is preferable to use a deterministic classification technique, such as Decision Trees, rather than other non-deterministic techniques, such as the Support Vector Machine which relies on optimization theory, or the Bayesian inference which is based on probability theory. Moreover, the Decision Trees classifier has general performance characteristics that stand out in comparison with other disaggregation algorithms, especially with regard to its tolerance for irrelevant attributes and its transparency in the classification process [132].

The Decision Trees algorithm performs its classification in two phases, the *tree building* and the *tree pruning* phases. Once the tree has been fully grown and then pruned, the decision tree model can be used to predict the class value for new patterns. For a detailed explanation of the decision tree classifier algorithm see Appendix E.

In a third stage, the evaluation stage, the prediction accuracy of the decision tree classifier is evaluated. When a large amount of data are available, a large sample can be used for training and a further independent and large sample of different data can be used for testing. For these cases, a typical validation method used is the *K-fold validation method*. This comprises the partitioning of a data set D into n subsets D_i and then running the decision tree classifier algorithm n times, each time using a different training set $(D - D_i)$ and validating the results on D_i . However, in many cases there is not a large supply of data available and this limits the amount of data that can be used for testing. In those cases, a certain amount of data can be exchanged for testing and training purposes. In the *holdout method*, the data is split randomly into two independent subsets: training and testing. Generally, $2/3$ of the data are selected for the training set and the remaining $1/3$ for the testing data set. The classification model is built using the training data, and later validated using the testing set. The holdout method is an alternative solution when there is not enough data for both training and testing separately. A detailed explanation of the

decision tree classifier validation algorithms used in this study is included in Appendix F.

5.2.4.1 Accuracy metric

To test the degree of confidence in the NIALM method implemented in the experimental study, the accuracy of the decision tree algorithm has been assessed by comparing the output results of the classifier with its expected targets using a confusion matrix.

The confusion matrix is a typical receiver operating characteristics (ROC) technique for supervised learning of classifier algorithms comprised of a specific table layout that allows visualization of the performance of the classifier algorithm. Each column of the matrix represents the instances in a predicted class, while each row represents the instances in an actual class (or vice versa). That is: if the instance is positive and it is classified as positive, it is counted as a True Positive (TP); if it is classified as negative, it is counted as a False Negative (FN). On the other hand: if the instance is negative and it is classified as negative, it is counted as a True Negative (TN); and if it is classified as positive, it is counted as a False Positive (FP). Table 5.2.4.1 presents the confusion matrix elements, where the numbers along the major diagonal represent the correct decisions made.

		PREDICTED CLASS	
		<i>Class=Yes</i>	<i>Class=No</i>
ACTUAL CLASS	<i>Class=Yes</i>	TP	FN
	<i>Class=No</i>	FP	TN

Several common metrics can be calculated from the confusion matrix, as the precision(5.12) and overall accuracy(5.13) of the classifier.

$$Precision = \frac{TP}{TP + FP} \quad (5.12)$$

$$\text{Overall Accuracy} = \frac{TP + TN}{TP + FN + TN + FP} \quad (5.13)$$

In the precision Equation 5.12, the True Positive predicted values are dividing between all the predicted positive values (true and false), and for the accuracy Equation 5.13, the True values are divided between all the values. The different metrics should be used based on the values considered "relevant" for each evaluation, precision for one specific class and accuracy for all the classes.

The decision trees algorithm and the confusion matrix evaluation are implemented using KNIME, a free discrete software tool for data analysis and visualization that integrates components for machine learning and data mining. For a detailed explanation of the KNIME implemented algorithm see Appendix G.

5.2.5 Individual profile database

To construct an *Individual Profile Database*, a small (around 150 m^2) office area in the University of Reading was chosen. This office contained: four heaters (H); two fans (F); eight personal computers, each with one screen (PC); four incandescent lamps (IL); and a small kitchen with two kettles (K), two coffee machines (CM), and one microwave (M). These appliances were considered to be suitable for the research purpose because they can usually be found in both an office⁵ and a dwelling.

Each individual appliances was switching ON/OFF during different periods, in order to register their typical operational modes. This process was repeated 10 times for each appliance. Table 5.1 presents the approximate monitoring periods, nameplate power rates and correspondent

⁵In accordance with Section 12 of Guide F "Electrical power systems and office equipment" [138].

amperages⁶ assuming a constant voltage of 230 volts, for each of the targeted appliance.

Table 5.1: ON period, power rate, and amperage for the different appliances under monitoring.

Appliance	Power (W)	Amperage (A)	ON period (s)
Kettle (K)	3000	13	30
Heater (H)	750	23.26	200
Coffee Machine (CM)	800	3.48	40
Fan (F)	30	0.13	200
Incandescent Lamp (IL)	40	0.17	200
Microwave (M)	1000	4.5	50
Personal Computer (PC)	270	1.17	200

5.3 Results analysis and discussion

In this section, the individual profiles are analysed graphically and numerically in order to understand the different monitoring requirements and electrical characteristics. The disaggregation capabilities of the different signature categories are also analysed for both individual and aggregated appliance loads.

5.3.1 Individual appliance signal patterns analysis

Graphical and numerical analyses of the different electrical signatures for each appliance have been undertaken and their specific characteristics are presented and discussed. For this purpose,

⁶The power and amperage values are based on the nameplate provided by the manufactures, these are usually greater than the operational values.

a set of four different signal profiles for each appliance is presented in this section. Sub-figures 5.6a, 5.6b, 5.7a, 5.7b, 5.8a, 5.8b, 5.9a, 5.9b, 5.10a, 5.10b, 5.11a, 5.11b correspond to the time-domain patterns (RMS averaged of the AC signal) and sub-figures 5.6c, 5.6d, 5.7c, 5.7d, 5.8c, 5.8d, 5.9c, 5.9d, 5.10c, 5.10d, 5.11c, 5.11d to the frequency domain patterns (FFT of the AC signal).

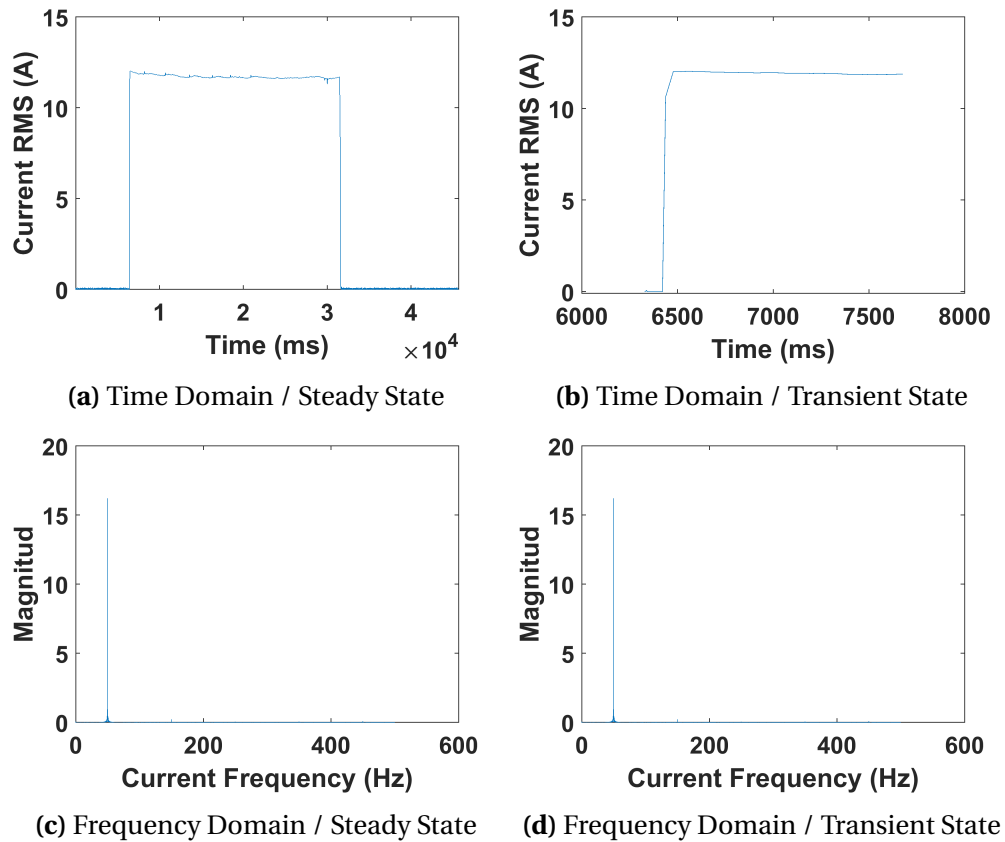


Figure 5.6: Kettle electrical signal profiles.

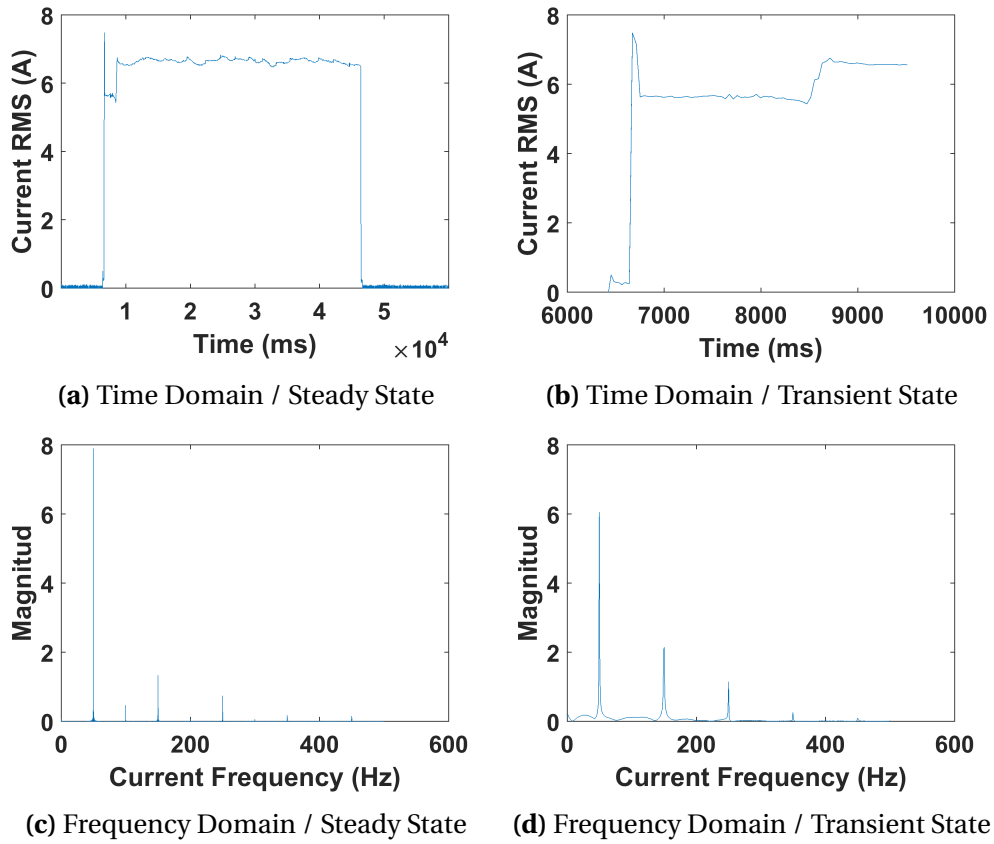


Figure 5.7: Microwave electrical signal profiles.

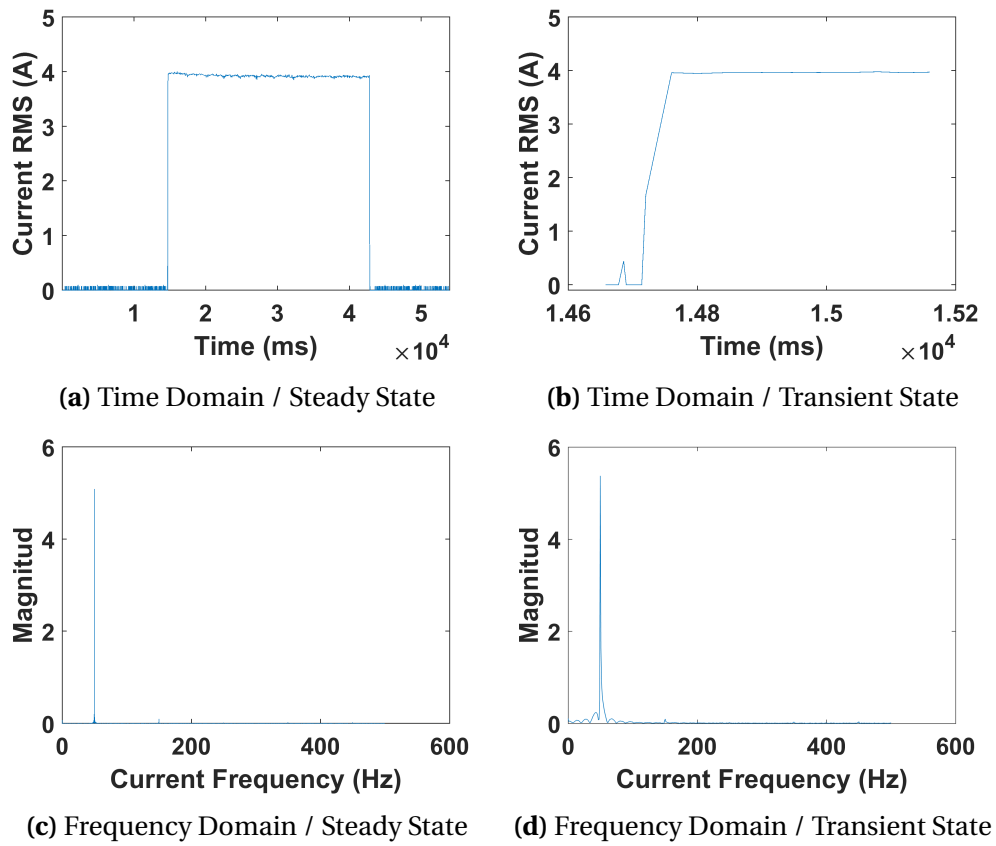


Figure 5.8: Coffee machine electrical signal profiles.

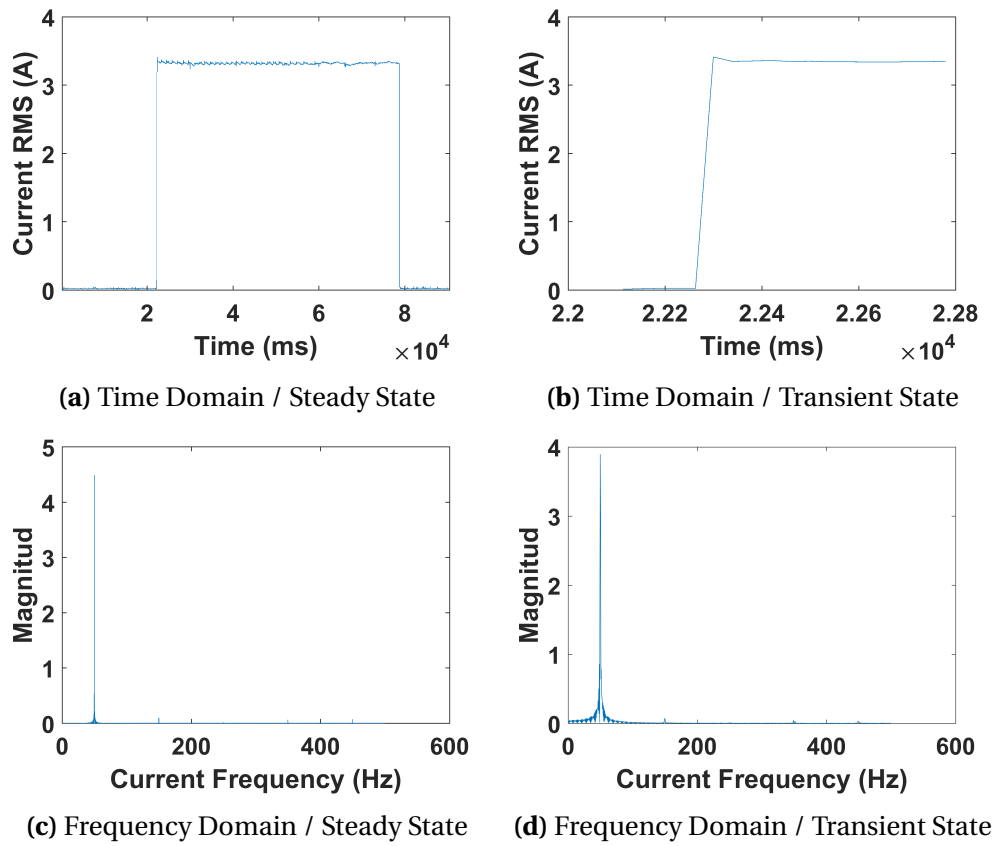


Figure 5.9: Heater electrical signal profiles.

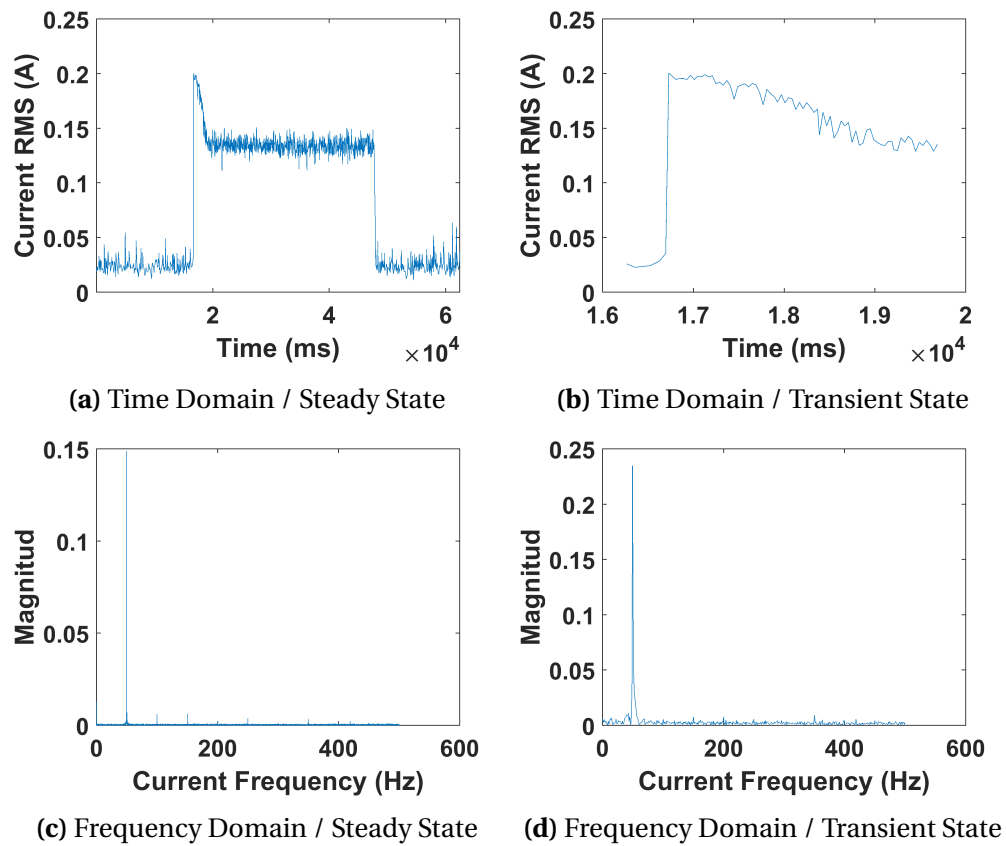


Figure 5.10: Fan electrical signal profiles.

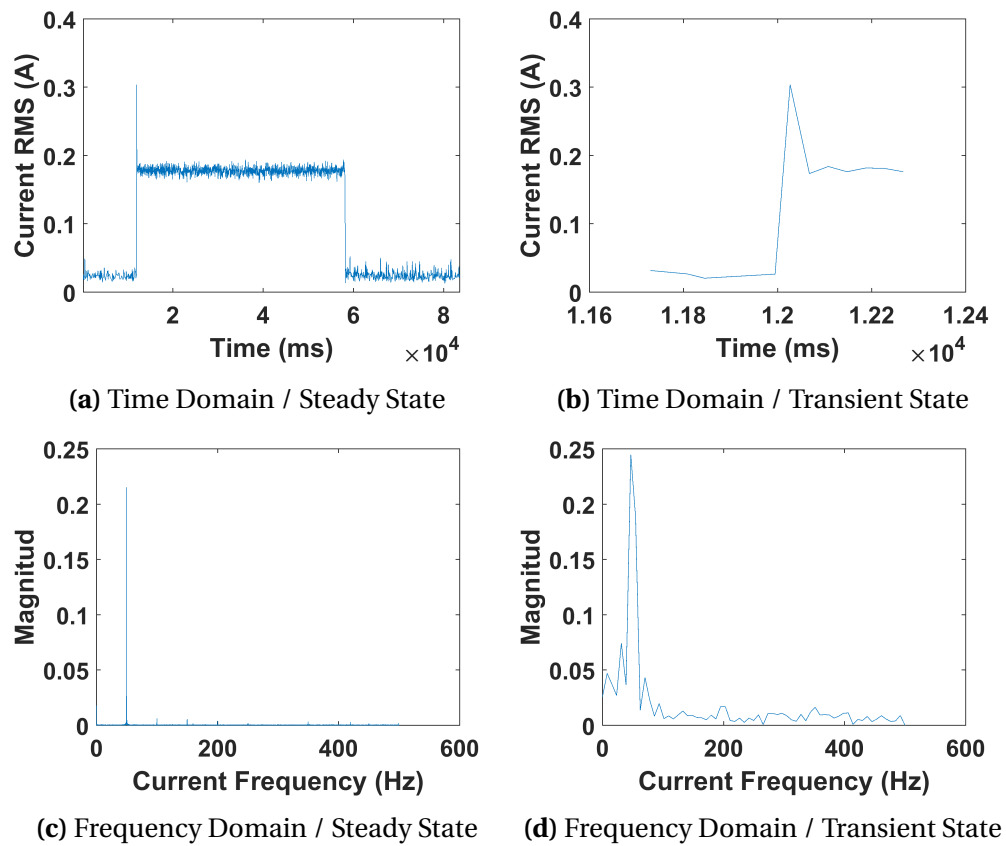


Figure 5.11: Incandescent lamp electrical signal profiles.

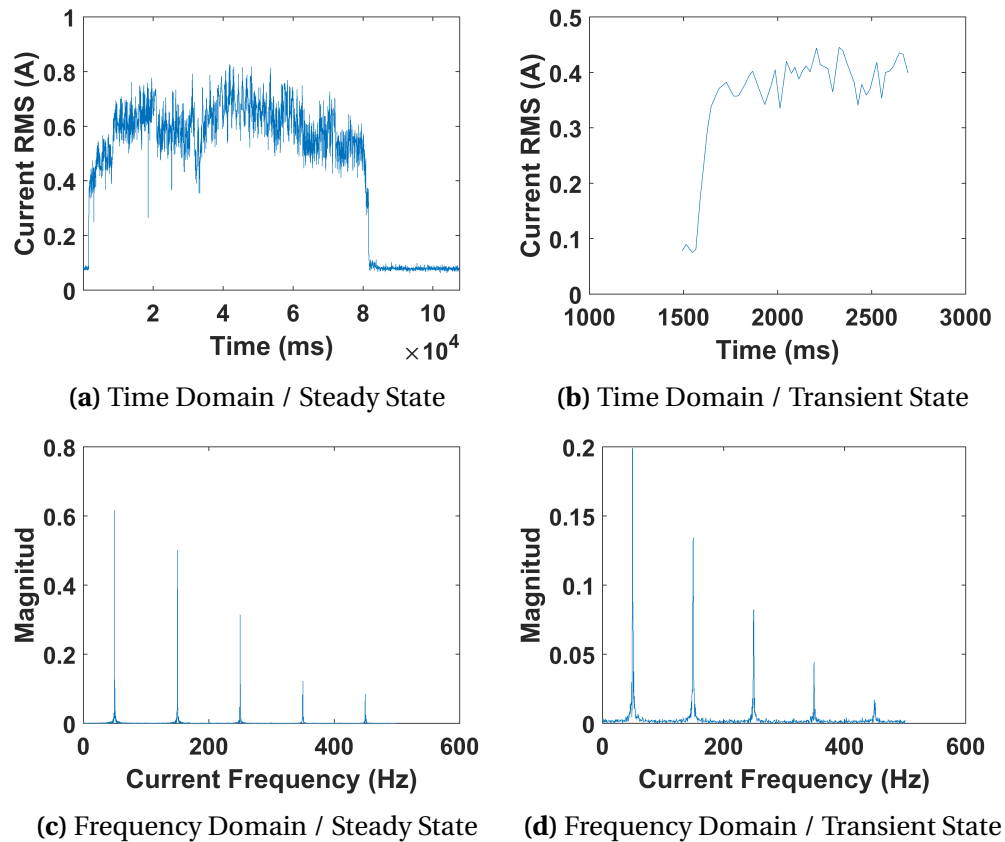


Figure 5.12: Desk (PC and screen) electrical signal profiles.

A preliminary visual analysis of these profiles provides relevant information about the electrical characteristics of the different appliances and allows the identification of some signature features, such as large switching on transient spikes and specific harmonic content.

Within each figure, each graph (a) provides information about the steady operational state of the different appliances in the time domain. Based on these profiles, the different appliances can be classified as large load appliances (i.e., K, CM, M, H), with a *RMS Increment* signature greater than one ampere, and low load appliances (i.e., PC, IL, F), with a *RMS Increment* smaller than 1 ampere. Small loads and pattern fluctuations (FI) in variable loads, as for PC, are susceptible to similar *RMS Increment* sizes.

Each graph (b) provides information about the transient behaviour of the appliance in the time domain. Flat pattern profiles, such as those for K, CM, and H, indicate a lack of significant transient behaviour and, consequently, absence of information from the transient time domain signatures. M, F, and IL, on the other hand, are expected to have distinguishable *Crest Factors*, and the PC, with a fluctuating profile, will have a variable *Crest Factor*.

Each graph (c) provides information about the harmonic content of the different appliances during their steady operational states, this harmonic content is strongly related to the type of load. Linear nonreactive loads, such as K, CM, and IL, do not generate harmonics of their own. Neither do linear reactive loads, such as H, F, and M, but their impedance changes with respect to the frequency and, therefore, each harmonic gives additional information about the load. The nonlinear loads, such as the PC, contain circuit components that distort the waveform and generate their own harmonic.

In each figure, each graph (d) provides information about the harmonic content of the different appliances during their transient operational states. The transient harmonic content is similar to steady state once, where only linear reactive and nonlinear loads present noticeable harmonics. However, the magnitude of the harmonics is amplified during the transient state, as can be clearly seen in the M profile, Figure 5.7d.

5.3.1.1 Signature characteristic parameters

The previous graphical analysis helps to understand the electrical behaviour of the different appliances and to set down a number of adjustable parameters for identification of the respective signatures. Four different parameters have been defined in this section and, although they are presented here specifically for this case study, the same considerations are required for the implementation of any NIALM method based on event detection. This is because the

establishment of those parameters determines the kind of appliance that can be disaggregated. The parameter m represents the number of cycles undertaken for the RMS average. The two cycle RMS average works well for detecting the large loads appliance (i.e., K, CM, M, H) switching events, but seems inadequate for low load appliances (i.e., PC, IL, F), particularly for the PC due to its fluctuations. Larger values for m smooth the signal and remove sharp fluctuations, however, averages over large numbers of cycles lead to loss of information, especially with small loads, such as F and IL. To overcome this problem, a value of $m=30$, experimentally tested, has been found to be suitable for use during the event detection stage. This new average considerably smooths the PC signal fluctuations, making the event detection process easier, although some fluctuations are still detected and need to be recognised as such in the disaggregation method and when the probability of event overlapping is incremented. Once the event locations have been detected, the previous two cycles RMS average is again considered and used for signature identification and extraction, thus avoiding the information loss associated with large m values⁷. The parameter α is the positive I_{RMS} threshold value that establishes the first condition for the event detection method, as stated in Equation 5.2. To establish this parameter, 75% of the smallest appliance's RMS current has been chosen as the condition in accordance with empirical testing and Meehan et al's method [114]. Thus, $\alpha = 0.075 A$, based on consideration of the *RMS Increment* of the smallest appliance, F, which is approximately 0.1. Smaller appliances initially considered in the study, such as the mobile charger, were discarded as their *RMS Increment*, at 0.03 A, was indistinguishable from the background noise.

The parameter p is the number of samples of the RMS signal sequence between consecutive events and accomplishes the second condition for the event detection method, according to Equation 5.3. This parameter established the steady and the transient sequences for

⁷Note that the probability of event overlapping is not reduced in this way.

each event. Large p -values ensure the detection of the characteristic whole transient signal shape, however, they also add the limitation that events that occur within $Transient\ time = (p \cdot m \cdot 0.02)$ seconds will not all be identified correctly, especially in scenarios which involve a large number of appliances. For this study, a value of $p=15$ has been chosen, allowing a transient identification time of 0.6 seconds, enough to capture the initial energy burst peaks of appliances such as M and F through the Crest Factor, and to minimize a potential event overlap⁸.

5.3.2 Signature dataset

Following the implementation of the third stage of the NIALM method, the *electrical signature extraction*, and in accordance with the representative signatures selected in section 5.2.3. and the adjustable parameters established in subsection 5.3.1.1., a *Signature Dataset* is obtained from the initial *Individual Profile Database*. For steady state signatures, ON and OFF events have been considered (20 values for each signature), and for the transient states signatures only ON events have been considered (10 values for each signature). Tables 5.2 and 5.3 present the average magnitude for each signature and appliance over the considered values and their corresponding standard deviation, σ , for time domain and frequency domain, respectively.

This new *Signature Dataset* is used for training the decision tree classifier and for an initial comparison of the electrical signature recognition capability. A first glance at the tables provides an idea of the distinguishable capacity of the different signatures, e.g., Φ magnitude values are quite different between appliances, however, they remain very similar for CM and M, and for F and the Fl. Others signatures are characteristic of some specific appliances, e.g., the *Crest Factor* for M and IL.

The harmonic analysis allows the identification of the type of load. Linear nonreactive loads

⁸Note that the RMS average for the event detection process is done over 30 cycles.

Table 5.2: Steady State Signature Dataset

SP	Time Domain		Frequency Domain	
	Ψ (A)	σ_{Ψ} (A)	Sh_3 (%)	σ_{Sh_3} (%)
K	11.52	0.06	2.03	0.37
M	6.46	0.12	23.71	3.62
CM	3.71	0.15	1.84	0.17
H	3.28	0.16	0.33	0.2
F	0.10	0.02	2.84	0.36
IL	0.14	0.01	2.81	0.40
PC	0.40	0.03	101.80	14.67
Fl	0.06	0.03	129.47	82.78

Table 5.3: Transient State Signature Dataset

SP	Time Domain		Frequency Domain	
	CF (A)	σ_{CF} (A)	Th_3 (%)	σ_{Th_3} (%)
K	0.25	0.06	0.25	0.34
M	1.98	0.88	57.00	1.41
CM	0.06	0.01	3.07	0.22
H	0.06	0.03	02.55	0.72
F	0.06	0.01	211.23	8.56
IL	0.14	0.26	11.81	7.43
PC	0.02	0.01	38.18	24.24
Fl	0.11	0.04	0	0

have low harmonic content (i.e, K, CM and H) and nonlinear loads have high harmonic content (i.e., PC).

The comparison of the standard deviation with their signature magnitude provides relevant information about the “quality” of the signature, where this concept is understood as the appliance identification capability of the signature, inversely proportional to the standard deviation value. For example, small appliances loads, such as F and IL, have relatively large standard deviation values with respect to their transient signatures, which means a poor signature “quality” due to background noise effecting transient signals in small loads.

5.3.3 Individual appliance identification

To test the individual appliance identification capability of each of the electrical signatures, the k-fold cross-validation method is implemented. This method realises a partition of the *Signature Dataset*, which contains 80 samples, into $k=10$ disjoint subsets, each of which contain eight samples, and taking one partition for testing purposes and using the remainder, 72 samples, for training the classifier algorithm. The process is repeated with each of the remaining nine folders and the mean accuracy is averaged over the 10 iterations. For each iteration, therefore, two datasets are created: the training dataset, with $72 * 10 = 720$ pieces of data to train the decision tree algorithm, and the testing dataset, with $8 * 10 = 80$ pieces of data to test the validity of the method.

A confusion matrix is used to test the effectiveness of the algorithm. In each iteration, the disaggregation precision for each individual appliance is calculated using Equation 5.12, and the overall disaggregation accuracy for all the appliances is calculated using Equation 5.13.

Table 5.4 presents the averaged results for the 10 iterations where each column corresponds to individual signatures. In the same way, each row corresponds to an individual load and the *All* row represents the total load aggregation.

In accordance with Table 5.5, Φ is the signature that achieves the highest overall accuracy. However, by consideration of Table 5.4, it can be seen that there are some identification issues between the F and the fluctuation, and between CM and H, as was suggested by the values in Table 5.2.

The remainder of the signatures (i.e., CF, Sh and Th) present similar overall accuracy, as can be seen in Table 5.5, however, their precision values depend on which appliances are considered, e.g., Fl have poor precision values for CF and Sh, but a very high value for Th.

Thus, Tables, 5.5 and 5.4, highlighted the different disaggregation capabilities of the signatures

App.	$Prec.\Psi$	$\sigma\Psi$	$Prec.CF$	σ_{CF}	$Prec.Sh$	σ_{Sh}	$Prec.Th$	σ_{Th}
K	1	0	1	0	0.04	0.05	0.07	0.08
M	1	0	1	0	1	0	1	0
CM	0.96	0.05	0.24	0.10	0.86	0.17	1	0
H	0.96	0.05	0.04	0.05	0.28	0.12	0.52	0.15
F	0.86	0.05	0.18	0.04	0.96	0.08	0.27	0.19
IL	1	0	0.82	0.16	0.56	0.08	0.23	0.01
PC	1	0	0.96	0.05	0.70	0.025	0.43	0.04
FI	0.86	0.05	0.16	0.02	0.28	0.04	1	0

Table 5.4: Individual loads precision recognition averaged over 10 iterations

* Precision (Prec.)

App.	$Accu.\Psi$	$\sigma\Psi$	$Accu.CF$	σ_{CF}	$Accu.Sh$	σ_{Sh}	$Accu.Th$	σ_{Th}
All	0.97	0.01	0.57	0.02	0.59	0.05	0.58	0.02

Table 5.5: Overall accuracy recognition averaged over 10 iterations

* Accuracy (Accu.)

depending on the appliances. However, their interpretation is very limited, as the training and testing datasets are populated by the same data.

5.3.4 Aggregated appliances identification

To create an *Aggregated Profile Dataset* for testing and comparing the disaggregation capabilities of the generic NIALM method in dwellings and offices, and considering the limitations of the monitoring hardware equipment (13 Amperes maximum), two different sets of scenarios have been created with a number of profiles chosen from the *Individual Profile Dataset* and randomly aggregated. The first set includes ten domestic scenarios comprised of seven appliance profiles: one kettle; one heater; one coffee machine; one fan; one incandescent lamp; one microwave; and one PC profile. The second is a set of ten office scenarios which includes 23 appliance profiles: two kettles; four heaters; two coffee machines; two fans; four incandescent lamps; one

microwave; and eight PCs. Ten different aggregated profiles have been created for each scenario and the NIALM method implemented in each to analyse the disaggregation capabilities of the different signature combinations.

5.3.4.1 NIALM for domestic appliance disaggregation

In accordance with the implementation stages of the generic NIALM method, the on/off switching events are first identified, and then the different electrical signatures are extracted from the set of ten domestic scenarios, providing 40 on-events signatures and 20 off-events signatures⁹ for each of the seven appliances, with a total of 420 signature for the whole set of ten scenarios, that constituted the *Signature Domestic Dataset* for each of the seven appliances, thus providing a total of 420 signatures for the whole set of ten scenarios to constitute the Signature Domestic Dataset. Figure 5.13 presents an example of the aggregated profiles from the set of domestic scenarios.

⁹Only the two steady state signatures can be extracted during off-events.

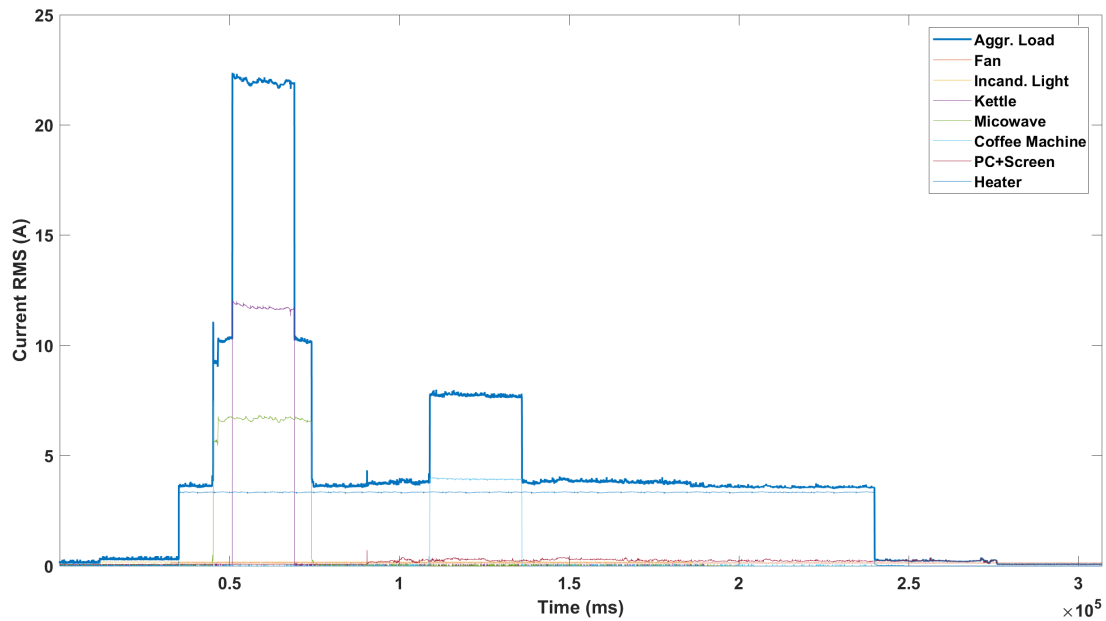


Figure 5.13: RMS aggregated MATLAB profiles for the domestic scenario.

To test the efficiency of the different electrical signatures when recognising individual appliances over aggregated load, the *holdout-validation* method is applied to the *Signature Domestic Dataset*. In the hold-out method the relevant data have been used in two different ways: the *Signature Dataset*, with 80 samples, in the learning process; and the *Signature Domestic Dataset*, with 420 samples, in the testing validation ¹⁰.

To find the optimal combination of signatures for disaggregating the different appliance sets, all the possible signature iterations or combination have been considered. Table 5.6 presents the averaged overall disaggregation accuracies obtained for each of the signature combinations, differentiating between large loads ¹¹ and low loads ¹².

The comparison of Tables 5.5 and 5.6 shows how the load disaggregation efficiency of the generic

¹⁰Note that these 420 signatures are from known appliances and, therefore, can be used for validation purposes.

¹¹With a *RMS Increment* signature greater than 1 Ampere

¹²With an *RMS Increment* smaller than 1 Ampere.

Table 5.6: Overall accuracy for all the possible Signature combinations for the domestic scenarios

Signature Combination	Large loads		Low loads	
	Acc. ON	Acc. OFF	Acc. ON	Acc. OFF
Φ	0.96	0.95	0.70	0.80
CF	0.60	—	0.5	—
Sh	0.53	0.75	0.54	0.38
Th	0.50	—	0.30	—
Φ + CF	1	—	0.75	—
Φ + Sh	0.97	0.95	0.54	0.75
Φ + Th	0.50	—	0.74	—
CF + Sh	0.53	—	0.54	—
CF + Th	0.50	—	0.50	—
Sh + Th	0.50	—	0.54	—
Φ + CF + Sh	1	—	0.54	—
Φ + CF + Th	1	—	0.80	—
Φ + Sh + Th	0.90	—	0.54	—
CF + Sh + Th	0.50	—	0.54	—
Φ + CF + Sh + Th	1	—	0.70	—

NIALM method is reduced when dealing with more than one appliance. Signatures with large standard deviation values negatively effect the disaggregation ability when used in combination with others signatures, which is a result of imprecise identification metrics, e.g., *Th* signature for large loads and *Sh* signature for low loads.

In general, low loads achieve lower accuracies than do large ones. This is mainly due to the variable electrical signal of the PC and the background noise which negatively affects the Φ disaggregation capabilities.

For the identified on-events, the higher accuracy for a single signature is achieved by Φ , with 96% and 95% accuracy for the large loads and 70% and 80% for low loads, in on and off events respectively. These accuracies are improved when also considering CF, achieving 100% of overall accuracy, as this signature reduces the identification issue caused by the similar Φ value between CM and H, and between F and Fl. For the low loads, the identifiable capability of Φ is improved

when combined with CF and Th , with 80% disaggregation accuracy for on-events.

In the identification of off-events, transient signatures are not considered as there are no electrical transient behaviours when the case study appliances are switched off. For these events, the higher accuracies are again achieved by Φ , but in this case they are not improved by the addition of Sh , as occurred in the on-events.

5.3.4.2 NIALM for office appliances disaggregation

The procedure followed for evaluating the disaggregation capabilities of the generic NIALM method in the set of office scenarios was the same as that for the domestic set, but it used 23 aggregated profile loads, thus creating the *Signature Office Dataset* comprised of 1380 signatures, 920 extracted from on-events and 460 from off-events. Figure 5.14 presents an example of the aggregated profiles from the set of office scenarios.

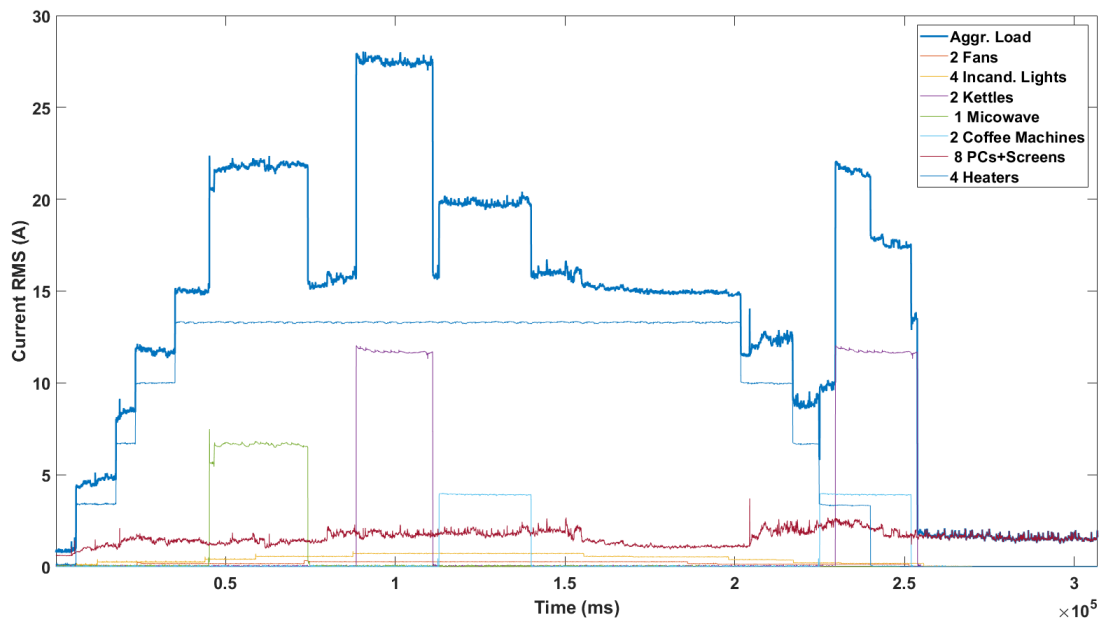


Figure 5.14: RMS aggregated MATLAB profiles for the office scenario.

As for the domestic scenarios, the *holdout-validation* method was applied over the aggregated load profiles and all the possible signature combinations considered. Table 5.7 presents the averaged overall disaggregation accuracies obtained for each of the signature combinations for the office set of ten scenarios.

Table 5.7: Overall accuracy for all the possible Signature combinations for the office scenario

Signature Combination	Large Loads		Low Loads	
	Acc. ON	Acc. OFF	Acc. ON	Acc. OFF
Φ	0.84	0.82	0.32	0.32
CF	0.54	—	0.25	—
Sh	0.50	0.65	0.24	0.22
Th	0.35	—	0.20	—
Φ + CF	0.88	—	0.30	—
Φ + Sh	0.88	0.85	0.34	0.30
Φ + Th	0.40	—	0.22	—
CF + Sh	0.38	—	0.30	—
CF + Th	0.30	—	0.25	—
Sh + Th	0.30	—	0.28	—
Φ + CF + Sh	0.90	—	0.34	—
Φ + CF + Th	0.82	—	0.38	—
Φ + Sh + Th	0.75	—	0.21	—
CF + Sh + Th	0.45	—	0.22	—
Φ + CF + Sh + Th	0.82	—	0.32	—

Comparing Tables 5.6 to Table 5.7, the reduction in the disaggregate accuracy with the appliances number increment can be seen. Nevertheless, a similar trend to that of the domestic scenarios is maintained, especially for large loads where the higher accuracy for a single signature is achieved again by Φ , with 84% for the on-events and 82% for off-events. These accuracies are again improved when combined with *CF* and Φ , achieving 88% of disaggregation accuracy with such a combination, and an even higher accuracy of 90% being reached by the Φ , *CF*, and *Sh* signature trio. Signature *Th* negatively affects the disaggregation ability when used in combination with other signatures.

For the low load appliances, by contrast, the identifiable capability of all signatures is significantly reduced, the higher percentage being achieved by the Φ , CF , and Sh signature trio, with only 38% overall accuracy in on-events.

5.4 Summary and discussion

The work presented in this chapter assesses the implementation of existing NIALM methods for the disaggregation of electricity consumption of small power equipment in office buildings, where the aim is to improve the accuracy of these methods in commercial energy audits.

Research in this field has led to the introduction of numerous NIALM methods since they were first developed in the early 1990s. These methods have been shown to work well for disaggregating small power in domestic dwellings. However, in the commercial domain NIALM has been largely unexplored, mainly due to the larger number of loads which exist in comparison to those of residential buildings. This increase in the complexity of energy disaggregation, from residential to commercial, means most NIALM methods made for residential use cannot be directly applied to commercial buildings.

In order to address this issue, based on a decision tree algorithm, a generic NIALM method is implemented in four stages. The analysis of the third stage, *the electrical signature extraction*, is recognised in the literature review chapter as a fundamental aspect of the disaggregation process. A set of seven different types of small appliances, typically found in both domestic and office environments, have been selected for this research. The results outline three aspects which influence the effectiveness of implementation of the NIALM method in this stage: the *adjustable* electrical parameters used in the monitoring process; the specific electrical signature combination chosen; and the number of aggregated appliances.

An initial analysis of the electrical behaviour of the different appliances reveals three relevant

adjustable parameters in the identification of the different electrical signatures:

1. The number of cycles taken to deduct the RMS average, this increment smooths the signal from background noise, but with the cost of eliminating electrical information.
2. The positive I_{RMS} threshold value that establishes the first condition for the event detection method. For this research, this parameter was defined as 75% of the RMS current of the smallest appliance, loads with I_{RMS} thresholds of the same order as the background noise were removed from the study.
3. The number of samples of the RMS signal sequence between consecutive events that accomplishes the second condition for the event detection method. This parameter established the steady and the transient sequences for each event. Large *p-values* ensure the detection of the characteristic whole transient signal shape, however, they also add the limitation that events that occur within transients may not be detected.

The specific electrical signature combination that better characterises the different small appliance loads in office buildings was also analysed in this chapter. To do so, a *Signature Dataset* was created which contained averaged signature magnitudes and their corresponding standard deviation for each appliance switching on/off event, thereby allowing an analysis of the individual recognition capability of each of the targeted electrical signatures. This revealed relevant information about the different appliance identification capability of each signature and their dependence on the appliance type.

Finally, an investigation into the number of aggregated appliances as a factor which affects the disaggregation capability of the different signatures was also undertaken. To do so, an *Aggregated Profile Dataset* was created to test and compare the disaggregation capabilities of the generic NIALM method in a set of domestic scenarios with seven aggregated appliances, and a set

of office scenarios with 23 aggregated appliances. The overall accuracy in the disaggregation process was found to be significantly smaller for office scenarios, mainly due to the larger number of loads in comparison to the domestic scenarios, thus incrementing the probability of events overlapping, especially for those classified *low loads*, with RMS current increments lower than 1 Ampere, where the use of the generic NIALM method failed to accurately disaggregate any appliances.

In this way, the chapter contributes towards meeting the objectives of the thesis, as it provides a better understanding of the electrical signatures which better characterize different small appliance loads and evidences that an initial analysis of the information provided by these signatures may address the existing limitation when implementing NIALM methods in office buildings, by increasing the accuracy and number of appliances that can be disaggregated (e.g., from 8 appliances, using current existing domestic methods, to 23 appliances, according with this study).

Further researches should therefore include follow-up work designed to evaluate the effectiveness of NIALM methods in real energy audits, incorporating findings from this thesis.

Chapter 6

Discussion and thesis conclusions

The evaluation of two main quantitative energy audit approaches has led to the proposal of three methods for ranking and quantifying uncertainty in small power estimation in commercial buildings; one for each of the research areas covered in this project. That is: the problems associated with uncertainty in small power energy estimations in calculation models; the challenges faced by the different energy measurement techniques; and the potential use of NIALM methods in office buildings for small power disaggregation. Although these methods undertake different approaches, they all pursue the same aim and there is no restriction to them being combined to complement each other in a holistic approach that can be used to inform auditors and researchers within the sector. Such an integrated approach will depend on the audit scenario and accuracy requirements. The experimental case study presented in Chapter 5, for instance, can make use of a generic NIALM method for disaggregation of the so called *Large loads*¹, for which 90% disaggregation accuracy was achieved, and a calculation model for the remaining *Low loads*². An additional comprehensive approach, suitable for scenarios with large numbers of a

¹With RMS current increments higher than 1 Ampere.

²With RMS current increments lower than 1 Ampere.

specific load, can make use of the extrapolation method proposed in Chapter 4 for the estimation purposes and again, can implement a calculation model for the remaining ones. To inform the selection of the optimal calculation model (i.e., the one with less uncertainty associated to its estimations), depending on the appliances and information available in both scenarios, the SA method proposed in Chapter 3 can be used.

The outcomes of this thesis not only contribute to the growing academic field of small power energy data analysis, but impact industrial practices through actual energy audits. This chapter aims to provide the final conclusions to the thesis, including discussion and evaluation of the research aims and contributions.

6.1 Research summary

Recent surveys [4, 11] have divided traditional quantitative audits into two approaches: *calculation*, which uses mathematical equations for energy estimations, and *measurement*, which involves some level of direct energy monitoring. Furthermore, the latter can be implemented through what has been defined in this thesis, in accordance with Swan and Ugursal's [75] classification, as *bottom-up* techniques, i.e., from end-users to total aggregate energy, and *top-down* techniques, i.e., breaking down total energy consumption into end-users.

The best energy estimation strategy depends on the audit requirements, the scenario under evaluation, and the information available. In accordance with the relevant literature reviewed in Chapter 2, calculation approaches have the advantage of little, or no, hardware installation. However, their accuracy is highly dependent on the quality of the input variables and their associated uncertainties. Measurement approaches, on the other hand, overcome some of the uncertainties by direct monitoring of the energy consumption, but at the cost of increasing complexity in the hardware installation. This complexity is proportional to the level of accuracy

obtained in the final estimations, going from a high level in bottom-up techniques, to a low level using top-down techniques, with possible intermediate levels when the techniques are combined.

The central problem of this research concerns the deficiencies identified in the implementation process for quantitative energy audits in office buildings in terms of small power load estimations through this classification. The motivation for the investigation of this problem arises from the importance of small power loads in energy audits, particularly in highly efficient buildings where they constitute an important part of the overall energy consumption, and errors in estimations can negatively affect the whole audit process.

The accuracy of small powers energy estimations achieved by the different audit approaches will be highly dependent on the sources of uncertainty associated with the input data or the monitoring technique used, for the calculation and measurement approach, respectively. The study of the effects of these uncertainties on the energy estimations is covered by three aspects: the identification of the source of uncertainty; the proposition methods used to assess this uncertainty; and the experimental tests of the methods. These research lines are undertaken by the three contribution chapters of this thesis where each proposes a different method for evaluating the uncertainty associated with a specific audit strategy. Figure 6.1 presents a framework of the three proposed methods proposed for addressing the different audit strategies for small power load estimations: the adapted SA method for the calculation approach; and the remaining two for the measurement approach, i.e., the extrapolation method for bottom-up techniques and the NIALM method for top-down techniques.

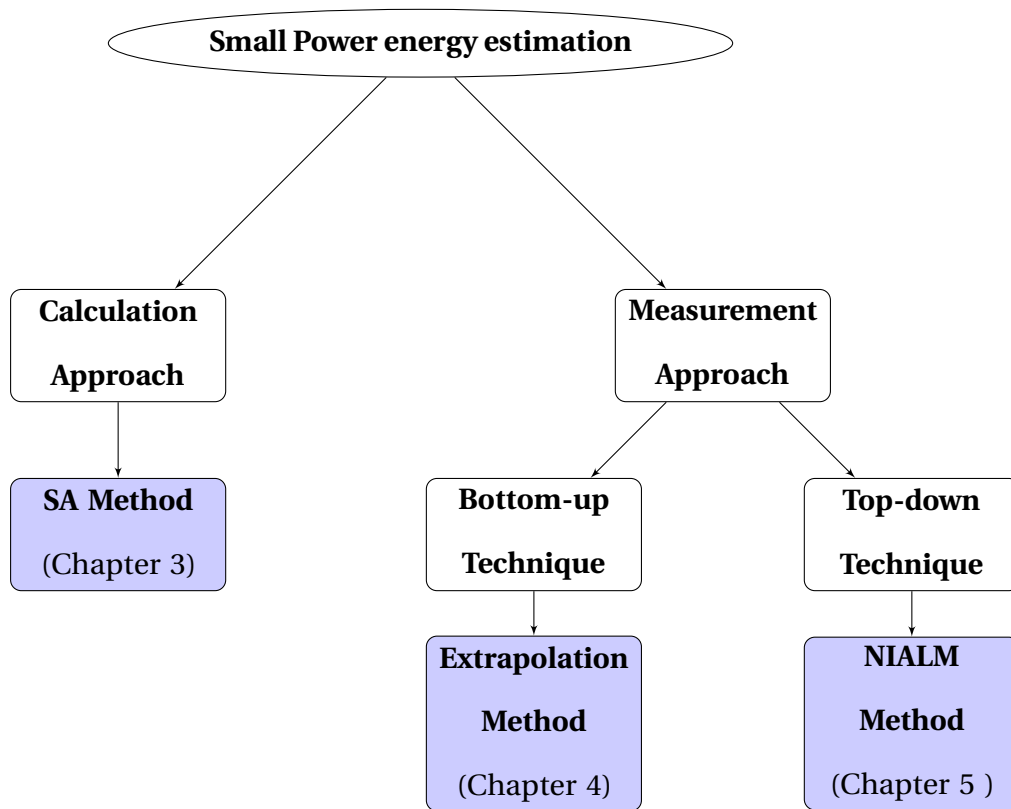


Figure 6.1: Proposed methods for overcoming the deficiencies detected in the different small power load estimations.

Calculation and metering approaches can be combined to optimise the audit process. For example, using calculation models for appliances with well-known input parameters (i.e., parameters with low uncertainty), and metering techniques for more uncertain ones. The proposed SA and extrapolation methods can help decide to which extent each of the approaches should be implemented to optimise the process.

Regarding NIALM methods, the contribution of this thesis is only in the electrical signature stage, other aspects of the method still need to be considered for it to be efficiently implemented in office buildings. However, as seen in the results described in this thesis, NIALMs may be considered as a solution for small power loads estimations in office buildings, overcoming the

uncertainties from the use of calculation methods at the low infrastructure cost of the top-down techniques.

6.2 Research contributions

The aim of this thesis, *to identify and propose methods to assess the uncertainty in quantitative energy estimations in office buildings for small power loads*, has been met by addressing five supporting research objectives.

The first objective, *to create a sensitivity analysis method for calculation models to evaluate how the variation in the output of a model can be apportioned to uncertainty in different input factors*, was addressed by the work presented in Chapter 3, where a new SA method was proposed for evaluation of the relevance of the input uncertainties in the energy audit process. SA methods to analyse the quality of calculation-based models have been used by modellers and practitioners from various disciplines [53–55], including in energy assessment models in buildings [56]. However, no practical studies have been undertaken for small power energy calculation methodologies.

The SA method proposed in this thesis is based on the Morris method [69], a well-established SA method with applications in different fields [59, 70]. The new method overcomes Morris' limitations for small power calculation models by implementing a number of adaptive refinement measures. The resultant adapted method was designed to be implemented in two stages: the Primary SA, providing an initial ranking of the input factors; and the Secondary SA, supplying additional information about the monotonicity and skewness of the output due to each of the inputs. This constituted the first SA method specific to small power energy estimations. Its capabilities were demonstrated through a case study where the new SA method was applied in four different energy calculation models, operating under the TM22 framework umbrella,

and using established industrial benchmarking sources and assumptions for the input values. Results from the case study present how the accuracy on the final energy estimation depends on the input information and the calculation model used. The new SA method will help energy auditors to select the optimal calculation model for a specific building scenario based on the quality of information available.

According to recent research into the current state of the art regarding work performed which relates to the electric energy consumption for small power loads, there remains great potential for energy savings through measurement techniques [4, 13], however, there has been a lack of practical studies which investigate the implementation of these techniques for small power energy estimation, especially in non-domestic buildings. To overcome this issue, objective 2, *to conduct a comparative study to identify the most efficient meter installation strategy in a typical office building for monitoring small power loads*, was addressed in Chapter 4. This was done through assessment of two common measurement technique, *bottom-up* and *top-down*, implementing both in an office case study scenario at the University of Reading, and using two databases obtained by two different monitoring systems, a set of smart plugs for monitoring at individual appliance level, and a centralised meter directly connected to the mains for monitoring at aggregated appliance level. The small power energy estimations obtained by top-down and bottom-up techniques at both monitoring levels were analysed and ways of improving them explored. Graphical tools to present and analyse the meter's data were included and compared, highlighting the benefits of chromo-maps to provide a picture of the overall energy performance to make occupancy pattern data visible and understandable at a glance. Additionally, possible appliance profile classifications were made based on occupancy and energy behaviour profiles, such as continuous-periodic appliance profile types (e.g., the fridge) where it is less disturbing to substitute the use of direct metering by benchmarking

or assumptions, and high-variable appliance profile types (e.g., the printer) where the use of individual meters will be more beneficial.

Kamilaris et al. [13] conducted a literature review survey on the state of the art work performed related to electric energy consumption for small powers in office and commercial buildings. They revealed the complexity of the current techniques used for measuring the energy consumption of office plug loads. According to Wang and Shengwei Yan [3], this complexity is the reason why these techniques are mainly being used to provide detailed energy data for research or validation purposes, while it is usually considered to be too expensive for practical applications in common buildings. As a result, a novel extrapolation method that provides accuracy of the total energy estimation for each of the possible permutations of the individual installed sub-meters has been proposed and tested in Chapter 4, fulfilling objective 3 of this thesis: *to evaluate the relationship between estimation uncertainty and cost of implementation of sub-metering techniques in terms of complexity and intrusiveness*. The method was implemented, through four stages, in the office case study scenario, and considered all the possible sub-meter combinations of the 12 individual meters installed in each of the desks over a period of 43 days, from 18th August to 3rd December 2017 (five no consecutive weeks). The relative percentage of uncertainty, measured against the percentage of the monitored desks calculated, showed a logarithmic relation that indicated the number of desks that need to be monitored depends on the relative uncertainty that the energy assessment is willing to accept. For example, to obtain a relative uncertainty lower than 10% it is necessary to monitor more than half the desks. The medians and confidence intervals of the different sets of energy estimations were also calculated to provide additional information. According to this last piece of information, the use of more than half of the meters is likely to result in a over-estimation of the total energy consumption values, and the use of fewer than the half is likely to result in an under-estimation. The information provided by this extrapolation

method can serve as a useful guide for auditors to determine the minimum level of metering granularity necessary to achieve the desired level of accuracy in their final energy estimates.

Based on the literature reviewed, NIALM methods are considered to be a metering technique able to provide information about the energy consumed by individual appliances using a top-down measurement approach. The benefits of NIALM methods for the disaggregation of small power in domestic buildings has also been tested by a number of researchers [88, 97], however, in the commercial domain NIALM has been largely unexplored by the academic community. The initial implementation of these methods is also described in Chapter 4, and attains objective 4: *to explore the capability of alternative measurement techniques for traditional load disaggregation methods for small power in office buildings.*

The first step in the implementation of a typical NIALM technique is the load status detection. Chapter 4 explained the exploration of the capabilities of a proposed detection method in a case study to understand the potential capabilities of NIALM techniques in office environments. The method relies on the identification of variations in the aggregated consumption power to detect the status (ON or OFF) of the loads. An event detection identification algorithm was implemented over the aggregated profiles collected by the centralised meter connected to the three electrical circuits feeding the office sockets. Monitoring of the first circuit, feeding only a fridge and an instant water boiler, and the third circuit, feeding seven PC desks, obtained a high degree of event detection. For this last circuit, although presenting some overlapping issues, an estimation of the energy consumed by the seven PCs, based on their averaged power rates and operational number of hours determined by the algorithm, was conducted and achieved an averaged relative error of 14.2%, with respect the plug meters installed in each of the office appliances (relative low considering the assumptions made). The second circuit, by contrast, with five PC desks, two printers, and one shredder, was less efficient regarding the event detection

algorithm implementation, not only due to the larger number of appliances, but also to the high operational variability of the printers' consumption profiles³. This case study does not claim to be a rigorous validation of the method, rather it constitutes an initial assessment of the potential capabilities of NIALM techniques and points out some of the issues which arise from its implementation in a real case and, introducing the research line taken in Chapter 5.

The work conducted in Chapter 5 took care of the final objective, *to analyse the electrical characteristic specifications and disaggregation capabilities for the different signatures for NIALM techniques in office buildings*. According to relevant literature in the field [28], the implementation of NIALM methods is limited to the domestic sector and most of these methods cannot be directly applied to commercial buildings. This limitation is thought to be due to, amongst other reasons, the lack of understanding of the optimal electrical signatures combination in the disaggregation process. In Chapter 5 this research gap is tackled by defining a typical generic NIALM method based on a set of electrical signatures, previously classified in the literature review section. The generic NIALM method is used to analyse the individual recognition capability of each of the electrical signatures for seven targeted appliance types. The results from this case study revealed information about the different appliance identification capability of each of the signatures, depending on the appliance type, e.g., the RMS current increment (Φ) is the signature that achieves the highest overall disaggregation accuracy across all the appliances. Finally, the generic NIALM method was implemented in both a domestic scenario (with seven aggregated appliances), and an office scenario (with 23 aggregated appliances) and the accuracy of the disaggregation process analysed. This accuracy was found to be significantly smaller for office scenarios, mainly due to the larger number of loads in comparison to the domestic scenarios, thus incrementing the probability of events overlapping.

³In comparison with the 10 second sample rate of the meter

The findings presented in this last chapter have built on the work conducted by Batra et al. [28], by assessing the validity of general NIALM methods for residential buildings when applied to commercial buildings, focusing on small power loads, and demonstrating, through a practical example, how a better understanding of the optimal electrical signatures combination is likely to enhance the disaggregation process.

The implementation of NIALM method in office audits can enable significant energy savings by tracking individual appliances over time, without having to install dedicated sensors across an entire building. This process can also help identify inefficient or malfunctioning appliances, and allows energy auditors to determine whether or not replacing them will ultimately be a cost-effective decision.

6.3 Further work

A set of assumptions, stated in Chapter 1, have been made during the research presented here due to the complexity of the energy estimation approaches reviewed, particularly for small powers, and issues related to implementation of the research solutions on real energy audits. Consequently, these assumptions can be considered in future works.

For calculation approaches, the SA method proposed in Chapter 5 is only able to provide a ranking of the input factors in their order of importance. A more sophisticated global SA method, able to quantify the input factors absolute significance over the output, would allow comparison between different audit scenarios. Although this SA method was conceived for the specific field of small power load calculations, it could be applied to other systems, such as Ventilation and Air-Conditioning systems, or areas of energy auditing, such as in gas consumption assessments. For the comparative study of the measurement approaches performed in Chapter 4, other analytic variables of the monitoring process, such as monitoring time or the number of appliances,

can also be assessed by more extensive case studies. This would allow consideration of all the potential aspects of the monitoring process that might have an impact on the information delivered.

Regarding NIALM techniques, the research conducted and reported in Chapter 5 has focused on the third implementation stage, *electrical signature identification*. However, the other three implementation stages, *hardware installation*, *event detection*, and *load disaggregation*, also present areas of improvement and further work needs to be done in these research areas. Additionally, it would be useful to evaluate the practicality of NIALM techniques by allowing experienced energy auditors to interact with a prototype system and share their opinions for the creation of more robust signature values and a more comprehensive coverage of appliance loads.

6.4 Concluding remarks

The importance of small loads in commercial building audits have been highlighted by the literature reviewed in this thesis, along with the deficiencies which exist regarding their energy assessment. For these reasons this thesis has sought to advance understanding in these areas, hoping that the research presented is taken further in the field, taking note of the recommendations for further work presented throughout.

Drawing on the existing knowledge base and industry experience that the EngD affords, this research project has brought together the fields of energy calculation models sensitivity analysis, metering techniques, and load disaggregation techniques. New methods for assessing calculation and metering energy estimation approaches for small powers have been generated, and a relevant contribution has been made towards amelioration of the problem of NIALM implementation in the commercial sector.

In summary, the three research areas covered in this thesis have built a foundation of methodolo-

gies that can be used both in industry and in academic fields. For the former, by providing a tool that can help auditors to choose the optimal energy assessment strategy for small power load estimations and, for the latter, by better understanding the significance of uncertainty within the different energy estimation methods.

References

- [1] R. B. Rouncefield-Swales, “ESOS Energy Audit Report Roadchef Norton Canes off M6 Toll UK,” tech. rep., AECOM, London, UK, 2015.
- [2] Ch. Malamatenios, “Energy Audits Guide Part A: Methodology and Technics,” tech. rep., Athens, Greece, 2000.
- [3] S. Wang, C. Yan, and F. Xiao, “Quantitative energy performance assessment methods for existing buildings,” *Energy and Buildings*, vol. 55, pp. 873–888, 2012.
- [4] T. Hong, C. Koo, J. Kim, M. Lee, and K. Jeong, “A review on sustainable construction management strategies for monitoring, diagnosing, and retrofitting the building’s dynamic energy performance: Focused on the operation and maintenance phase,” *Applied Energy*, vol. 155, pp. 671–707, 2015.
- [5] BSI Group, “Draft BS ISO 50002 Energy audits,” Tech. Rep. 0, London, UK, 2013.
- [6] CIBSE, “Energy efficiency in buildings. CIBSE guide F,” tech. rep., London, UK, 2015.
- [7] K. C. Armel, A. Gupta, G. Shrimali, and A. Albert, “Is disaggregation the holy grail of energy efficiency? The case of electricity,” *Energy Policy*, vol. 52, pp. 213–234, 2013.

- [8] L. Pérez-Lombard, J. Ortiz, R. González, and I. R. Maestre, “A review of benchmarking, rating and labelling concepts within the framework of building energy certification schemes,” *Energy and Buildings*, vol. 41, no. 3, pp. 272–278, 2009.
- [9] L. Pérez-Lombard, J. Ortiz, and C. Pout, “A review on buildings energy consumption information,” *Energy and Buildings*, vol. 40, no. 3, pp. 394–398, 2008.
- [10] Department for Communities and Local Government (DCLG), *A guide to Display Energy Certificates and advisory reports for public buildings*. 2008.
- [11] N. Fumo, “A review on the basics of building energy estimation,” *Renewable and Sustainable Energy Reviews*, vol. 31, pp. 53–60, 2014.
- [12] Energy Information Administration, “<https://www.eia.gov/energyexplained/>,” 15 January, 2018.
- [13] A. Kamilaris, B. Kalluri, S. Kondepudi, and T. Kwok Wai, “A literature survey on measuring energy usage for miscellaneous electric loads in offices and commercial buildings,” *Renewable and Sustainable Energy Reviews*, vol. 34, pp. 536–550, 2014.
- [14] S. Frank, L. Gentile Polese, E. Rader, M. Sheppy, and J. Smith, “Extracting operating modes from building electrical load data,” *2011 IEEE Green Technologies Conference, Green 2011*, 2011.
- [15] A. Menezes, A. Cripps, R. Buswell, J. Wright, and D. Bouchlaghem, “Estimating the energy consumption and power demand of small power equipment in office buildings,” *Energy and Buildings*, vol. 75, pp. 199–209, 2014.

- [16] D. Kaneda and B. Jacobson, "Plug Load Reduction: The Next Big Hurdle for Net Zero Energy Building Design," *ACEEE Summer Study on Energy Efficiency in Buildings*, pp. 120–130, 2010.
- [17] The David and Lucile Packard Foundation, "www.packard.org/about-the-foundation," 23 January, 2018.
- [18] J. Waltz, *Computerized Building Energy Simulation Handbook*. Lilburn, GA: The Fairmont Press, 2000.
- [19] P. Hill, "Energy use by office equipment: reducing long-term running costs," tech. rep., 2015.
- [20] D. Coakley, P. Raftery, and M. Keane, "A review of methods to match building energy simulation models to measured data," *Renewable and Sustainable Energy Reviews*, vol. 37, pp. 123–141, 2014.
- [21] P. de Wilde, "The gap between predicted and measured energy performance of buildings: A framework for investigation," *Automation in Construction*, vol. 41, pp. 40–49, 2014.
- [22] CIBSE, "Energy Assessment and Reporting Methodology : Office Assessment Method," tech. rep., London, UK, 1999.
- [23] A. Leiper, "Report, ESOS Energy Audit Roadchef North, Strensham M5No Title," tech. rep., AECOM, London, UK, 2015.
- [24] H. Lee, "ESOS Energy Audit Report Roadchef Stafford off M6 Southbound Junction 15-14 Stone Staffordshire," tech. rep., London, UK, 2015.

- [25] H. Lee, “ESOS Energy Audit Report Roadchef Killington Lake, M6 Southbound Cumbria UK,” tech. rep., London, UK, 2015.
- [26] M. Zeifman and K. Roth, “Viterbi algorithm with sparse transitions (VAST) for nonintrusive load monitoring,” in *IEEE Symposium on Computational Intelligence Applications In Smart Grid*, pp. 1–8, 2011.
- [27] G. Hart, “Nonintrusive appliance load monitoring,” *Proceedings of the IEEE*, vol. 80, no. 12, pp. 1870–1891, 1992.
- [28] N. Batra, O. Parson, M. Berges, A. Singh, and A. Rogers, “A comparison of non-intrusive load monitoring methods for commercial and residential buildings,” 2014.
- [29] BS, “Energy audits Part 1 : General requirements,” tech. rep., London, UK, 2012.
- [30] R. Bell and J. Harris, “Asset Management and Maintenance Audits,” tech. rep., BSRIA, 2012.
- [31] CIBSE, “Energy Assessment and Reporting Methodology : Office Assessment Method,” tech. rep., London, UK, 2006.
- [32] BS EN, “Energy audits Part 2 : Buildings,” tech. rep., London, UK, 2014.
- [33] ASHRAE, “Procedures for commercial energy audits ASHRAE.pdf,” tech. rep., Atlanta, USA, 2011.
- [34] DECC, “Approaches to ESOS audits,” Tech. Rep. March, London, UK, 2015.
- [35] A. Lewry, “Energy survey and audits,” tech. rep., 2015.
- [36] W. Lee, F. Yik, and J. Burnett, “A method to assess the energy performance of existing commercial complexes,” *Indoor and Built Environment*, vol. 12, no. 5, pp. 311–327, 2003.

- [37] B. Poel, G. van Cruchten, and C. Balaras, “Energy performance assessment of existing dwellings,” *Energy and Buildings*, vol. 39, no. 4, pp. 393–403, 2007.
- [38] H. Akbari, “Validation of an algorithm to disaggregate whole-building hourly electrical load into end uses,” *Energy*, vol. 20, no. 12, pp. 1291–1301, 1995.
- [39] R. E. Moffatt, “Guide A: Environmental Design,” Tech. Rep. 4, The Chapter Institution of Building Services Engineers, London, UK, 1983.
- [40] C. Yan, S. Wang, and F. Xiao, “A simplified energy performance assessment method for existing buildings based on energy bill disaggregation,” *Energy and Buildings*, vol. 55, pp. 563–574, 2012.
- [41] M. S. Al-Homoud, “Computer-aided building energy analysis techniques,” *Building and Environment*, vol. 36, no. 4, pp. 421–433, 2001.
- [42] C. Yan, S. Wang, F. Xiao, and D.-c. Gao, “A multi-level energy performance diagnosis method for energy information poor buildings,” *Energy*, vol. 83, pp. 189–203, 2015.
- [43] J. Field, J. Soper, P. Jones, and W. Bordass, “Energy performance of occupied non-domestic buildings : Assessment by analysing end-use energy consumptions,” *Building Serv. Eng. Res. Technol.*, vol. 18, no. 1, pp. 39–46, 1997.
- [44] H. Gonçalves, A. Ocneanu, and M. Bergés, “Unsupervised disaggregation of appliances using aggregated consumption data,” in *Workshop on Data Mining Applications in Sustainability (SIGKDD)*, (San Diego, CA, USA), 2011.
- [45] M. Sheppy, C. Lobato, O. V. Geet, S. Pless, K. Donovan, and C. P. Nrel, “Reducing Data Center Loads for a Large- scale , Low-energy Office Building : NREL ’ s Research Support Facility,” no. December, 2011.

- [46] N. F. Esa, M. P. Abdullah, and M. Y. Hassan, "A review disaggregation method in Non-intrusive Appliance Load Monitoring," *Renewable and Sustainable Energy Reviews*, vol. 66, pp. 163–173, 2016.
- [47] G. Dunn and I. Knight, "Small power equipment loads in UK office environments," *Energy and Buildings*, vol. 37, no. April 2004, pp. 87–91, 2005.
- [48] D. Williams and Y. Tang, "The Impact of Office Productivity Cloud Computing on Greenhouse Gas Emissions," *Environmental Science & Technology*, vol. 47, pp. 4333 – 4340, 2013.
- [49] A. C. Menezes, A. Cripps, D. Bouchlaghem, and R. Buswell, "Predicted vs. actual energy performance of non-domestic buildings: Using post-occupancy evaluation data to reduce the performance gap," *Applied Energy*, vol. 97, pp. 355–364, 2012.
- [50] W. L. Lee, F. W. H. Yik, and J. Burnett, "Assessing energy performance in the latest versions of Hong Kong Building Environmental Assessment Method (HK-BEAM)," *Energy and Buildings*, vol. 39, no. 3, pp. 343–354, 2007.
- [51] D. Coakley, P. Raftery, P. Molloy, and G. White, "Calibration of a Detailed BES Model to Measured Data Using an Evidence-Based Analytical Optimisation Approach," *Proceedings of Building Simulation 2011: 12th Conference of International Building Performance Simulation Association*, pp. 374–381, 2011.
- [52] A. Saltelli, S. Tarantola, F. Campolongo, and M. Ratto, *Sensitivity Analysis*. Ispra, Italy: JohnWiley&Sons, 2004.
- [53] E. E. Leamer, "American Economic Association Sensitivity Analyses Would Help," *The American Economic Review*, vol. 75, no. 3, pp. 308–313, 1985.

- [54] O. Pilkey and L. Pilkey-Jarvis, *Useless Arithmetic. Why Environmental Scientists Can't Predict the Future*. New York.: Columbia University Press, 2007.
- [55] T. Santner, B. Williams, and W. Notz, *Design and Analysis of Computer Experiments*. Springer-Verlag, 1st ed., 2003.
- [56] E. Azar and C. C. Menassa, "A comprehensive analysis of the impact of occupancy parameters in energy simulation of office buildings," *Energy and Buildings*, vol. 55, pp. 841–853, 2012.
- [57] S. De Wit and G. Augenbroe, "Analysis of uncertainty in building design evaluations and its implications," *Energy and Buildings*, vol. 34, no. 9, pp. 951–958, 2002.
- [58] C. J. Hopfe and J. Hensen, "Uncertainty analysis in building performance simulation for design support," *Energy and Buildings*, vol. 43, no. 10, pp. 2798–2805, 2011.
- [59] D. Garcia Sanchez, B. Lacarrière, M. Musy, and B. Bourges, "Application of sensitivity analysis in building energy simulations: Combining first- and second-order elementary effects methods," *Energy and Buildings*, vol. 68, no. PART C, pp. 741–750, 2014.
- [60] H. Rabitz, "Systems Analysis at the Molecular ScaleNo Title," *Science*, vol. 246, no. 4927, pp. 22–226, 1989.
- [61] D. M. Hamby, "A review of techniques for parameter sensitivity analysis of environmental models," *Environmental Monitoring and Assessment*, vol. 32, no. 2, pp. 135–154, 1994.
- [62] E. M. Saltelli, A. Chan, K. Scott, *Sensitivity Analysis*. Chichester, UK: Wiley and Sons, first edit ed., 2000.

- [63] G. Sin and K. V. Gernaey, “Improving the Morris method for sensitivity analysis by scaling the elementary effects,” *Computer Aided Chemical Engineering*, vol. 26, pp. 925–930, 2009.
- [64] D. G. Cacuci, *Sensitivity & Uncertainty Analysis, Volume I: Theory*. Boca Raton, Florida: Chapman & Hall/CRC, 2003.
- [65] M. Spivak, “Calculus on Manifolds,” *The American Mathematical Monthly*, vol. 75, no. 5, p. 567, 1968.
- [66] A. Saltelli and P. Annoni, “How to avoid a perfunctory sensitivity analysis,” *Environmental Modelling and Software*, vol. 25, no. 12, pp. 1508–1517, 2010.
- [67] I. M. Sobol and S. S. Kucherenko, “Global sensitivity indices for nonlinear mathematical models and their Monte Carlo estimates,” *Mathematics and Computers in Simulation*, vol. 55, pp. 271–280, 2001.
- [68] F. Campolongo, J. Cariboni, and A. Saltelli, “An effective screening design for sensitivity analysis of large models,” *Environmental Modelling and Software*, vol. 22, no. 10, pp. 1509–1518, 2007.
- [69] M. D. Morris, “Factorial Sampling Plans for Preliminary Computational Experiments,” *Technometrics*, vol. 33, no. 2, pp. 161–174, 1991.
- [70] D. M. King and B. J. C. Perera, “Morris method of sensitivity analysis applied to assess the importance of input variables on urban water supply yield - A case study,” *Journal of Hydrology*, vol. 477, pp. 17–32, 2013.
- [71] C. Yan, S. Wang, and F. Xiao, “A simplified energy performance assessment method for existing buildings based on energy bill disaggregation,” *Energy and Buildings*, vol. 55, pp. 563–574, 2012.

- [72] S. Lanzisera, S. Dawson-Haggerty, H. Y. I. Cheung, J. Taneja, D. Culler, and R. Brown, "Methods for detailed energy data collection of miscellaneous and electronic loads in a commercial office building," *Building and Environment*, vol. 65, pp. 170–177, 2013.
- [73] A. C. Menezes, A. Cripps, D. Bouchlaghem, and R. Buswell, "Analysis of Electricity Consumption for Lighting and Small Power in Office Buildings," *CIBSE Technical Symposium*, 2011.
- [74] V. Amenta and G. Marco, "Load Demand Disaggregation based on Simple Load Signature and User ' s Feedback," *Energy Procedia*, vol. 83, pp. 380–388, 2015.
- [75] L. G. Swan and I. V. Ugursal, "Modeling of end-use energy consumption in the residential sector: a review of modeling techniques.," *Renew Sustain Energy Rev*, vol. 13, pp. 1819–35, 2009.
- [76] A. Grandjean, J. Adnot, and G. Binet, "A review and an analysis of the residential electric load curve models," vol. 16, pp. 6539–6565, 2012.
- [77] Episensor, "<http://episensor.com/documentation/product-zem-30/>," 22 August, 2014.
- [78] Energy Inc, "<https://www.theenergydetective.com/downloads/>," 16 August, 2015.
- [79] Clancy, Heather, "www.zdnet.com/article/energyhub-manages-home-power-consumption-green-gadget-of-the-week/," 02 May, 2017.
- [80] Power Meter Store, "www.powermeterstore.com/pdfs/cache/www.powermeterstore.com/99333/manual/99333-manual.pdf," 20 May, 2017.

- [81] ASTREL GROUP SRL, “<https://www.4-noks.com/shop/elios4you-accessories/smart-plug/?lang=en>,” 16 July, 2017.
- [82] A. Ridi, C. Gisler, and J. Hennebert, “A survey on intrusive load monitoring for appliance recognition,” *Proceedings - International Conference on Pattern Recognition*, pp. 3702–3707, 2014.
- [83] R. Cohen, M. Standeven, B. Bordass, and A. Leaman, “Assessing building performance in use 1: the Probe process,” Tech. Rep. 2, 2001.
- [84] A. Zoha, A. Gluhak, M. A. Imran, and S. Rajasegarar, “Non-intrusive load monitoring approaches for disaggregated energy sensing: a survey.,” *Sensors (Basel, Switzerland)*, vol. 12, pp. 16838–66, jan 2012.
- [85] M. Zeifman and K. Roth, “Nonintrusive appliance load monitoring: Review and outlook,” *IEEE Transactions on Consumer Electronics*, vol. 57, no. 1, pp. 76–84, 2011.
- [86] J. Kelly and W. Knottenbelt, “‘uk-dale’: A dataset recording uk domestic appliance-level electricity demand and whole-house demand,” *CoRR*, vol. abs/1404.0284, 2014.
- [87] M. L. Marceau and R. Zmeureanu, “Nonintrusive load disaggregation computer program to estimate the energy consumption of major end uses in residential buildings,” *Energy Conversion and Management*, vol. 41, no. 13, pp. 1389–1403, 2000.
- [88] H. Park, “Load Profile Disaggregation Method for Home Appliances Using Active Power Consumption,” *Journal of Electrical Engineering and Technology*, vol. 8, pp. 572–580, may 2013.
- [89] L. Norford, H. Xing and D. Luo., “Detection of HVAC Equipment Turn On-Turn O Events with Non-Intrusive,” tech. rep., Massachusetts Institute of Technology, MA, USA., 2001.

- [90] K. D. Lee and L. Norford, "Fully Automated Analysis of Equipment Scheduling and Cycling," tech. rep., Technical report, Massachusetts Institute of Technology, MA, USA, 2001.
- [91] M. E. Berges, E. Goldman, H. S. Matthews, and L. Soibelman, "Enhancing Electricity Audits in Residential Buildings with Nonintrusive Load Monitoring," *Journal of Industrial Ecology*, vol. 14, no. 5, pp. 844–858, 2010.
- [92] A. Kamilaris, B. Kalluri, S. Kondepudi, and T. K. Wai, "A literature survey on measuring energy usage for miscellaneous electric loads in of fi ces and commercial buildings," *Renewable and Sustainable Energy Reviews*, vol. 34, pp. 536–550, 2014.
- [93] M. E. Berges, *A Framework for Enabling Energy-Aware Facilities Through Minimally-Intrusive Approaches*. PhD thesis, Carnegie Mellon University, 2010.
- [94] S. J. Kang, K. Shin, R. Yang, S. Y. Lee, and J. Sohn, "Cost effective disaggregation mechanism for the NIALM system," *International Journal of Smart Grid and Clean Energy*, pp. 364–370, 2013.
- [95] M. Baranski and J. Voss, "Detecting Patterns of Appliances from Total Load Data Using a Dynamic Programming Approach," *Fourth IEEE International Conference on Data Mining (ICDM'04)*, pp. 327–330, 2004.
- [96] H. Chang, "Non-Intrusive Demand Monitoring and Load Identification for Energy Management Systems Based on Transient Feature Analyses," *Energies*, vol. 5, pp. 4569–4589, nov 2012.
- [97] S. N. Patel, T. Robertson, J. A. Kientz, M. S. Reynolds, and G. D. Abowd, "At the flick of a switch: Detecting and classifying unique electrical events on the residential power line,"

- in *Proceedings of the 9th International Conference on Ubiquitous Computing*, (Innsbruck, Austria), pp. 271–288, 2007.
- [98] Armel, Carrie, “Energy disaggregation [power point slides] <https://web.stanford.edu/group/peec/cgi-bin/docs/events/2011/becc/presentations/3-20Disaggregation-20The-20Holy-20Grail-20-20Carrie-20Armel.pdf>,” 2011.
- [99] I. Abubakar, S. N. Khalid, M. W. Mustafa, H. Shareef, and M. Mustapha, “An overview of Non-intrusive load monitoring methodologies,” *2015 IEEE Conference on Energy Conversion, CENCON 2015*, pp. 54–59, 2016.
- [100] K. Anderson, A. F. Ocneanu, D. Benitez, D. Carlson, A. Rowe, and M. Bergés, “BLUED : A Fully Labeled Public Dataset for Event-Based Non-Intrusive Load Monitoring Research,” *Proceedings of the 2nd KDD Workshop on Data Mining Applications in Sustainability (SustKDD)*, no. October 2011, pp. 1 – 5, 2012.
- [101] A. N. Milioudis, G. T. Andreou, V. N. Katsanou, K. I. Sgouras, and D. P. Labridis, “Event detection for load disaggregation in Smart Metering,” *2013 4th IEEE/PES Innovative Smart Grid Technologies Europe, ISGT Europe 2013*, pp. 1–5, 2013.
- [102] J. Kim, T. Le, and H. Kim, “Nonintrusive Load Monitoring Based on Advanced Deep Learning and Novel Signature,” vol. 2017, 2017.
- [103] A. I. Cole and A. Albicki, “Data extraction for effective non-intrusive identification of residential power loads,” in *Instrumentation and Measurement Technology Conference, 1998. IMTC/98. Conference Proceedings. IEEE*, vol. 2, pp. 812 –815 vol.2, may 1998.

- [104] H. Y. Lam, G. S. K. Fung, and W. K. Lee, "A Novel Method to Construct Taxonomy of Electrical Appliances Based on Load Signatures," *IEEE Transactions on Consumer Electronics*, vol. 53, no. 2, pp. 653–660, 2007.
- [105] Y. Jin, E. Tebekaemi, M. Berges, and L. Soibelman, "A time-frequency approach for event detection in non-intrusive load monitoring," *Proceedings of SPIE - The International Society for Optical Engineering*, vol. 8050, pp. 80501U–80501U–13, 05 2011.
- [106] H. Chang, C. Lin, and H. Yang, "Load recognition for different loads with the same real power and reactive power in a non-intrusive load-monitoring system," in *Comput. Support. Coop. Work Des. 2008. CSCWD 2008. 12th Int. Conf.*, pp. 1122–1127, 2008.
- [107] M. Ito, R. Uda, S. Ichimura, K. Tago, T. Hoshi, Y. Matsushita, and K. Hachioji, "A Method of Appliance Detection Based on Features of Power Waveform," *2004 International Symposium on Applications and the Internet (SAINT'04)*, 2004.
- [108] H. Najmeddine, K. El Khamlichi Drissi, C. Pasquier, C. Faure, K. Kerroum, A. Diop, T. Jouanet, and M. Michou, "State of art on load monitoring methods," *2008 IEEE 2nd International Power and Energy Conference*, no. PECon 08, pp. 1256–1258, 2008.
- [109] L. Jiang, J. Li, S. Luo, J. Jin, S. West, and C. Scientific, "Literature Review of Power Disaggregation," *Neural Networks*, no. June, pp. 38–42, 2011.
- [110] D. H. D. Bailey and P. P. N. Swarztrauber, "A Fast Method for the Numerical Evaluation of Continuous Fourier and Laplace Transforms," *SIAM Journal on Scientific Computing*, vol. 15, no. 5, pp. 1–8, 1994.

- [111] G. Hart, E. Kern, J. Lincoln, and F. Schweppe, “Non-Intrusive appliance monitor apparatus,” tech. rep., Massachusetts Institute of technology, Cambridge, Mass; Electric Power Research Institute, Inc., Palo Alto, Calif., 1989.
- [112] S. B. Leeb and M. S. LeVan, “Transient Event Detection in Spectral Envelope Estimates for Nonintrusive Load Monitoring,” *IEEE Transactions on Power Delivery*, vol. 10, no. 3, pp. 1200–1210, 1995.
- [113] D. Srinivasan, W. S. Ng, and A. C. Liew, “Neural-network-based signature recognition for harmonic source identification,” *IEEE Transactions on Power Delivery*, vol. 21, no. 1, pp. 398–405, 2006.
- [114] P. Meehan, C. McArdle, and S. Daniels, “An efficient, scalable time-frequency method for tracking energy usage of domestic appliances using a two-step classification algorithm,” *Energies*, vol. 7, no. 11, pp. 7041–7066, 2014.
- [115] H. H. Chang, “Non-intrusive demand monitoring and load identification for energy management systems based on transient feature analyses,” *Energies*, vol. 5, no. 11, pp. 4569–4589, 2012.
- [116] K. Khairrell Khazin, F. Mahdi, I. Sallehuddin, A. Mohd, and Y. Md, “Artificial_Neural_Network for Non-Intrusive Electrical Monitoring System,” *Indonesian Journal of Electrical Engineering and Computer Science*, vol. Vol. 6, pp. pp 124–131, 2017.
- [117] C. Laughman, K. Lee, R. Cox, S. Shaw, S. Leeb, L. Norford, and P. Armstrong, “Power signature analysis,” *IEEE Power and Energy Magazine*, vol. 1, no. 2, pp. 56–63, 2003.

- [118] S. R. Shaw, S. B. Leeb, L. K. Norford, and R. W. Cox, “Nonintrusive Load Monitoring and Diagnostics in Power Systems,” *Instrumentation and Measurement, IEEE Transactions on*, vol. 57, no. 7, pp. 1445–1454, 2008.
- [119] H. Y. Lam, *Voltage-Current Trajectory: A 2-Dimensional Approach to Understand Electrical Load Signatures*. PhD thesis, The University of Hong Kong, 2007.
- [120] L. K. Norford and S. B. Leeb, “Non-intrusive electrical load monitoring in commercial buildings based on steady-Statistics and transient load-detection algorithms,” *Energy and Buildings*, vol. 24, no. 1, pp. 51–64, 1995.
- [121] G. Shueli, N. R. Patel, and P. C. Bruce, *Data Mining for Business Inteligence*. New Jersey: John Wiley and Sons, second ed., 2010.
- [122] B. Baykara, *Impact of Evaluation Methods on Decision Tree Accuracy*. PhD thesis, University of Tampere, 2015.
- [123] I. Witten and E. Frank, *Data Mining*. San Francicso: Morgan Kaufmann, second ed., 2005.
- [124] H. Shao, V. Tech, and M. Marwah, “A Temporal Motif Mining Approach to Unsupervised Energy Disaggregation,” *1st International Workshop on Non-Intrusive Load Monitoring*, pp. 1–2, 2012.
- [125] E. Alpaydin, *Introduction to Machine Learning*. Cambridge, Massachusetts: The MIT Press, second ed., 2014.
- [126] G. Linoff and M. Berry, *Data mining techniques*. Indianapolis: Wiley and Sons, third ed., 2011.

- [127] H. Blockeel and J. Struyf, “Efficient algorithms for decision tree cross-validation,” *Journal of Machine Learning Research*, vol. 3, no. 4-5, p. 9, 2001.
- [128] Z. Yu, F. Haghghat, B. Fung, and H. Yoshino, “A decision tree method for building energy demand modeling,” 2010.
- [129] C. Bishop, *Pattern Recognition and Machine Learning*. New York, EEUU: New YorkInc: Springer-Verlag, 2006.
- [130] A. Marchiori, D. Hakkarinen, Q. Han, and L. Earle, “Circuit-Level Load Monitoring for Household Energy Management,” *IEEE Pervasive Computing*, vol. 10, no. 1, pp. 40–48, 2011.
- [131] T. Saitoh, Y. Aota, T. Osaki, R. Konishi, and K. Sugahara, “Current Sensor based Non-intrusive Appliance Recognition for Intelligent Outlet,” *The 23rd International Technical Conference on Circuits/Systems, Computers and Communications (ITC-CSCC 2008)*, vol. 37, pp. 349–352, 2008.
- [132] S. B. Kotsiantis, I. D. Zaharakis, and P. E. Pintelas, “Supervised Machine Learning: A Review of Classification Techniques,” *Informatica*, vol. 31, pp. 501–520, 2007.
- [133] T. A. Nguyen and M. Aiello, “Energy intelligent buildings based on user activity: A survey,” *Energy and Buildings*, vol. 56, pp. 244–257, 2013.
- [134] O. T. Masoso and L. J. Grobler, “The dark side of occupants’ behaviour on building energy use,” *Energy and Buildings*, vol. 42, no. 2, pp. 173–177, 2010.
- [135] A. C. Menezes, *Improving Predictions of Operational Energy Performance Through Better Estimates of Small Power Consumption*. PhD thesis, Loughborough University, 2013.

- [136] D. Cheshire, “Evaluating operational energy performance of buildings at the design stage. CIBSE TM54.,” tech. rep., London, UK, 2013.
- [137] Department of the Environment, Transport and the Regions (DETR), BRECSU, “Energy Efficiency in Offices – Small Power Equipment Loads, Energy Consumption Guide 35,” tech. rep., Garston, UK, 1993.
- [138] CIBSE, “Energy efficiency in buildings. CIBSE Guide F,” tech. rep., London, UK, 2013.
- [139] CIBSE, “Environmental design. CIBSE Guide A,” tech. rep., London, UK, 2013.
- [140] CarbonTrust, “Advanced metering for SMEs Carbon and cost savings,” tech. rep., London, UK, 2007.
- [141] A. C. Menezes, A. Cripps, R. A. Buswell, and D. Bouchlaghem, “Benchmarking small power energy consumption in the United Kingdom: A review of data published in CIBSE Guide F,” *Building Services Engineering Research and Technology*, pp. 1–14, 2012.
- [142] Eurachem, “<https://eurachem.org/index.php/publications/guides/quam>,” 06 September, 2017.
- [143] J. O. Mundy and K. Livesey, “CIBSE Guide F : Energy efficiency in buildings Page,” tech. rep., The Chapter Institution of Building Services Engineers, London, UK, 2015.
- [144] L. K. Norford and S. B. Leeb, “Non-intrusive electrical load monitoring in commercial buildings based on steady-state and transient load-detection algorithms,” *Energy and Buildings*, vol. 24, no. 1, pp. 51–64, 1996.
- [145] Mount Auto Equipment Services, “www.autoequipment.com.au,” 06 November, 2017.

- [146] A. G. Ruzzelli, C. Nicolas, A. Schoofs, and G. M. P. O'Hare, "Real-time recognition and profiling of appliances through a single electricity sensor," *SECON 2010 - 2010 7th Annual IEEE Communications Society Conference on Sensor, Mesh and Ad Hoc Communications and Networks*, no. July, 2010.
- [147] C. F. Lai, R. H. Hwang, H. C. Chao, and Y. H. Lai, "A dynamic power features selection method for multi-appliance recognition on cloud-based smart grid," *Proceedings - 17th IEEE International Conference on Computational Science and Engineering, CSE 2014, Jointly with 13th IEEE International Conference on Ubiquitous Computing and Communications, IUCC 2014, 13th International Symposium on Pervasive Systems*, pp. 780–785, 2015.
- [148] Y. X. Lai, C. F. Lai, Y. M. Huang, and H. C. Chao, "Multi-appliance recognition system with hybrid SVM/GMM classifier in ubiquitous smart home," *Information Sciences*, vol. 230, pp. 39–55, 2013.
- [149] A. Zoha, A. Gluhak, M. A. Imran, and S. Rajasegarar, "Non-intrusive Load Monitoring approaches for disaggregated energy sensing: A survey," *Sensors (Switzerland)*, vol. 12, no. 12, pp. 16838–16866, 2012.
- [150] J. Shafer, R. Agrawal, and M. Mehta, "SPRINT: A Scalable Parallel Classifier for Data Mining," *Proceedings of the 22th International Conference on Very Large Data Bases (VLDB)*, pp. 544–555, 1996.
- [151] A. Barron, J. Rissanen, , and B. Yu, "Principle in Coding and Modeling," *IEEE Transaction on Information Theory*, vol. 44, no. 6, pp. 2743–2760, 1998.

Appendix A

CIBSE TM22 methodology

The TM22 quantitative energy assessment framework used in Chapter 3, was originally developed by the PROBE studies and first published in 1999. It provides a systematic way of undertaking an energy survey, reporting the results, and calculating likely savings from changes in use, technology or management [22]. In 2006, a second edition of the TM22 was published, updating the previous edition by describing procedures for compliance with emerging energy performance legislation and included treatment of on-site energy generation and renewable energy sources [31].

The TM22 methodology establishes three levels of detail for creating energy end-use breakdowns. Figure A.1 illustrates the underlying structure of the TM22 assessment framework, depicting the breakdown of energy consumption into three levels of information subcategories.

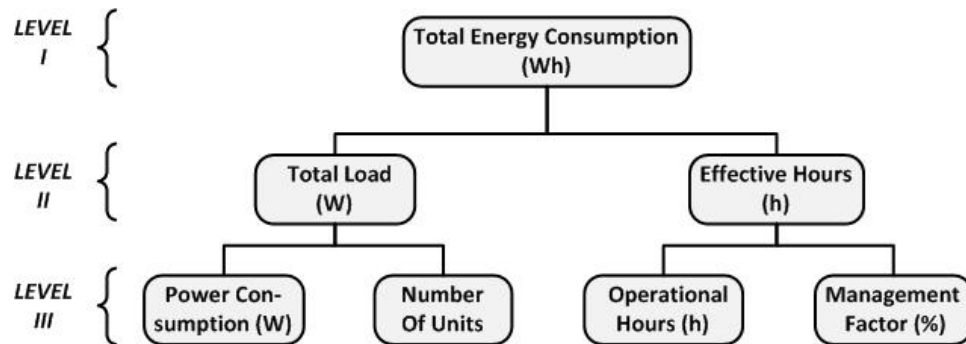


Figure A.1: TM22 tree diagram illustrating the breakdown of energy use.

Each level provide a degree of energy assessment:

Level 1: Simple building assessment: Assessment for a simple building, which has just one building type with at most two energy suppliers including grid electricity, with no special energy use or occupancy features.

Level 2: General building assessment: An overall assessment of a more complex building that can include areas of different building types, with up to five energy suppliers and special features or non-standard usage, accounted for by exclusion or adjustment.

Level 3: System assessment: Assessment of the energy performance of individual systems in a building against benchmarks for that building. This level is applicable to the estimation of small power loads.

Each of those level, requires different inputs factor:

- *Level I:*
 - *Total Annual Energy (Wh):* the aggregated energy consumed by each appliance type in one year.
- *Level II:*
 - *Total Load (W):* the total installed power for the appliance type.

- *Effective Hours (h)*: the total time (in hours) that each appliance is using its nominal full load.
- *Level III*:
 - *Power Consumption (W)*: the power consumed per individual unit in order to provide service.
 - *Number of Units*: the number of installed individual appliances.
 - *Operational Hours (h)*: the number of hours per year that the appliance is delivering a required service. This is not necessary the same that *Occupational Hours (h)*¹.
 - *Management Factor (%)*: the fraction of the time enabled the appliance is working.

Those inputs can be obtained from different sources, table A.1 presents some of the mains typical input data used depending on the assessment level.

¹*Occupational Hours* is the number of hours per year that the building is occupied.

Input data	Level 1	Level 2	Level 3
Annual energy consumption (kWh): gas and electricity bills for at least one year	Yes	Yes	Yes
Total gross area (m ²)	Yes	Yes	Yes
Building type (Benchmarking)	Yes	Yes	Yes
Annual energy consumption (kWh) for each energy suppliers.	No	Yes	Yes
Sub-areas types: natural ventilated, AC, etc	No	Yes	Yes
Main system specifications: lighting, ventilation/cooling	No	Yes	Yes
Effective occupancy hours per year	No	Yes	Yes
Modelling including weather	No	Yes	Yes
CHP and others existing renewables	No	Yes	Yes
The system energy use data that can be obtained from: sub-metered, a detailed survey or modelling	No	No	Yes

Table A.1: TM22 methodology input data by assessment levels.

Appendix B

Informative monitored appliances table for Chapter 4 case study

This appendix presents a table with the appliances monitored in the case study of Chapter 4. The summary table specifies the plug meter number connected to each appliance, the appliance type (e.i. Desk or Shared), a brief description and the power rate for operative and sleep mode. Plug meters are connected to a single devices (e.i. PC, laptop, monitor) or a combinations of them (e.i. PC and monitor, laptop and monitor) depending on the offices set up. However, for the case study experimental design each desk has been considered as an individual appliance. The so called *Desk 0* corresponds to the laptop used only during the data collection. This desk, although monitored by plug meter 98, had not been used in the case study. The instant water boiler is directly connected to the mains, for what a plug meter cannot be connected to this appliance that is only monitored by the MTU.

Plug No	Type	Appliances Description	Nominal Power	Sleep Mode
98	Desk 0	Laptop SANGSUNG Model NP370R5E	60	8
16	Desk 1	Laptop TOSHIBA Tecra R850 119 + Monitor Viewsonic 19"	85.23	9
17	Desk 2	Laptop TOSHIBA Tecra R850 119	65	8
22	Desk 2	Monitor DELL 19"	20	0.5
18	Desk 3	PC Viglen Compact Small + Monitor DELL 19"	270.23	12.5
68	Desk 3	Monitor DELL 19"	20.23	0.5
20	Desk 4	Monitor DELL 19"	20.23	0.5
56	Desk 4	PC Viglen Compact Small + Monitor DELL 19"	270.23	12.5
40	Desk 5	PC Viglen Compact Small + Monitor DELL 19"	270.23	12.5
91	Desk 6	PC hp small compact + Monitor EliteDisplay 27"	280	12.5
99	Desk 7	Laptop TOSHIBA Tecra R850 119 + Monitor DELL 19"	85.23	8.5
96	Desk 8	PC Viglen Compact Small + Monitor DELL 19"	270.23	12.5
47	Desk 8	Monitor DELL 19"	20.23	0.5
106	Desk 9	Laptop TOSHIBA Tecra R850 119	65	8
110	Desk 10	PC Viglen Compact Small + Monitor	270.23	12.5
98	Desk 10	Monitor DELL 19"	20.23	0.5
44	Desk 11	Monitor DELL 19"	20.23	0.5
55	Desk 11	Monitor DELL 19"	20.23	0.5
38	Desk 11	PC Viglen Compact Small	250	12
65	Desk 12	Monitor DELL 19"	20.23	0.5
56	Desk 12	PC Viglen Compact Small	250	12
42	Shared	Small Fridge Cooler King Model KKWBR 130	85	0
36	Shared	Konica Minolta Laser mult. printer bizhub C302300	1580	18
93	Shared	Konica Minolta Laser mult. printer bizhub C302300	1580	18
119	Shared	Auto Feed Micro Cut Shredder	220	0.1
/	Shared	Filtered instant boiling water Zip Hydroboil	2400	0

Appendix C

Schematic layout of smart plugs for the bottom-up metering techniques

This appendix presents the wireless smart plugs distribution layout used for the bottom-up monitoring of the 16 individual appliances targeted for chapter 4 study. The case-study scenario consist in a $30m^2$ naturally ventilated office area, divided into two rooms: office A, occupied by the energy management team of the university; and office B, occupied by the cleaning management team of the university.

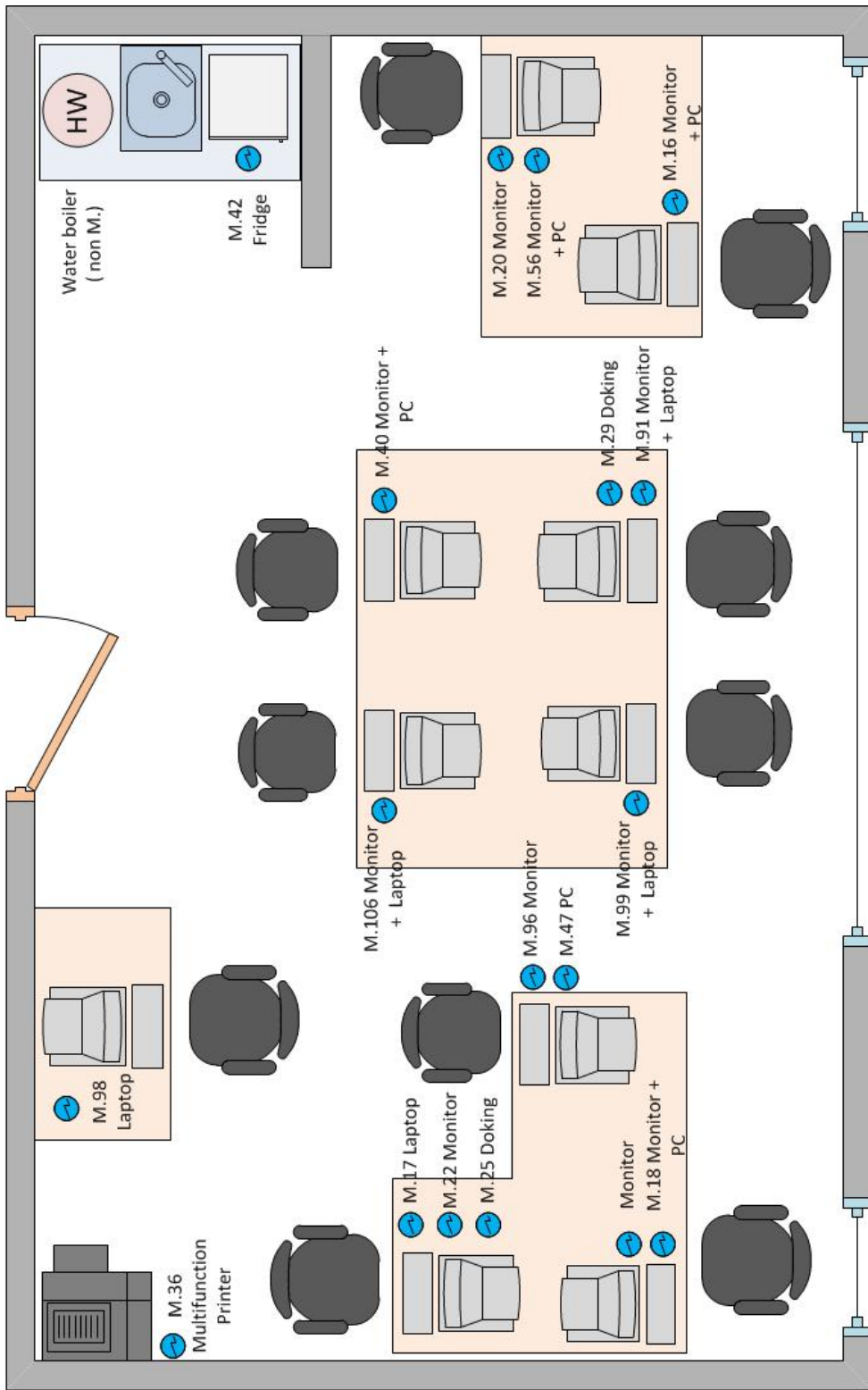


Figure C.1: Smart plugs schematic layout for room A

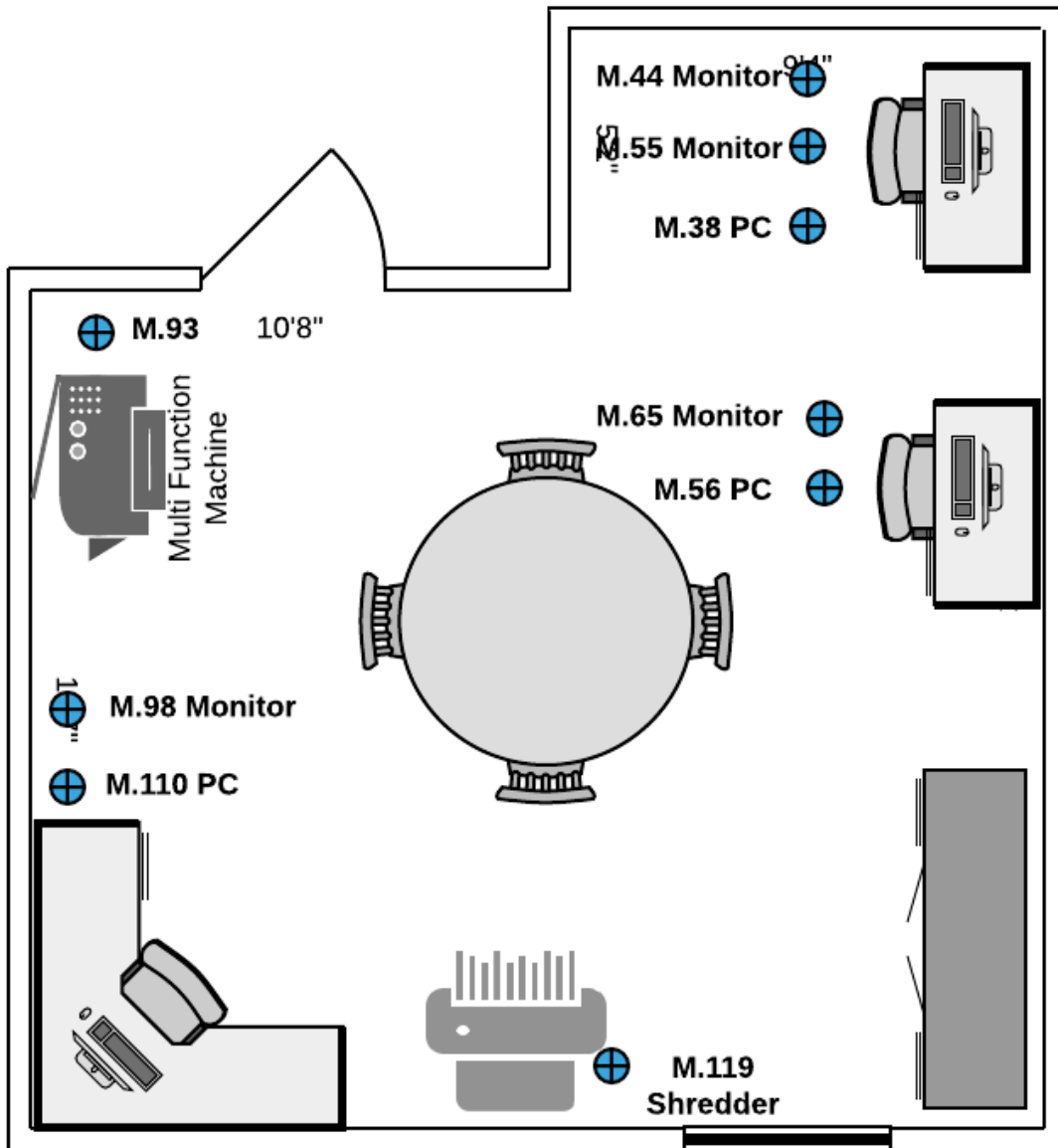


Figure C.2: Smart plugs schematic layout for room B

Appendix D

Individual power consumption profiles for appliances with high frequency content

This appendix presents the consumption profile of two appliances with high frequency content from the case study in Chapter 4. A high-resolution monitoring system, composed by a Pico current meter system connected to a 2204 PicoScope, allows input readings at a sample frequency of 100Hz. Profile peaks are detected and their distances measure.

Figure D.1 shows one printer power consumption profile. It presents high variability on their peaks, or fluctuation, achieving nearly 1000 W of magnitude and a time interval between them of 8 to 20 millisecond approximately.

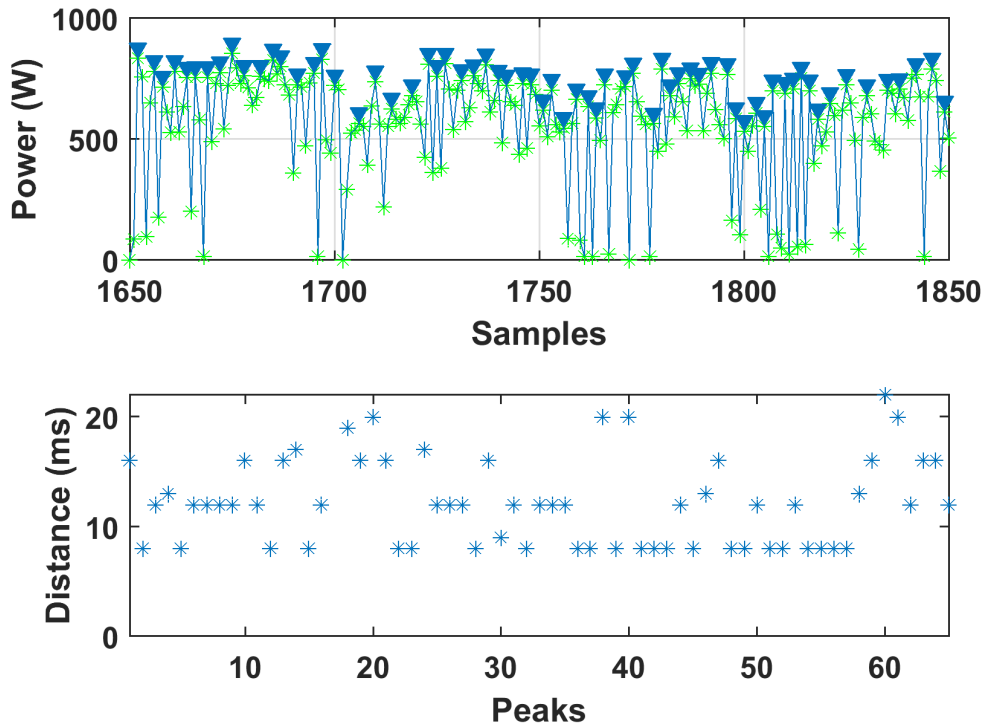


Figure D.1: Printer power profile at 100Hz sample rate.

Figure D.2 shows one PC power profile. It presents a smoother variability on the peaks or fluctuation magnitudes (around 20 W) and a time interval between them of 40 to 260 millisecond approximately.

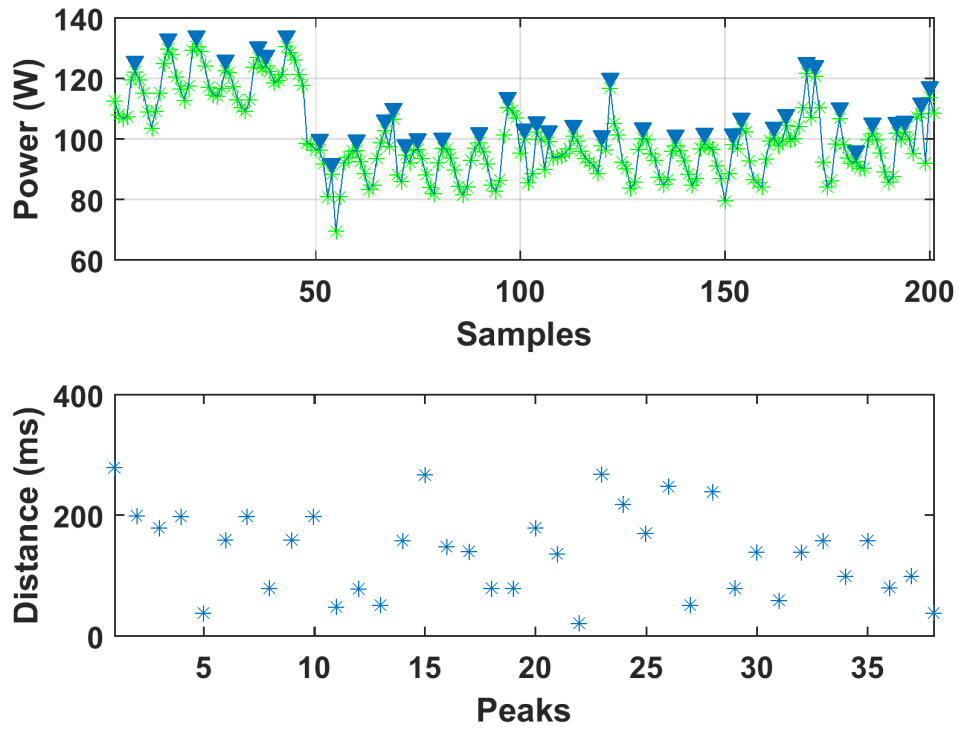


Figure D.2: PC power profile at 100Hz sample rate.

Appendix E

Decision tree classifier algorithm

This appendix contains further details on the Decision Trees algorithm used in Chapter 5. The algorithm performs classification in two phases and is evaluated in a third stage, in accordance to Shafer et al. [150]:

1. *The tree building phase*: or growth phase, in which the tree is built by recursively splitting the data into two or more branches. The value of a split point depends upon how well separate or "pure" the differences between appliance signatures are. The most popular technique for evaluating the quality of the split is the *Gini Index* [121].

The *Gini Index* Gini index is an impurity-based criterion that measures the divergences between the probability distributions of the target attributes or appliances' signatures values. It has the advantage that its calculation requires only the distribution of the load type in each of the partitions level or node. When a node t containing n samples, is split in k partitions, the quality of the split can be computed by Equation E.1:

$$Gini_{split} = \sum_{i=1}^k \frac{n_i}{n} GINI(i) \quad (\text{E.1})$$

Where n_i is the the number of samples at partition i and GINI is the Gini Index for the node t , given by equation E.2.

$$Gini(t) = 1 - \sum_j p_j^2 \quad (E.2)$$

Where p_j is the relative frequency of the appliance j at node t .

When a split divides the node into two branches, the quality of the split is computed as:

$$Gini_{split} = \frac{n_1}{n} Gini_1 + \frac{n_2}{n} Gini_2 \quad (E.3)$$

To find the best split point for a node, each of the node's signatures lists is scanned and splits are evaluated based on that signature. The signature containing the split point with the lowest value for the Gini index is then used to split the node.

2. *The tree pruning phase:* In the three building phase the algorithm three keeps growing by splitting nodes as long as the new splits increase brunches that increase "purity". The tree creation process is optimized by the training data set, so eliminate any leave will increase the error rate ¹ of the tree, however, this fact does not implies that the full tree does the best job for for predictions on new data [126].

A decision tree algorithm makes its best split first, at the root node, where there are the largest number of samples. As the nodes gets smaller, idiosyncrasies of the particular training samples at a node come to dominate the process, in a way that, the smaller the node become, the grater the danger of over-fitting ². One way to overcome this issue, is to

¹The error rate is the proportion of error make over a whole set of instances, and it measures the overall performance of the classifier.

²Insufficient samples in a node causes the tree to use other training samples data that are irrelevant for the classification task, which in decision trees that are more complex that necessary.

set up a minimum leaf size. Another approach is to allow the tree to grow as long as there are splits that appear to be significant in the training data and then eliminate the splits that prove to be unstable by cutting away leaves through a process called *pruning* [126]. A common pruning method used in NIALMs, based on the minimum description length principle, replaces each node with its most popular class, starting at the leaves, but only if the prediction accuracy doesn't decrease, thus extracting the maximum amount of information from the data without over-fitting [151].

3. *The performance evaluation phase:* Once the tree has been fully grown and then pruned, the decision tree model can be used to predict the class value for new patterns. In the evaluation stage the prediction accuracy of the decision tree classifier is evaluated. To do so, the error rate on a data set that did not play a part in the formation of the classifier, the *test or evaluation data set*, is calculated. When a lot of data is available, a large sample can be used for training; and another, independent large sample of different data for testing. Provided both samples are representative, the error rate on the test set will give a good indication of future performance. However, in many cases there is not a vast supply of data available. This limits the amount of data that can be used for testing, and the problem becomes how to make the most of a limited dataset. In those cases, a certain amount is held over for testing, this is called the holdout procedure, and the remainder used for training. In order to find the optimal balance between training and testing, there are several validation methods. Tenfold cross-validation is the standard way of measuring the error rate of a learning scheme on limited data; for reliable results, 10 times 10-fold cross-validation. But many other reliable methods, as the leave-one-out cross-validation, can be used instead [123].

Appendix F

Validation methods for the decision tree algorithm

This appendix presents additional information for the practical study conducted in chapter 5, in which two different validation methods have been used, the *K-fold* and the *holdout* methods.

The *K-fold validation method* consists of partitioning a data set D into n subsets D_i and then running a given algorithm n times, each time using a different training set $D - D_i$ and validating the results on D_i . The *K-fold validation method* allows to alternate between training and testing when the dataset is relatively small to maximize the error estimation [127].

In cross validation a fixed number k is decided as the number of folds that is going to be used. According to the fold number that is selected, the data is portioned into k mutually exclusive subsets which are of approximately equal size. Data D is then divided into k subsets: D_1, D_2, \dots, D_k , where each of these subsets is referred to as a fold. All the folds, except the first one are taken and the subset D_2, D_3, \dots, D_k , becomes the training data and the decision tree model is trained and is tested on the first fold D_1 . On the next iteration, the second fold D_2 becomes the testing subset, and another tree model is trained on the rest of the subsets D_1, D_3, \dots, D_k . This procedure

is repeated k times since every fold is going to act as a testing subset for once, as is graphically represented in Figure F.1.

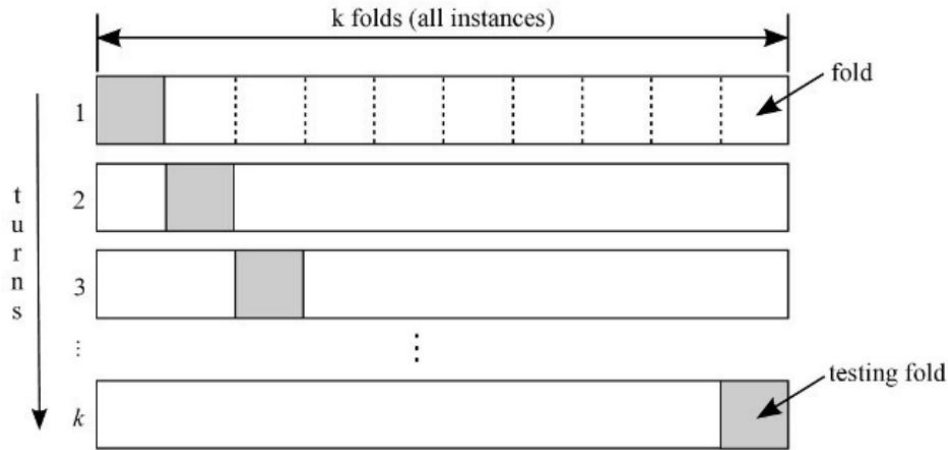


Figure F.1: k-fold cross validation method.

When all the iterations are completed, the accuracy rates that are calculated at the end of each iteration using the testing subset are summed, and then divided by the number of folds to find the average classification rate. Cross validation accuracy (CVA) is calculated as follows;

$$CVA = \frac{1}{k} \sum_{i=1}^k A_i \quad (F.1)$$

where k is the number of folds and A_i is the accuracy measure that belongs to a specific fold.

The *holdout method* is also referred to as the simplest cross-validation method. This method is probably the simplest and most commonly used practice among the evaluation methods. The data is split randomly into two independent subsets: training and testing. The split ratio that is preferred generally is; selecting the training set from 2/3 of the data and testing data from the remaining 1/3 [123]. After the data is split into training and testing, a classification model is built by the inducer using the training data. Later on, this model is used to calculate the misclassification rate or the performance of the built model. Predictions are made based

on the classification model by using the testing data as it can be seen from Figure F.2 The holdout method is used when there is enough data that can be used for both training and testing, separately [122].

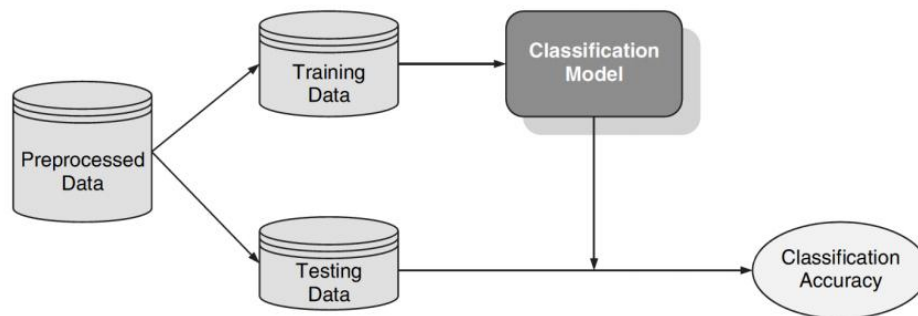


Figure F.2: Holdout validation method.

Appendix G

Decision Tree code in KNIME

This appendix contains the disaggregation and validation work flow for the decision tree algorithm implement in Chapter 5.

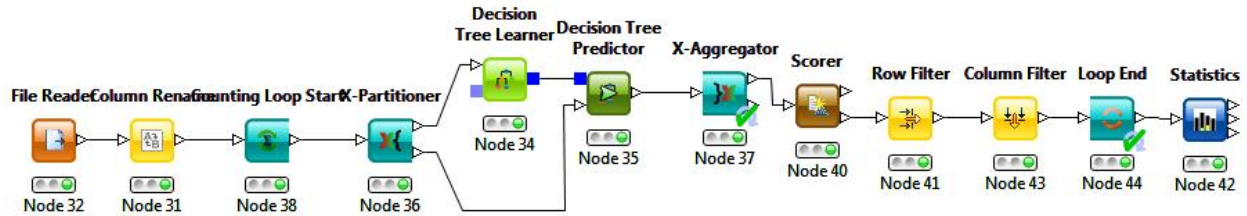


Figure G.1: Decision Tree code in KNIME

Each unit-element of the algorithm in Figure G.1 is represented by a node and linked to others by pipelines. The specific configuration of those nodes are presented below.

- *File Reader*: This node reads data from a URL location.
- *Column Rename*: This node gives each data column a electrical signatures name.
- *Counting Loop Start*: This node starts a loop that is executed a predefined number of times. At the end of the loop, the *Loop-End*, collects the results from all loop iterations. All nodes

in between are executed as many times as specified in the *Loop-Start*, twenty for the case study of Chapter 5.

- *X-Partitioner*: This node is the first in a cross validation loop. At the end of the loop the *X-Aggregator* collects the results from each iteration. All nodes in between these two nodes are executed ten times (number of cross validation iterations). The partitions for the cross validation are sampled randomly.
- *Partitioning*: This node is the first in a hold validation loop (does not appear in the example provided by Figure G.1). It splits data into two partitions, train and test data.
- *Decision Tree Learner*: This node induces the classification decision tree, with a nominal target attribute (the signature type). The other attributes from the case study are numerical. Numeric splits are always binary (two outcomes), dividing the domain in two partitions at a given split point. The quality measure for split calculation used is the gini index. The minimum number of records per node selected for the case study is one, meaning that if the number of records is smaller or equal to this number the tree is not grown any further.
- *Decision Tree Predictor*: This node uses the existing decision tree to predict the class value for new patterns. In this node the *target column* (column containing the true class label) and the *prediction column* (column containing the prediction label) are determined.
- *X-Aggregator*: This node is the end of a cross validation loop and follows a X-Partitioner node. It collects the result from the predictor node, compares predicted class and real class and outputs the predictions for all rows and the iteration statistics.
- *Scorer*: Compares the target and predict columns by their attribute value pairs and shows the confusion matrix.

- *Row Filter*: The node allows for row filtering.
- *Column filter*: This node allows columns to be filtered from the input table while only the remaining columns are passed to the output table, including the column names.
- *Loop End*: This node, at the end of a loop, is used to mark the end of a workflow loop and collects the intermediate results by row-wise concatenation of the incoming tables. The start of the loop is defined by the loop start node, which defines how often the loop should be executed. All nodes in between are executed that many times.
- *Statistics*: This node calculates statistical moments